



Research review paper

A navigation guide of synthetic biology tools for *Pseudomonas putida*

Maria Martin-Pascual<sup>a,1</sup>, Christos Batianis<sup>a,1</sup>, Lyon Bruinsma<sup>a,1</sup>, Enrique Asin-Garcia<sup>a</sup>, Luis Garcia-Morales<sup>a</sup>, Ruud A. Weusthuis<sup>b</sup>, Richard van Kranenburg<sup>c,d</sup>, Vitor A. P. Martins dos Santos<sup>a,e,\*</sup>

<sup>a</sup> Laboratory of Systems and Synthetic Biology, Wageningen University & Research, Wageningen 6708 WE, The Netherlands

<sup>b</sup> Bioprocess Engineering, Wageningen University and Research, Droevendaalsesteeg 1, 6708 PB Wageningen, The Netherlands

<sup>c</sup> Corbion, Gorinchem 4206 AC, The Netherlands

<sup>d</sup> Laboratory of Microbiology, Wageningen University & Research, Wageningen 6708 WE, the Netherlands

<sup>e</sup> LifeGlimmer GmbH, Berlin 12163, Germany

## ARTICLE INFO

## Key words:

*Pseudomonas putida*  
Genetic toolbox  
Genome editing  
Synthetic biology  
Chassis  
Metabolic engineering

## ABSTRACT

*Pseudomonas putida* is a microbial chassis of huge potential for industrial and environmental biotechnology, owing to its remarkable metabolic versatility and ability to sustain difficult redox reactions and operational stresses, among other attractive characteristics. A wealth of genetic and *in silico* tools have been developed to enable the unravelling of its physiology and improvement of its performance. However, the rise of this microbe as a promising platform for biotechnological applications has resulted in diversification of tools and methods rather than standardization and convergence. As a consequence, multiple tools for the same purpose have been generated, whilst most of them have not been embraced by the scientific community, which has led to compartmentalization and inefficient use of resources. Inspired by this and by the substantial increase in popularity of *P. putida*, we aim herein to bring together and assess all currently available (wet and dry) synthetic biology tools specific for this microbe, focusing on the last 5 years. We provide information on the principles, functionality, advantages and limitations, with special focus on their use in metabolic engineering. Additionally, we compare the tool portfolio for *P. putida* with those for other bacterial chassis and discuss potential future directions for tool development. Therefore, this review is intended as a reference guide for experts and new 'users' of this promising chassis.

## 1. Introduction

The quest for the optimal chassis in Synthetic Biology (SynBio) has shown how utopian the idea of one single and perfect chassis is. Thus, it is more realistic to consider a defined repertoire of characterized and standardized chassis for specific scenarios (de Lorenzo et al., 2021). *Pseudomonas putida* KT2440 is recognized as a qualified SynBio chassis for metabolic engineering purposes due to its unique properties to adapt to harsh environmental conditions, especially high concentrations of organic solvents and oxidative stress. Additionally, its simple nutritional requirements, fast growth, flexible metabolism, large volume of knowledge, extensive genetic toolbox and genome-scale metabolic models reinforce the implementation of *P. putida* as a platform for industrial biotransformations (Dos Santos et al., 2004; Nikel et al., 2016;

Poblete-Castro et al., 2012). Furthermore, the biosafety credentials of *P. putida* make it suitable for a very large range of applications (Dos Santos et al., 2004; Kampers et al., 2019b; Weimer et al., 2020). The continuous and fast expansion of the repertoire of genetic tools since its original sequencing in 2002 (Nelson et al., 2002), reflects the great importance of *P. putida* for the scientific community and its potential for the bioeconomy.

This review is envisioned as a reference guide, in which the thus far published tools for regulatory genetic elements, genome editing, transcriptional, post-transcriptional and post-translational regulation, as well as genome-scale metabolic models and available databases are included, with a main focus on the last 5 years. The aspects that make this review attractive not only for experts in the field, but also for new users are: (i) the principles and functionality of each tool, (ii) advantages

\* Corresponding author at: Laboratory of Systems and Synthetic Biology, Wageningen University & Research, Wageningen 6708 WE, The Netherlands.

E-mail address: [vitor.martinsdosantos@wur.nl](mailto:vitor.martinsdosantos@wur.nl) (V.A.P. Martins dos Santos).

<sup>1</sup> These authors contributed equally.

and limitations for each of them, including a comparative analysis between different tools for the same purpose and, (iii) their applicability with special focus on metabolic engineering. Additionally, we explore future directions for the development of synthetic biology tools for *P. putida*, by comparing its current toolbox with those from other important bacterial chassis.

## 2. Genetic regulatory elements to tune bacterial gene expression

Fine-tuning gene expression is essential for constructing efficient bacterial chassis with predictable behavior to elicit the desired output upon implementing heterologous synthetic circuits. Different gene and protein expression levels can be achieved by inferring regulation at transcriptional and translational level (Freed et al., 2018). To such end, we highlight gene copy number, promoters, ribosome binding sites (RBS) and transcriptional terminators as crucial factors to tune expression (Fig. 1).

### 2.1. Replicative plasmids and gene copy number

Plasmids, extrachromosomal DNA with autonomous replication, are crucial cloning vectors for genetic engineering (Jahn et al., 2016). They are also important vehicles for transferring genetic information across bacteria and play an important role in bacterial evolution and adaptation (Shintani et al., 2015). With the advent of sequencing technology, plasmid availability and diversification have increased considerably, resulting in more than 13,000 annotated plasmid sequences (Galata et al., 2019). A few of the most commonly used plasmids comprise the pVLT and pBRR1MCS backbones (de Lorenzo et al., 1993; Kovach et al., 1995).

However, during the last decade, new avenues in SynBio are directed towards robustness and standardization to create controllable chassis whose behaviors can be predicted. The first initiative came in 2003 with the Registry of Standard Biological Parts (Biobrick platform: <http://biobricks.org>), followed by the Standard European Vector Architecture (SEVA) platform in 2013 (Silva-Rocha et al., 2013). Later, in 2015 and 2020, SEVA 2.0 and SEVA 3.0 versions were respectively launched, expanding and improving the plasmid collection and the web interface (Martínez-García et al., 2015, 2020b). Yet, the most updated version, recently published, is SEVA 3.1, which enables compatibility between the SEVA and the Biobrick platforms together with the type IIS assembly method (Damalas et al., 2020). In the field of *P. putida* engineering, numerous laboratories have chosen the SEVA platform as the way

towards data reproducibility and interoperability. SEVA vectors are composed of four functional variable modules: (i) antibiotic resistance marker, (ii) origin of replication, (iii) cargo (DNA sequence with specific function) and, (iv) gadget (DNA sequences that add new features to the vectors, e.g. stabilization). Each vector receives a code, which is a multi-digit cipher. Thus, each module has a specific position in the code; the antibiotic resistance marker module is represented in the first position, the origin of replication module is represented in the second position, the cargo in the third position and the gadget in the fourth position (Martínez-García et al., 2015). For example, the SEVA231 $\alpha$  is a backbone with the kanamycin Ab resistance gene, BBR1 ori, standard multi-cloning site (MCS) and *hok-sok* gadget.

#### 2.1.1. Origin of replication

The origin of replication (ORI) allows the multiplication and segregation of plasmid molecules to daughter cells and determines the plasmid copy number (PCN). This is an important characteristic for biotechnological applications, being responsible for the cargo gene dosage, which has a direct impact on protein production (Jahn et al., 2016). In addition to replicative plasmids, suicide plasmids, also named integrative plasmids, are used to integrate recombinant DNA in the genome of *P. putida* (see Section 3.2 Integrative plasmids). They harbor the ORI R6K, which needs the  $\pi$  protein for plasmid replication. The  $\pi$  protein is encoded by the *pirR6K*, a 1370 bp DNA fragment present in *pir*<sup>+</sup> bacteria, such as *E. coli* DH5 $\alpha$  *pir* (Roberto et al., 1978; Silva-Rocha et al., 2013). Consequently, plasmids with this ORI cannot replicate in *pir*<sup>-</sup> bacteria, such as *P. putida*.

Of particular interest are temperature sensitive replicons, widely applied in fast plasmid-curing strategies since the increase in temperature from 30 to 42 °C leads to plasmid instability and its final loss. To date, there are some inconsistencies regarding their functionality in *P. putida*. There are reports in which temperature sensitive replicons based on the broad-host-range RK2 *oriV* are applied to *P. putida* (Choi and Lee, 2020; Lauritsen et al., 2017; Sun et al., 2018a). However, a recent publication has reported the absence of functionality of previously reported temperature sensitive replicons in *P. putida* (Volke et al., 2020a). The major problem is the almost complete inability of *P. putida* to survive at 42 °C. Besides, the functionality of RK2 strongly depends on the species (Karunakaran et al., 1998).

#### 2.1.2. Antibiotic resistance markers

The antibiotic (Ab) resistance marker module consists of the Ab resistance gene and its native promoter (Silva-Rocha et al., 2013). There

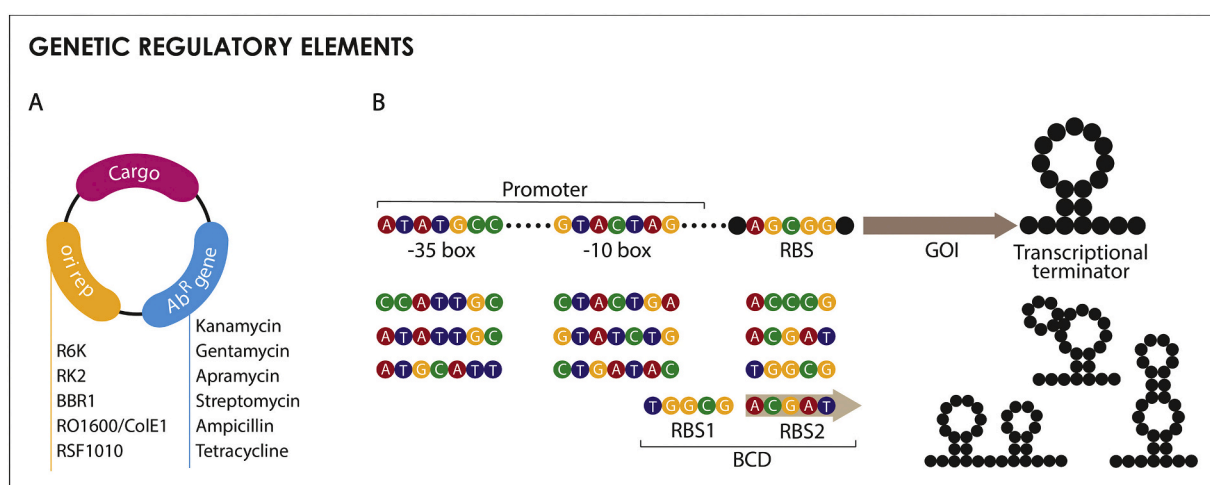


**Fig. 1.** Genetic regulatory elements in *P. putida*. A) Replicative plasmid with the cargo (pink), the antibiotic resistance gene (blue) and the origin of replication (yellow). B) Library of promoters, ribosome binding sites (RBS) and transcriptional terminators. Gene of interest (GOI) (dark brown arrow). Bicistronic design element (BCD) is comprised by two RBSs (RBS1 and RBS2) and encodes a small peptide (light brown arrow). (For interpretation of the references to color in this figure legend, the reader is referred to the web version of this article.)

are six different antibiotic markers: ampicillin, kanamycin, streptomycin/spectinomycin, tetracycline, gentamycin, and apramycin widely applied to *P. putida* (Table 1) (Martínez-García et al., 2015). However, it is important to notice that *P. putida* is natively resistant to chloramphenicol (Fernández et al., 2012) and the apramycin gene *aac(3)-IV* confers additionally resistance to gentamycin as it does for other *Enterobacteriaceae* such as *E. coli* and *Salmonella*. Such cross-resistance is due to the production of aminoglycoside 3-N-acetyltransferase, which can use both apramycin and gentamicin as substrates, and inactivates them (Chaslus-Dancla et al., 1991, 1986; Davies and O'Connor, 1978). Moreover, ampicillin is needed in very high concentrations. Alternatively, other  $\beta$ -lactams with lower intrinsic resistance might also be used to select for  $\beta$ -lactamase bearing plasmid backbones, e.g. piperacillin (Day et al., 1984; Martínez-García and de Lorenzo, 2011).

## 2.2. Promoters

### 2.2.1. Constitutive promoters

Promoters are essential for gene expression and their difference in strength allows to fine tune gene expression. Most of the native bacterial promoters are *cis*-acting sequences with two functional sites,  $-35$  and  $-10$  elements, upstream of the transcription start site (TSS), that are recognized by the RNA polymerase (RNAP) (e Silva and Echeverriagaray, 2012). Several studies have shown the functionality of the same  $\sigma^{70}$  promoter in both *P. putida* and *E. coli*, indicating a high conservation of some regions involved in the interaction with the consensus  $-35$  and  $-10$  elements (Zobel et al., 2015). Therefore, most of the constitutive promoters initially tailored in *E. coli*, such as the *lac* family promoters (without the *lacI* repressor), iGEM Anderson promoters or the PEM7, are directly applied in *P. putida* (Batianis et al., 2020; Calles et al., 2019; Damalas et al., 2020; Zhou et al., 2020; Zobel et al., 2015). When using constitutive promoters as regulatory tools, two strategies can be pursued: (i) characterization of native promoters and, (ii) engineering of synthetic promoters. To date, two high degeneracy synthetic promoter libraries have been developed in *P. putida*. The first was constructed by fusing the monomeric superfolded GFP gene (*msfGFP*) to a library of synthetic promoters and integrating it into a special attachment site (*attTn7*) downstream of the *glmS* gene (Zobel et al., 2015). The design of the synthetic promoters was based on the study published by Hammer et al. (2006), in which the  $-35$  (TTGACA) and  $-10$  (TATAAT) elements were maintained invariable while the surrounding nucleotides were randomized, obtaining variations in promoter strength. As a result, nine promoters with different gene expression levels, spanning three order of magnitude in *P. putida* KT2440 were identified (Zobel et al., 2015). The second library was based on the *tac* promoter, achieving different gene expression levels by modifying the  $-35$ ,  $-10$  and UP-elements (upstream sequences to the  $-35$  motif) in contrast with the previous library, in which those were kept constant (Elmore et al., 2017). Six variants of the  $-35$  and  $-10$  elements and four variants of the UP-elements were included and the promoter strength was calculated by measuring mNeonGreen production, once being integrated in the *P. putida* genome using the BxB1 serine integrase. As a result, 36 constitutive  $\sigma^{70}$  promoters were generated by only combining all the  $-35$  and  $-10$  elements. From this library, three synthetic promoters with high and medium-high strength were chosen to further increase the library variability by incorporating in each of them four distinct UP-elements from native ribosomal RNA promoters of *P. putida* since the UP-elements are known to increase transcription rates. In total, the library accounts for 72 different combinations with a  $\sim 150$ -fold range span (Elmore et al., 2017). In an effort to elucidate how the genetic context influences the activity of synthetic promoters, Köbbing et al. (2020) made different libraries of two concatenated promoters based on the above-mentioned library of Zobel et al. (2015) and analyzed their activity. Despite the poor correlation of different tested factors with promoter activity, it was concluded that the length of the spacer between the two promoters and its position in single promoter-spacer combinations significantly affects

protein expression, independently of the spacer sequence. Only with a specific spacer length of 80 bp, the combination of two promoters yielded higher transcript levels than the single promoters, but those were lower than the sum of the activities of the individual promoters. Further studies are needed for better understanding how the surrounding sequences affect genetic elements, such as promoters. This information can improve the predictability and composability of genetic element combinations, important parameters in SynBio (Köbbing et al., 2020).

### 2.2.2. Inducible promoters

In contrast to constitutive promoters, inducible promoters turn a cellular function or a chosen pathway on or off in response to an external signal. Well-studied inducible systems for gene expression have been proven to be efficient in *P. putida* (Table 2). Among them, the native XylS/Pm expression system from *P. putida* mt-2 receives special attention, being the most widely used as it tightly controls gene expression levels in a broad-host range of applications (Gawin et al., 2017). In *P. putida*, it has been used for multiple purposes, including (i) genome engineering, e.g. gene deletions via I-SceI (Martínez-García and de Lorenzo, 2011) or RecET (Choi et al., 2018), integrations by the mini-transposon Tn5 (Nikel and de Lorenzo, 2013) or single-nucleotide mutations by Ssr recombinase (Aparicio et al., 2016), (ii) transcriptional and post-transcriptional regulation using CRISPRi and sRNAs, respectively (Apura et al., 2020; Batianis et al., 2020), (iii) metabolic engineering such as docosahexaenoic acid production (Gemperlein et al., 2016) and, (iv) recombinant antibody fragments production (Dammeyer et al., 2011). Nevertheless, when working with inducible expression systems, the OFF state generally does not give the ideal zero basal transcription or zero 'leakiness' levels. The numerous factors contributing to the promoter leakiness levels (promoter architecture, PCN, the locus of genome integration, genetic background of the organism, medium composition, cell growth stage, among others) make the engineering of non-leaky promoters challenging (Chen et al., 2018b; Grossman et al., 1998; Reisbig, 2003). Regardless, some attempts to tightly control gene expression levels in *P. putida* have resulted in two different strategies. On one hand, the XylS regulatory element has been physically decoupled from the Pm promoter and the product of the gene of interest was subjected to conditional proteolysis (see Section 3.7 Post-translational regulation). Leakiness levels close to zero were achieved, independent of the PCN (Volke et al., 2020b). On the other hand, a synthetic module was designed and placed downstream of the XylS/Pm expression system, enabling tight control of the highly toxic colicin E3 in *P. putida* as zero basal expression was achieved (Calles et al., 2019).

## 2.3. Ribosome binding sites

RBSs work independently of the promoter and are a vital part of SynBio as they directly affect translation (Salis, 2011). Bacterial translation is divided in four phases: initiation, elongation, termination and ribosome turnover, of which initiation is the most critical and often the most rate-limiting step. Several factors can influence the formation of the 30S initiation complex, including the secondary structure of the mRNA, the RBS spacer and the distance between the RBS and the start codon, being optimal at 5–6 base pairs (Salis et al., 2009). One of the niftiest programs that tackles all these factors is the RBS calculator (Salis et al., 2009). This program uses biophysical methods and computational optimization algorithms to design RBS sequences with well-predicted functions. Despite their essentiality in SynBio, only few studies have reported the characterization of different RBSs in *P. putida*. In the first study, ten different RBS sequences were generated by Elmore et al. (2017), mutating four nucleotides within the core RBS sequence and combined with three different promoters using mNeonGreen as readable output. Protein production levels between the strongest and weakest RBS reached up to 6–7-fold difference. Later, Damalas et al. (2020) predicted six different RBS sequences, ranging from strong to weak,

**Table 1**  
Antibiotic resistance genes and origins of replication applied in *P. putida*.

	Plasmid	Type	Size (bp)	Features	References
Origin of replication	pSEVAx1xx	R6K	389	Suicide vector	Silva-Rocha et al., 2013
	pSEVAx2xx	RK2	2073	Broad-host-range plasmid Composition: <i>trfA</i> Rep protein and <i>oriV</i> 30 ± 10 copies	Cook et al., 2018
	pSEVAx3xx	pBBR1	1435	Broad-host-range plasmid from <i>Bordetella bronchiseptica</i> Composition: pBBR Rep protein and <i>oriV</i> 30 ± 7 copies	Cook et al., 2018
	pSEVAx4xx	pRO1600 /ColE1	3405	Broad-host-range plasmid from <i>Pseudomonas aeruginosa</i> Composition: pRO1600 Rep protein and <i>oriV</i> Inconsistency related to the PCN	Jahn et al., 2016
	pSEVAx5xx	RSF1010	3664	Broad-host-range plasmid Composition: <i>repA</i> , <i>repB</i> , <i>repC</i> and <i>oriV</i> Hyper-promiscuous 130 ± 40 copies	Cook et al., 2018
	pSEVAx6xx	p15A	732	Narrow-host-range plasmid Plasmids containing the p15A origin of replication can be propagated in <i>E. coli</i> cells that contain a second plasmid with the ColE1 origin. Copy number is not determined	Cook et al., 2018; Jahn et al., 2016
	pSEVAx8xx	pUC	929	Narrow-host-range plasmid Composition: CAP binding site for the <i>E. coli</i> catabolite activator protein. CAP binding activates transcription in the presence of cAMP. Copy number is not determined	Cook et al., 2018; Jahn et al., 2016
Ab resistance marker	pSEVA1xxx	Ampicillin	1039	Working concentration is 600 $\mu\text{g/mL}$	
	pSEVA2xxx	Kanamycin	927	Working concentration is 50 $\mu\text{g/mL}$	
	pSEVA4xxx	Streptomycin/ Spectinomycin	989	Working concentration is 100 $\mu\text{g/mL}$	Silva-Rocha et al., 2013
	pSEVA5xxx	Tetracycline	1267	Light sensitive Ab Working concentration is 50 $\mu\text{g/mL}$	
	pSEVA6xxx	Gentamycin	805	Working concentration is 10 $\mu\text{g/mL}$	
	pSEVA8xxx	Apramycin	980	Incompatible with the gentamycin resistance gene Working concentration is 50 $\mu\text{g/mL}$	Martínez-García et al., 2020b

**Table 2**  
Inducible expression systems applied in *P. putida*.

Name	Type	Inducer	TF	Induction	Features	References
XylS/Pm	Native	3-MB	XylS	Linear: 0.05–0.1 mM Maximum: 0.5 mM	Low basal expression. Inconsistence related to the leakiness. High expression levels in exponential phase	Calero et al. (2016)
XylR/Pu	Native	3-MBA	XylR	Maximum: 3 mM	Leaky in stationary phase. Low expression levels in exponential phase	Blatny et al. (1997)
AlkS/PalkB	Native	DCPK	AlkS	Maximum: 0.05 %	Low basal expression levels. Low leakiness. Low expression levels in exponential phase	Calero et al. (2016)
NahR/Psal	Native	SA acid	NahR	Maximum: 1 mM	Low leakiness. High expression levels in exponential phase	Calero et al. (2016)
XylR/PxylA	Native	Xylose	XylR	Maximum: 2 mM	ND	Wang et al. (2018)
Pvan		Vallinic acid	ND	Maximum: 15 mM	ND	Lin et al. (2016)
PRox306 PRox3061 PRox132	Native	OD <sub>578</sub> = 1.5	–	–	Medium expression levels High expression levels Low expression levels	Meyers et al. (2019)
AraC/ParaB	Heterologous	Arabinose	AraC	Maximum: 100 mM	Low basal expression levels. No leakiness. High levels of expression in exponential phase	Calero et al. (2016)
RhaRS/PrhaB	Heterologous	Rhamnose	RhaRS	Linear: 1–3.75 mM Maximum: 10 mM	Low basal expression levels. Low leakiness. High levels of expression in exponential phase	Calero et al. (2016)
LacIQ/Ptrc, Plac, Ptac	Heterologous	IPTG	LacIQ	Maximum: 10 mM	Strong basal expression High leakiness	Bagdasarjan et al. (1983); Calero et al. (2016)
TetR/Ptet MekR/PmekA	Heterologous Heterologous	ATC MEK	TetR MekR	ND Maximum: 90 mM	Inconsistency related to its efficiency Low basal expression levels. No leakiness. High levels of expression in exponential phase.	Cook et al. (2018) Graf and Altenbuchner (2013)
MtlR/PmtIE	Heterologous	Mannitol	MtlR	ND	Low basal expression levels. Low leakiness. High levels of expression in exponential phase	Hoffmann and Altenbuchner (2015)
PT5, PT7	Heterologous	Several		Maximum: 10 mM	High leakiness. Low expression levels in exponential phase	Calero et al. (2016)
ChnR/PchnB	Heterologous	Cyclohexanone	ChnR	Maximum: 1 mM	Low basal expression levels. Low leakiness. High levels of expression in exponential phase	Benedetti et al. (2016)
ClcR/PclcA	Heterologous	3- or 4-chlorocatechol	ClcR	Maximum: 100 μM	ND	Guan et al. (2000)
NagR/PnagA	Heterologous	SA acid	NagR	Maximum: 1 mM	High levels of expression in exponential phase	Hüsken et al. (2001)
CprK1/PDB3	Heterologous	CHPAA	CprK1	Maximum: 1 mM	ND	Batianis et al. (2020); Kemp et al. (2013)
ci857/PL	Heterologous	Temperature = 42 °C	ci857	–	Exposure time = 15–30 min pBBR1 (medium CPN) performs the best at 42 °C with highest expression levels.	Aparicio et al. (2019)
BC-ciIPTG-LacI/Ptac	Heterologous	UV-A light exposure at 365 nm (~1 mW cm <sup>-2</sup> )	LacI	–	Exposure time = 30 min	Hogenkamp et al. (2021)
ccaS-psyA-ho1-ccaR/ P <sub>epc62-172</sub> (mutated improved version)	Heterologous	Green light	ccaS-psyA-ho1-ccaR	–	Exposure time = 8–16 h	Hueso-Gil et al. (2019)

ND (Not defined), TF (transcriptional factor), 3-methylbenzoate (3-MB), 3-methylbenzyl alcohol (3-MBA), Dicyclopropylketone (DCPK), Salicylic acid (SA), Isopropyl β-D-1-thiogalactopyranoside (IPTG), Anhydrotetracycline (ATC), Methyl ethyl ketone (MEK), 3-chloro-4-hydroxyphenylacetic acid (CHPAA), 4,5-bis(carboxymethoxy)-2-nitrobenzyl protecting group (BC, 10b) IPTG.

specifically for sfGFP translation in *P. putida* using the RBS calculator. RBS strength was assessed using the BioBrick BBa\_B0034 RBS as a control and experimental data showed that three of the six predictions were correct. Whereas the strongest predicted RBS showed a significant higher production (2.5-fold) and the two weakest significant lower (3-fold), the other three roughly gave the same output. Recently, Aparicio et al. (2020) integrated a *gfp* into the genome of *P. putida* without a functional Shine-Dalgarno (SD) sequence, which is needed for translation initiation. By using recombineering mediated by degenerated oligos with six or nine nucleotides, a library of 33 RBS variants with a 20-fold difference was created. Moreover, the strongest RBS showed a perfect match with the last 9 nucleotides of the 3' end of the 16S ribosomal RNA of *P. putida*, an interaction which is known to highly impact

ribosome stability and promote translation.

An alternative way to improve the heterologous protein expression is with bicistronic design elements (BCD). In *P. putida*, the translational coupler BCD2 has been used to significantly increased protein expression from heterologous genes inserted in the genome (Wirth et al., 2019; Zobel et al., 2015). The BCD2 was positioned downstream of the promoter, harboring two SD sequences and encoding a small peptide. The first SD sequence mediates the translation of the small peptide, whereas the second SD sequence is translationally coupled to the gene of interest (GOI). In this way, the translation efficiency of the GOI significantly increases by preventing the formation of inhibitory secondary structures at the 5' end of the mRNA, which otherwise would disrupt ribosome binding (Mutalik et al., 2013).

## 2.4. Transcriptional terminators

Whereas the promoter is the starting point for RNA synthesis, the transcriptional terminator marks its end. Terminators are an essential component of the transcription process as they affect mRNA stability and can therefore have a severe impact on protein synthesis. As SynBio comprises often complex circuits, the reuse of parts, e.g. terminators, can lead to homologous recombination (Amarelle et al., 2019). Therefore, a variety of wide-host terminators is required for a proper SynBio genetic toolbox. Transcriptional termination within bacteria, including *P. putida* occurs through two main mechanisms: intrinsic termination and Rho-dependent termination. In intrinsic termination, the nascent RNA forms strong secondary structures at the 3' end, detaching the RNAP in the process. Rho-dependent termination requires the ATP-dependent RNA translocase Rho, which binds to the RNA transcript and dissociates the elongation complex (Ray-Soni et al., 2016). The SEVA collection contains two standard predefined transcriptional terminators: the T1 phage lambda terminator and T0 terminator of the *rrnB* operon of *E. coli* (Silva-Rocha et al., 2013). Whereas no data are available about the effectiveness of the T0 terminator in *P. putida*, the T1 terminator has been reported as not fully functional and allowing transcriptional readthrough when placed in broad host-range vectors (Amarelle et al., 2019).

In general, terminators within *P. putida* have not been subjected to broad research yet with only one case described so far by Amarelle et al. (2019). Using a functional genomics approach, several soil microbial communities were explored to find novel transcriptional terminators, creating a metagenomic library. Terminator strength within this library was determined by placing the terminators between the promoter and a GFP<sub>Iva</sub> reporter, a GFP with reduced half-life. Strong terminators were quantified by their transcriptional readthrough, in which reduced or an absence of GFP signal was detected. Of this database, four unique terminator sequences significantly decreased GFP levels.

## 3. The current 'wet' genetic toolbox

### 3.1. Transposons

Transposon vectors are one of the oldest and most versatile tools for genetically modifying *P. putida* (de Lorenzo, 1992). In recent years, they have been deployed to integrate and express heterologous genes chromosomally instead of plasmid born. Chromosomal integration of expression modules ensures stable inheritance and production, tighter transcriptional control and less burden on the strain (de Lorenzo et al., 1998; Li et al., 2019). The two main modules used for this purpose are the Tn5 and Tn7 mini transposon-vectors. Both have minimal requirements for their functionality: (i) an antibiotic selection marker between two specific flanking sequences and, (ii) their corresponding transposase (Fig. 2). The selected cargo that is to be introduced into the genome is cloned within the flanking sequences where the selection marker is also located. Both the Tn5 and Tn7 transposon vectors have a R6K origin of replication, unable to replicate in *P. putida*. The transposases recognize their respective flanking sequences and transfer the mini-transposon module containing the cargo and antibiotic selection marker from the vector towards the genome. The Tn5 mini transposon vectors integrate in random places in the chromosome, whereas the Tn7 mini transposon vectors integrate unidirectionally in *attTn7* site (Zobel et al., 2015). While the Tn5 transposons allow subsequent Tn5-integrations, Tn7-transposition can occur only once unless additional *attTn7* sites have been introduced. However, taking into account that the Tn5-transposons can integrate everywhere and possibly disturb cell vitality, integrations into the *attTn7* locus are considered to be more innocuous (Lambertsen et al., 2004; Tan et al., 2018). A limitation of both approaches is the integration of an undesired antibiotic markers in the chromosome. However, this marker can be excised from the genome by any subsequent deletion strategies (see Section 3.4 Site-specific

recombination).

The Tn5 mini transposon vectors have undergone a number of improvements over time in terms of standardization and modularity (Table 3). In this way, first the pBAM1 plasmids were streamlined by removing non-essential DNA sequences and restriction sites as well as by incorporating non-frequent restriction sites between the functional modules for their easy exchange (Martínez-García et al., 2011). Suicide delivery of the pBAM1 plasmids in *P. putida* was tested by either electroporation or conjugation, in which transposon insertion frequencies were  $1.02 \times 10^{-7}$  and  $1.8 \times 10^{-3}$ , respectively, showing a preference for conjugation. Later, the pBAM1 plasmids were eventually restructured to create the pBAMD vectors, which have an architecture of the SEVA format and still contain all the advantages of the pBAM1 plasmids. Using the pBAMD vectors with different antibiotic markers, it was showcased that three rounds of transpositions were possible, enabling accumulation of several insertions in the same genetic background (Martínez-García et al., 2014). Another further development of the Tn5-transposons is called TREX, which allows the transfer and expression of entire biosynthetic pathways between bacterial hosts (Loeschcke et al., 2013). When these large pathways are transferred to another bacterium, transcription is not guaranteed as heterologous promoters associated with the biosynthetic pathways might not be recognized by the RNA polymerases of the host-strain. Consequently, they are randomly integrated into the genome through Tn5-transposition, where expression becomes dependent on read-through from chromosomal promoters. However, if biosynthetic pathways often comprise complex genetic structures in which genes are in bidirectional orientations, this will likely impede expression. Therefore, the TREX system was developed as an expression system, allowing transcription of biosynthetic pathways irrespective of the hosts natural promoters by using T7 RNA polymerase (T7RP)-dependent promoters. This polymerase is prone to ignore bacterial termination sites and able to produce long transcripts. Thus, the biosynthetic clusters are flanked by two T7RP-dependent promoters, ensuring their bidirectional transcription, crucial when the genes within such biosynthetic clusters are not unidirectionally organized. However, it must be noted that these promoters can only be used by the introduction of a T7RP-encoding plasmid.

With the TREX method, the zeaxanthin (6.9 kb) and prodigiosin (21.9 kb) gene clusters were successfully integrated into *P. putida*'s genome. Despite their size differences, transposition rates ( $10^{-5}$  to  $10^{-6}$ ) were similar for both clusters. Using the TREX-prodigiosin plasmid, Domröse et al. (2019) located the most favourable loci for chromosomal integration. A transposon-library of ~ 50.000 clones was created and 50 clones that showed strong expression of prodigiosin were subjected to in-depth analysis. In all these 50 clones, integration occurred within the rRNA-encoding operons of *P. putida*. This not only resulted in high expression but also long term-stability after subsequent cultivation for over 2 years. Recently, the TREX system was further improved to yTREX by combining it with yeast recombinational cloning (Domröse et al., 2017). Whereas the TREX method relied on conventional restriction/ligation methods, the yTREX method allowed cloning and modification of gene clusters in a single cloning step, overcoming the time-consuming bottleneck of its predecessor. Rearrangements of existing gene clusters like the violacein pathway, which yields different end products depending on the combination of genes, were further achieved. Additionally, facile detection of clusters which do not give visible outputs was demonstrated. To this end, a promoter-less *lacZ* reporter gene was successfully implemented downstream of the gene clusters, allowing identification of clones in which the whole cluster was transcribed.

### 3.2. Integrative plasmids

Whereas transposons are deemed efficient for genetic insertions, they cannot delete genes, only disrupt them. Instead, integrative plasmids are widely used to delete specific genes. The most established two-step deletion method in *P. putida* is via homologous recombination with

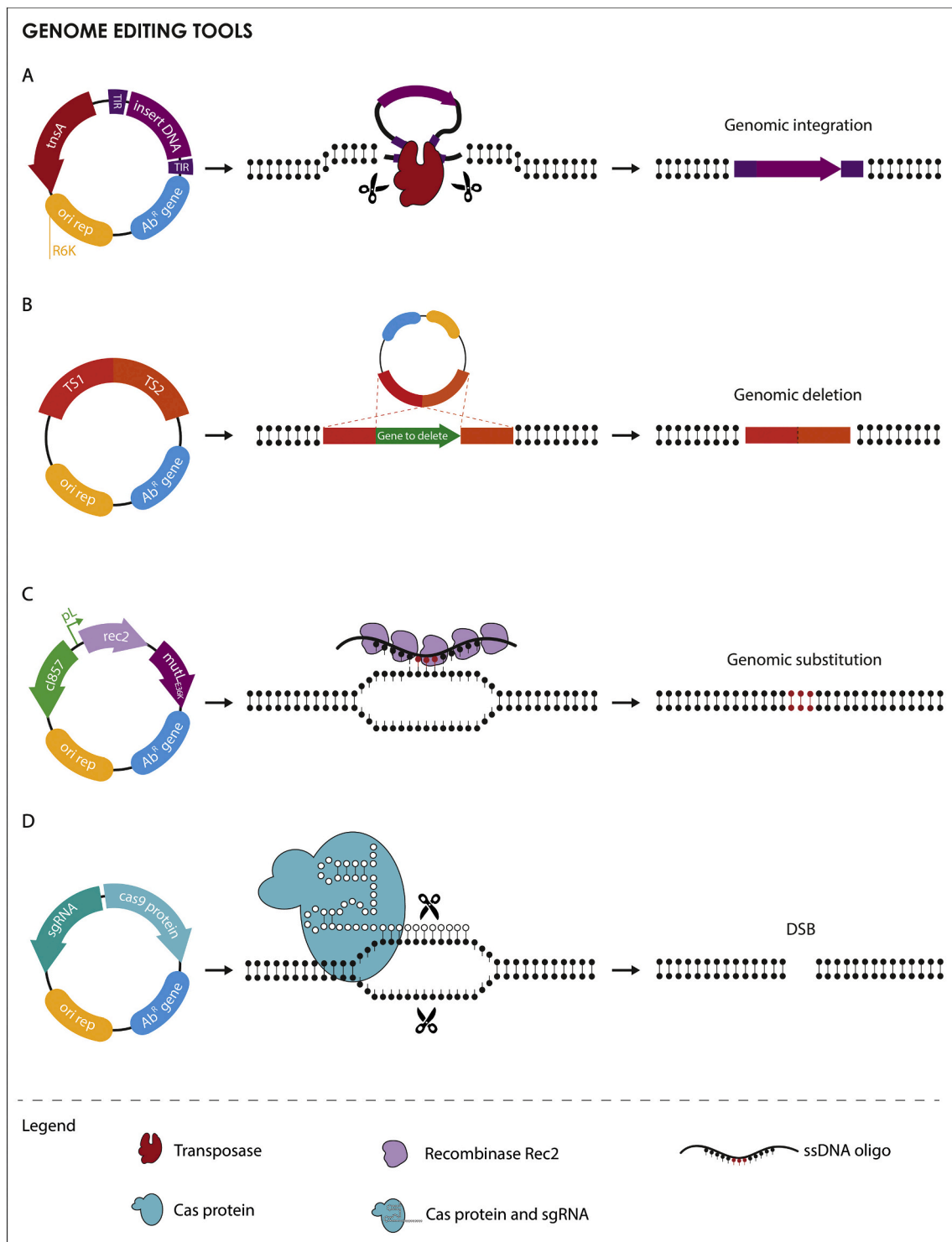


**Fig. 2.** Genome editing tools of *P. putida*. A) Transposon vector. The transposase encoded by the *tnsA* binds to the terminal inverted repeats (TIR), excises the element (DNA to insert) surrounded by the TIRs and introduces it in the bacterial genome. The result is a genomic integration. B) Integrative plasmids. The key features are the flanking regions TS1 (upstream the target locus) and TS2 (downstream the target locus) and the R6K origin of replication, which cannot replicate in *P. putida*. Homologous recombination events of TS1 and TS2, will lead to genomic deletions or genomic integrations if a target gene would be between TS1 and TS2. C) Recombineering. The recombinase gene *rec2* and the *mutL* are under the control of the temperature-inducible cI857/pL system. At 42 °C, both genes are expressed, promoting the incorporation of linear single-stranded DNA oligo in the replication fork during lagging-strand synthesis of DNA replication. In this scenario, the oligo carries a nucleotide mutation (red nucleotides), which will be inherited and spread across the cell population, resulting in a genomic substitution. If the oligo would bear other type of mutations, such as insertions or deletions, the editing outcome will be in accordance to those. D) CRISPR-Cas technology. The active Cas9 and the sgRNA, directed by the spacer, bind to the target site and induce a double strand break (DSB) in the genome, causing bacterial death. CRISPR-Cas9 technology can be used as counter selection tool allowing to select for rare genomic recombination events by eliminating wild-type sequences. Mutant cells with genome deletions, integrations or substitutions can be selected depending on the DNA template.

**Table 3**  
Comparison of different mini-transposon and integrative vectors applied in *P. putida*.

Tool	Purpose	Limitations	Applications	Efficiency	Time spent	References
<b>Mini-Transposon vectors</b>						
<b>pBAM1</b>	Insertions	Conventional cloning	Engineering <i>P. putida</i> for arsenic methylation.	Electroporation: $1.02 \times 10^{-7}$ Mating: $1.8 \times 10^{-3}$	ND	Martínez-García et al. (2011)
<b>pBAMD</b>	Insertions	Conventional cloning	Engineering <i>P. putida</i> to catabolize cellobiose	ND	ND	Dvořák and de Lorenzo, 2018; Martínez-García et al. (2014)
<b>TREX</b>	Insertions of large biosynthetic clusters with bidirectional transcription	Conventional cloning	Production of prodigiosin (94 mg/L)	Mating $10^{-5}$ to $10^{-6}$	ND	Loeschcke et al. (2013)
<b>yTREX</b>	Construction of biosynthetic clusters through yeast-based recombination and integration using TREX		Production of prodigiosin, violacein, deoxyviolacein and phenazine	ND	< 2 weeks	Domrose et al. (2017)
<b>Mini Tn7-transposon-vectors</b>	Insertions	Continuous rounds of integrations are not possible	Synthetic promoter characterization	ND	ND	Bruckbauer et al. (2015)
<b>Integrative plasmids</b>						
<b>pEMG</b>	Scarless deletions and insertions	Heavy PCR screening of cointegrates	Reducing the genome of KT2440	Theoretically 50 % chance of knockout/insertion	~ 5 days	Martínez-García et al. (2011)
<b>pGNW</b>		The expression of GFP is locus dependent	Insertion of fluorescent markers		~ 5 days	Wirth et al. (2019)
<b>pSNW</b>			Reducing the genome of EM42		~ 5 days	Volke et al. (2020b)
<b>pK18mobsacB</b>			Reducing the genome of KT2440. Insertion of catabolic pathways		ND	Elmore et al. (2020); Liang et al. (2020)

ND (Not defined).

the assist of the pEMG or pK18mobsacB integrative vectors (Martínez-García and de Lorenzo, 2011; Schäfer et al., 1994). The loci of integration are dependent on the homology arms that are built in these plasmids. When deleting a gene, approximately 500 – 800 bp upstream and downstream of the gene of interest are amplified and cloned into either vector. The homology arms in the pEMG vector are flanked by two unique I-SceI sites, which are recognized by the I-SceI endonuclease, encoded on the pSW-1 plasmid under the XylS/Pm expression system. Once the pEMG vector is integrated into the genome through homologous recombination over either one of the homology arms, the expression of the I-SceI endonuclease introduces a lethal double strand break in the single crossover (SCO) recombinants. The resolution of the SCO can eventually leave two possible outcomes: deletion of the gene of interest or restoration of the wild-type genotype (Wirth et al., 2019). One of the biggest highlights using the above mentioned protocol was the construction of a genome-reduced variant of *P. putida* KT2440, in which a span of 300 genes was deleted (~4.3 % of the entire genome) with the largest single deletion stretching 69 kb (Martínez-García et al., 2014). This new strain, designated EM42, showed a net increase of ATP and NADPH availability and superior growth properties with shorter lag phases in rich and minimal media, and a higher final biomass yield.

As time developed, both the pEMG and pSW-I plasmids went through several improvements (Table 3). The suicide vector pEMG was recently improved and transformed into pGNW, which allow a fast and accurate assembly of the homology arms. Additionally, a monomeric superfolded GFP was incorporated, allowing direct visualization of successful integrations (Wirth et al., 2019). Using this method, not only fast deletions were demonstrated, but also insertions. Recently, Volke et al. (2020b) observed that GFP derived fluorescence of the pGNW vectors was highly locus dependent. Consequently, these plasmids were enhanced by the addition of a BCD in front of the GFP, which showed significantly higher expression in low expression loci, compared to the pGNW plasmids and were named pSNW vectors.

The first major transfiguration of the pSW-I plasmid was performed

by Aparicio et al. (2015). The plasmid was rebuilt to be coherent with the SEVA format, adding several antibiotic markers and therefore expanding its functionality and use. Aside from the inducible versions, constitutive versions were also created (Wirth et al., 2019). Recently, these plasmids were further improved for easy self-curing, one of the most time-consuming steps in genome engineering (Volke et al., 2020a). These plasmids, branded as pQURE, have the initiator protein TrfA under the control of the XylS/Pm expression system, making plasmid replication reliant on the presence of 3-MB. Cells that were cultured without inducer for 24 h, lost in 92 % of the cases their plasmid. Both newly developed plasmids pSNW and pQURE were recently deployed to reduce the genome of *P. putida* strain EM42 even further (Volke et al., 2020a).

Like the pEMG and its successors, the pK18mobsacB also integrates through a single crossover event over either one of the homology arms. However, this system does not require the help of an additional plasmid for the second crossover event. The pK18mobsacB is equipped with the sacB selection marker from *Bacillus subtilis*. This gene encodes a levansucrase which hydrolyses sucrose and produces levans. This synthesis exerts a toxic effect in primarily gram-negative bacteria, where an accumulation of levans is hypothesized to obstruct the periplasm due to their high molecular weight (Pellic et al., 1996). Therefore, growing colonies on a medium with sucrose will select for cells that excised the plasmid through a second cross-over event. Unlike *E. coli* in which counterselection is performed on plates containing 5 % sucrose, the optimal working solution frequently used for *Pseudomonas putida* is 25 % (Elmore et al., 2017; Khetrapal et al., 2015). Like the pEMG series, this technique can be deployed for both deletions and insertions. Recently, through this method, the catabolic pathways for xylose and arabinose were introduced in KT2440, allowing this strain to grow on the five major sugars of lignocellulosic biomass (Elmore et al., 2020). In general, these suicide vectors are still a widely used concept, going through several rearrangements in the last decade. They have constantly been improved and remain a powerhouse for scarless deletions and insertions.

### 3.3. Recombineering

Recombineering is an efficient and sophisticated bioengineering technique for *in vivo* manipulation of genomes. Recombinase proteins (also known as single-stranded DNA-annealing proteins, SSAPs) are the methods core component promoting the incorporation of linear single-stranded DNA (ssDNA) segments in the replication fork during DNA replication (Ellis et al., 2001). Additional exonuclease activity is required for double-stranded DNA (dsDNA) recombineering systems in order to degrade one of the strands to generate the final ssDNA substrate (Datsenko and Wanner, 2000). If that DNA segment was designed to bear modifications, these would be inherited and spread across the cell population. On that account recombineering enhances the frequency of homologous recombination, allowing the generation of genomic deletions, insertions, and single nucleotide substitutions, as well as *in vivo* cloning, mutagenesis of bacterial artificial chromosomes and phasmids, and the construction of genomic libraries (Court et al., 2002; Marinelli et al., 2012). For *P. putida*, recent years have been marked by a constant search for an efficient recombineering system (Table 4). This exploration was primarily motivated by the somewhat poor direct applicability of the pioneer Red $\beta$  recombinase and dsDNA  $\lambda$  Red recombineering system from the *E. coli*  $\lambda$  phage (Martínez-García and de Lorenzo, 2019). Attempts to establish this powerful option have been numerous but, alas, the significant efficiency levels obtained in *E. coli* have been reached only by using phenotypic selection. Luo et al. (2016) applied the  $\lambda$  Red recombineering system for markerless gene deletions that ranged from 1.1 to 9.3 kb. Their two-step method started with a 3-MB-induced  $\lambda$  Red-mediated replacement of the target gene with a targeting dsDNA fragment that consisted of a kanamycin resistance gene flanked by *loxP* sites and 500 bp homologous arms. Recombinant clones were then selected on kanamycin and, subsequently, marker removal was conducted by expressing Cre recombinase from a different plasmid that  $\lambda$  Red and the dsDNA fragment, achieving replacement efficiencies > 70 % (see Section 3.4 Site-specific recombination). Shortly after, the same laboratory published an improved gene deletion protocol that did not rely on Cre/*lox*-mediated recombination anymore. In turn, I-SceI restriction sites flanking the antibiotic resistance gene were incorporated (Chen et al., 2016).

The previous studies inspired other authors to combine the  $\lambda$  Red

system with other selection methods such as CRISPR-Cas. Thanks to the Cas cleavage of wild type cells' chromosome, the yield of mutants approaches 100 % of the total remaining cells, which is translated into a boost of the net efficiency of recombineering (Cook et al., 2018; Sun et al., 2018a). CRISPR-Cas-mediated counter-selection will be thoroughly discussed later in the Section 3.5.1 CRISPR for gene editing.

Efforts with  $\lambda$  Red-like counterparts from other prophages have also been reported, namely the dsDNA recombineering RecET system from the *E. coli* Rac prophage. While the Red $\beta$  recombinase works more efficiently with low GC content DNA (Rybalchenko et al., 2004), RecT recombinase performs independently of this factor (Noirot and Kolodner, 1998) which is advantageous for *P. putida*, given its high GC content. Consequently, a new method combining RecET and Cre/*lox* site-specific recombination was presented (Choi et al., 2018; Choi and Lee, 2020). Mimicking the aforementioned study, the two-steps protocol began with a 3-MB-induced RecET-mediated replacement of the target gene with a dsDNA fragment consisting of a tetracycline resistance gene flanked by *lox* sites and 100 bp homologous arms. Furthermore, a multi cloning site was included between the homologous arms but outside of the *lox* region to allow markerless insertion of heterologous genes. After antibiotic selection, marker removal was performed correspondingly via IPTG-induced Cre recombination using a two-plasmid system. Like in the aforementioned two-step protocols, each plasmid of the two-plasmid system contained the elements for each step: one included RecET and the dsDNA fragment, and the other the Cre machinery. Though similar in approach, better results were obtained with this method including: i) 100 % successful knock-outs of multiple genetic loci with lengths ranging from 0.6 to 101.7 kb; ii) integration of different heterologous genes (1.2 kb) with an efficiency >74 %; and, iii) integration of different gene clusters (3.6–7.4 kb) with efficiencies ranging from 10 to 85 %. Moreover, marker removal was also 100 % successful in every case.

The efficiency, accuracy and the markerless modifications make the mentioned recombineering systems a competitive option over other deletion and insertion methods. Additionally, authors stressed the rapidness of the protocols which could be performed in 4–6 days. However, we must bear in mind that these systems incorporate selection methods (e.g. antibiotic resistance or cleavage of wild type cells) which are needed to maintain the high recombineering capabilities and can be a drawback for certain specific applications.

**Table 4**  
Recombineering tools applied in *P. putida*.

Tool	Purpose	Recombinase induction	Limitations	Applications	Efficiency	Time spent	References
$\lambda$ Red – Cre/ <i>lox</i>	Deletions (1.1–9.3 kb)	3-MB (Preculture from OD600 ~0.2 to ~0.6)	Antibiotic selection required, <i>lox</i> scar	–	70–100 %	4–6 days	Luo et al. (2016)
$\lambda$ Red – I-SceI	Deletions (1.1–64.3 kb)	3-MB (Preculture from OD600 ~0.2 to ~0.6)	Antibiotic selection required	Deletion of 16 drug exporter genes Strain LS3476 - 3.76 % genome reduction	25–100 %	4–6 days	Chen et al. (2016)
RecET <sub>Rac</sub> – Cre/ <i>lox</i>	Deletions (0.6–101.7 kb), insertions (1.2–7.4 kb)	3-MB (Preculture until OD600 ~2)	Antibiotic selection required, <i>lox</i> scar	Insertion of biosynthetic gene clusters for bioproducts	100 % (deletions), 10–85 % (insertions)	5 days	Choi et al. (2018); Choi and Lee (2020)
Red $\beta$	Point mutations	3-MB (30 min)	Low efficiency in absence of selection	–	0.0015–0.066 %	2 days (1 cycle)	Ricaurte et al. (2018)
Ssr	Point mutations, small deletions, small insertions	3-MB (30 min)	Low efficiency in absence of selection	–	0.023–0.013 % (point mutations), 0.0043 % (small deletions), 0.0088 % (small insertions)	2 days (1 cycle)	Aparicio et al. (2016); Ricaurte et al. (2018)
Rec2	Point mutations, small deletions, small insertions	3-MB (30 min)	Moderate efficiency in absence of selection	Determination of MMR system single nucleotide replacement hierarchy	0.086–0.18 % (point mutations), 0.0047 % (small deletions), 0.041 % (small insertions)	2 days (1 cycle)	Ricaurte et al. (2018)
HEMSE (with Rec2)	Point mutations	42 °C (15 min)	Low efficiency when multiplexing	Diversification of RBSS	~10 % (single), ~2 × 10 <sup>-4</sup> % (4 changes) and ~6 × 10 <sup>-6</sup> % (5 changes)	11 days (10 cycles)	Aparicio et al. (2020)

Besides the heterologous *E. coli* phage systems, functional homologs have been searched in the genomes of Pseudomonads. The quest for an optimal recombinase that would work efficiently in *P. putida* in absence of selection has so far resulted in two SSAP candidates: Ssr and Rec2. They were identified through bioinformatic mining in the genomes of *P. putida* strains DOT-T1E (Aparicio et al., 2016) and CSV86 (Ricaurte et al., 2018), respectively, and have been experimentally validated in multiple publications.

The ssDNA recombineering ability of Ssr was first demonstrated by generating small changes in the *pyrF* gene using mutagenic oligonucleotides. These mutants are resistant to 5-fluoroorotic acid (5-FOA) which allows an easy screening of the engineered cell population. The use of Ssr controlled by the Pm promoter to mediate small deletions (100 bp) and small insertions (9 bp) increased by  $\sim 6 \times 10^3$ -fold and  $\sim 2 \times 10^2$ -fold, respectively, in respect to the basal 5FOA resistance rate. Alas, these numbers of mutated cells still represented  $<0.1$  % of the total population (Aparicio et al., 2016). To overcome these low modification frequencies, the authors brought counter-selection into play once again. Hence, by merging Ssr-mediated recombineering with CRISPR-Cas9 technology, mutated clones were selected yielding higher efficiencies (Aparicio et al., 2018). The exploration for a better recombinase resulted in the discovery of Rec2. This enzyme first stood out among other Pm-controlled putative recombinases for its ability to mediate single nucleotide substitutions in the *rpsL* gene. The K43T amino acid substitution derived from one-point mutation in this specific gene confers streptomycin resistance facilitating the screening of mutants. While Red $\beta$  and Ssr exhibited a respective average of 0.066 % and 0.023 %, Rec2 reached 0.18 % of recombineering efficiency. This superiority was conserved while producing *pyrF* mutants: i) with single nucleotide changes the obtained efficiencies were 0.086 % for Rec2, 0.013 % for Ssr and 0.0015 % for Red $\beta$ , ii) with small insertions (9 bp), 0.041 % for Rec2 and 0.0088 for Ssr and, iii) with small deletions (100 bp), 0.0047 % for Rec2 and 0.0043 % for Ssr (Ricaurte et al., 2018). Thus, Rec2 surpassed previous standards, and was postulated as the new archetype to develop further.

Besides the two recombinases, these studies brought to light an extra limitation for single nucleotide changes: the sensitivity to the host's mismatch repair (MMR) system. *P. putida* ensures fidelity during DNA replication thanks to its native MMR machinery which comprises the *mutS* and *mutL* genes. The hierarchy of recognition of different types of base mispairings in *P. putida* was elucidated and described as follows: A: G < C:C < G:A < C:A, A:A, G:G, T:T, T:G, A:C, C:T < G:T, T:C (Aparicio et al., 2020). In order to overcome this obstacle during the recombineering process, a strategy of transient disruption of the MMR was proposed. The expression of a dominant negative E36K version of *mutL* linked to the expression of the recombinase interrupts the MMR generating a time gap during which any kind of single nucleotide changes is tolerated (Nyerges et al., 2016).

Convergence of Rec2 ssDNA recombineering and reversible disruption of the endogenous MMR machinery brought about the High-Efficiency Multi-site Genomic Editing system (HEMSE) for *P. putida*. Inspired by the MAGE platform (Gallagher et al., 2014; Wang et al., 2009), though lacking the automation feature, HEMSE was proposed as the way to go for entering multiple simultaneous changes in the chromosome of *P. putida*. Both *rec2* and *mutL*<sub>E36K</sub> were located under the thermo inducible control of the P<sub>L</sub>/cI857 system and were subjected to multiple cycles of expression/mutagenic oligonucleotide transformation. First, 5 different loci were targeted independently with efficiencies ranging from 8.5 % to 21 %, after 10 cycles of recombineering. Whereas these levels seemed promising, efficiency dropped dramatically when multiplexing:  $\sim 2 \times 10^{-4}$  % and  $\sim 6 \times 10^{-6}$  % mutated population after 10 cycles for four and five changes, respectively (Aparicio et al., 2020).

In view of the above, recombineering already represents a powerful tool for genome editing in *P. putida*, with available protocols for large deletions, insertions and single nucleotide changes. However, much

remains to be done to reach the yields reported in *E. coli* with Red $\beta$ . Despite the successful cases reported here, and next to what seems as an intrinsically rather poor ability of *P. putida* to capture exogenously provided DNA, the efficacy of the core recombinase remains the main bottleneck of the technique. A better enzyme is still required for optimal multiplexing of the technique and to stop depending on selection methods.

#### 3.4. Site-specific recombination: site-directed recombinases

In contrast to homologous recombinases, which promote the recombination between similar sequences, site-specific recombinases only promote recombination between specific recognition sites. These recombinases are found across many different hosts regulating key functions, but the most typically used are those found in phages (e.g. Cre,  $\lambda$  integrase,  $\phi$ C31 integrase, Bxb1 integrase) and in the yeast *Saccharomyces cerevisiae* (Flippase recombinase, FLP) (Gaj et al., 2014). They are classified into tyrosine and serine recombinases, depending on the active residue in the catalytic domain. These two types differ in the mechanism by which the recombination occurs. Briefly, tyrosine recombinases promote the recombination through a Holliday junction intermediate while serine recombinases cleave and religate the two molecules of DNA (Chen and Rice, 2003; Grindley et al., 2006). While some tyrosine recombinases (e.g. Cre, FLP) are bidirectional, other tyrosine recombinases (e.g.  $\lambda$  integrase) and all the serine recombinases (e.g.  $\phi$ C31 integrase, Bxb1 integrase) show recombination only in one direction (Wang et al., 2011).

In particular, the site-specific recombinases used for synthetic biology applications show a precise sequence specificity, which gives to the researchers a tight control over desired DNA reorganizations. Their recognition sites are short, usually ranging from 21 to 48 nucleotides, and similar in structure, consisting of two inverted repeats surrounding a spacer sequence where recombination occurs (Gaj et al., 2014).

Researchers have designed different strategies for the use of these recombinases in genome engineering that have allowed the insertion of heterologous DNA, and the inversion or deletion of a targeted DNA sequences (Table 5). In all these strategies, the specific recognitions sites must be previously inserted in the desired location of the genome. This is accomplished by other genetic manipulation tools, usually homologous recombination or transposition.

A remarkable example was the streamlining of *P. putida* KT2440 genome using a combinatorial deletion method based on mini-transposon insertion and the FLP-*FRT* recombination system (Leprince et al., 2012a, 2012b). This method combines random insertions of the mini-Tn5 derivative transposon vectors and the site-specific FLP-*FRT* recombination system to generate successive random deletions in a single strain in which parts of the genome are excised via the action of the cognate FLP. These mini-Tn5 transposons carry different selectable markers and each has a Flippase Recognition Target (*FRT*) site. Mapping of the position of both mini-Tn5 transposons in the chromosome of *P. putida* was conducted by Arbitrary Primed-PCR (AP-PCR). Subsequent sequencing of the PCR fragments led to the identification of the coordinates of the transposons and the orientation of both *FRT* sites. Under specific laboratory conditions, both *FRT* sites were recognized by the FLP, and the deletion of a nonessential intervening genomic segment along with the transposon backbones occurred without inheritance of any marker genes. Based on these libraries, they generated single-deletion mutants lacking  $\sim 4.1$  % of the genome ( $\sim 3.7$  % of the gene repertoire). A cyclical application of the method generated four double-deletion mutants of which a maximum of  $\sim 7.4$  % of the chromosome ( $\sim 6.9$  % of the gene count) was excised. This procedure demonstrates a new strategy for rapid genome streamlining and enabled to gain of new insights into the molecular interactions and regulations in *P. putida* (Leprince et al., 2012a, 2012b, 2012c).

More recently, the Cre recombinase from bacteriophage P1 has been used in combination with recombineering to produce scarred markerless

**Table 5**  
Site-directed recombinases applied in *P. putida*.

Tool	Purpose	Limitations	Applications	Efficiency	Time spent	References
FLP <i>FRT</i>	Deletions (41–253.9 kb)	(1) Random insertion of FRT sites. (2) Active FRT scar	Genome streamlining	100 %	2 days	Leprince et al. (2012a)
Cre <i>loxP-loxP</i>	Marker excision	(1) Active <i>lox</i> scar (2) Continuous rounds of deletions are not possible	Markerless deletions	100 %	2 days	Luo et al. (2016)
Cre <i>lox71-lox66</i>	Marker excision	(1) Inactive <i>lox</i> (2) Continuous rounds of deletions are not possible	Markerless deletions	100 %	2 days	Choi et al. (2018)
Cre <i>lox71-lox66</i>	Marker excision	(1) Inactive <i>lox</i> scar (2) Continuous rounds of integrations are not possible	Markerless insertions	100 %	2 days	Choi et al. (2018)
Cre <i>loxP-loxPlox5171-lox5171</i>	Insertions (10–49.1 kb)	(1) Antibiotic marker (2) Continuous rounds of integrations are not possible	Insertion of BGCs	33 %	2 days	Wang et al. (2019)
Bxb1 <i>attP-attB</i>	Insertions (> 6kb)	(1) Insertion of whole plasmid; antibiotic marker (2) Continuous rounds of integrations are not possible	Rapid insertions, screenings	100 %	2 day	Elmore et al. (2017); Peabody et al. (2019)

gene deletions in *P. putida* (Choi et al., 2018; Luo et al., 2016). Using this strategy, the gene of interest was replaced by a selectable marker flanked by *loxP* sites by homologous recombination using  $\lambda$  Red (Luo et al., 2016) or RecET (Choi et al., 2018). In both cases, the selectable marker was removed upon Cre recombination through the *lox* sites, which showed a 100 % efficiency in both works.

Luo et al. (2016) used the natural *loxP* sites from bacteriophage P1 to excise the antibiotic resistance marker. Cre-mediated recombination through natural *loxP* sites is bidirectional and, more importantly, leaves an active *loxP* scar in the genome after the excision. The presence of multiple active *loxP* scars causes genome instability and hinders the accumulation of mutations using the same system (Arakawa et al., 2001; Lambert et al., 2007). To prevent this situation of genome instability, few years later Choi et al. (2018) used the engineered *lox71-lox66* recognition sites instead of the natural *loxP* sites, enabling a quasi-irreversible recombination while maintaining 100 % efficiency on marker excision. This recombination leaves a *lox72* scar in the genome, which is poorly recognized by Cre recombinase and therefore, is considered inactive. This is an advantage over the use of native *loxP* sites as it allows reusing the system several times in the same cells (Arakawa et al., 2001). As stated before, this technology was only used in combination with recombineering to perform scarred markerless deletions (up to 101.7 kb) and insertions (up to 7.4 kb). However, Wang et al. (2019) used, for the first time, the Cre recombinase to directly integrate larger biosynthetic gene clusters (BGCs) by recombinase-mediated cassette exchange (RMCE). This strategy was based on the introduction of a landing pad that contained two heterospecific *lox* sites unable to recombine together (*loxP* and *lox5171*) flanking the Cre recombinase and the kanamycin resistant marker, in the genome of the target bacteria by transposition. The same *lox* sites were also introduced in a plasmid surrounding the desired BGC and an apramycin resistant marker. Upon transformation of this plasmid, Cre promoted recombination between the two *loxP* and the two *lox5171* sites independently, which produced a cassette exchange integrating the BGC in the genome and removing the kanamycin marker. In a high-throughput way, 9 BGCs from *Photobacterium luminescens* ranging from 10 kb to 49.1 kb were introduced in 25 diverse  $\gamma$ -Proteobacteria. In particular, the integration of these BGCs in *P. putida* ranged from 8 % to 75 % of the transformed cells, independently of the size of the BGC (Wang et al., 2019).

Serine integrases have also been used to introduce heterologous DNA into the genome of *P. putida*. These integrases promote recombination between *attP* (from the original Phage) and *attB* sites (from the original Bacterium). This recombination was used to integrate whole plasmids containing an *attP* site into a genome where an *attB* site has been previously introduced by homologous recombination. The efficiency of

several serine integrases has been tested in *P. putida*, from which the integrase of phage Bxb1 of *Mycobacterium smegmatis* showed the highest efficiency reaching  $2.28 \times 10^4$  CFU/ $\mu$ g of plasmid, in comparison with RV,  $\Phi$ BT1 and  $\Phi$ C1, which reached  $2.45 \times 10^3$  CFU/ $\mu$ g, 2.8 CFU/ $\mu$ g and 0.6 CFU/ $\mu$ g, respectively (Elmore et al., 2017). The authors tested this method to integrate plasmids of 6 kb and was applied in a high-throughput experiment to test a library of promoters in *P. putida* (Elmore et al., 2017). This approach was further used by Peabody et al. (2019) to express a heterologous GalP transporter at different levels and analyze the effect on growth of this bacterium using galactose as carbon source.

In summary, all site-specific recombinases leave scars in the final mutant strain, which is a downside when compared with other markerless gene deletion strategies. However, the high efficiency of site-specific recombinases makes them amenable for high-throughput applications (Luo et al., 2016), especially for integrating different DNA fragments into the same location of the chromosome and construct libraries. Strategies such as RMCE have been extensively adapted for high-throughput engineering experiments of different eukaryotic cell lines (Bouwman et al., 2013; Ebinuma et al., 2015; Krebs et al., 2014; Turan et al., 2013). Although these site-specific recombinase-based experiments are still very limited in bacteria, including *P. putida*, they represent a robust alternative to integrate multiple variants of complex synthetic pathways in these cells (Peabody et al., 2019; Urtecho et al., 2019; Wang et al., 2019).

### 3.5. CRISPR tools

#### 3.5.1. CRISPR for gene editing

The ever-expanding CRISPR-Cas systems have become an unprecedented molecular tool with endless possibilities, revolutionizing biotechnology, medicine and agriculture research fields. Owing to its simplicity, efficiency, flexibility and robustness, this powerful technique has propelled the genome editing technology throughout all kingdoms of life (Choi and Lee, 2016; Jaganathan et al., 2018; Schuster and Kahmann, 2019; Wang et al., 2016). The site-specific DNA-targeting and cleaving of the Cas endonuclease protein is reprogrammed by simply designing the spacer region of a short guide RNA molecule. The spacer sequence has to be complementary to a specific target region, denoted as protospacer, in the genome of interest. Additionally, a short protospacer adjacent motif (PAM) must be present upstream or downstream of the protospacer in the target DNA. Type-II CRISPR-Cas9 and type V CRISPR-Cas12a (or CRISPR-Cpf1) are the most widely adopted systems for precise genome engineering of both eukaryotes and prokaryotes (Adli, 2018; Pickar-Oliver and Gersbach, 2019). The Cas9 RNA-guided

nuclease is characterized by the two conserved HNH and RuvC nickase domains conferring the endonuclease activity. Cas9 requires two RNA elements, the CRISPR RNA (crRNA) and trans-activating RNA (tracrRNA). To gain simplicity, both RNAs have been fused together into a chimeric, single-guide RNA (sgRNA). The most widely used Cas9 is from *Streptococcus pyogenes* (SpCas9) and needs the PAM sequence 5'-NGG-3' downstream of the 20-nt long-spacer sequence (Jiang and Doudna, 2017). SpCas9 recognizes the target DNA via Watson-Crick base pairing by the complementary sgRNA, and introduces a primarily blunt, but occasionally a staggered double-stranded DNA break (DSB) (Gisler et al., 2019; Molla and Yang, 2020; Moon et al., 2019). Alternatively, the three Cas12a varieties (AsCas12a, LbCas12a and FnCas12a from *Acidaminococcus* sp., *Lachnospiraceae* bacterium and *Francisella novicida*, respectively) have the RuvC domain, but lacks the HNH domain, having a putative nuclease (Nuc) domain instead. Differently to Cas9, Cas12a only requires of the RuvC domain to cut both, the template and the non-template strands. As well, only the crRNA, containing the 20-nt long spacer and the PAM sequence 5'-TTN-3' or 5'-TTTN-3' located upstream of a target protospacer is necessary to introduce staggered 5'-overhangs in the cleavage site (Moon et al., 2019). The DSB is lethal for most bacteria since the non-homologous end joining (NHEJ) repair machinery is absent or not functional, a feature that makes Cas proteins extraordinarily powerful counter-selection tools. Only in the presence of a homologous recombination template, the desired modifications can be introduced in the genome by homology-directed repair (HDR) usually catalyzed by the RecA protein, assuring survival. It is noteworthy, however, that the native bacterial HDR is generally suboptimal for efficient and high-throughput applications. Consequently, heterologous recombinases are often simultaneously introduced with the donor template, boosting recombination efficiencies (Selle and Barrangou, 2015) (Tables 6 and 7).

The CRISPR-Cas technology reached the *P. putida* field in 2017 when, for the first time, a ThermoCas9-sgRNA tool for genome engineering of obligate thermophiles was additionally proven to be efficient as a counter-selection system in *P. putida* KT2440, despite its mesophilic nature (Mougiakos et al., 2017). A one-plasmid strategy, consisting of a two-step process, was pursued. During the first step, a suicide plasmid, carrying the ThermoCas9 under the XylS/Pm expression system, the sgRNA under the P3 constitutive promoter and the homologous recombination regions, was integrated in the bacterial genome. The ThermoCas9 was induced during the second step, introducing a DSB within the gene sequence to be deleted, in this case, *pyrF*. The only requirement of this Cas9 is the presence of the PAM sequence, 5'-NNNNCNRA-3', in the targeted gene. Comparing non-induced with induced conditions, the knockout efficiency increased from 2 % to 50 %, though the strategy was still dependent on the native recombination efficiencies (Mougiakos et al., 2017). Later, the wild type SpCas9-crRNA-tracrRNA system was employed also as counter-selection method, but in this case, in combination with Ssr-mediated ssDNA recombineering as an effort to increase the recombination efficiency (Aparicio et al., 2018). Besides this, the SpCas9's 5'-NGG-3' PAM sequence is notably simpler than the one recognized by ThermoCas9, increasing the number of potential target sites. In this particular study, different parameters for alternative goals were analyzed: (i) the deletion efficiency of different genes (*pyrF*, *endA-1* and *flgM*) individually and multiplexed targeted, (ii) the deletion efficiency of different DNA fragment sizes (1.9, 4.9 and 69.1 kb) and, (iii) the single nucleotide mutation efficiency depending on the nucleotide change and its position related to the PAM (2, 6 and 17 nt distant from the PAM). The results showed that ~50 to ~80 % of the colonies had the expected deletion when single genes (*pyrF*, *endA-1* and *flgM*) of less than 1 kb were targeted. However, when *endA-1* and *flgM* were simultaneously deleted, the achieved efficiency decreased to 3 %. Similarly, with the increase of DNA fragment length to 4.9 and 69.1 kb, the deletion efficiency dramatically dropped to 13 % and 1 %, respectively. Additionally, the counter-selection of single-nucleotide substitutions within the *pyrF* gene showed that 97 % of

**Table 6**

Technical specifications of CRISPR-based Cas9 editing strategies applied in *P. putida*.

Study	Strategy	Strain	Elements
Mougiakos et al. (2017)	One-plasmid system:  (1) pEMG-suicide plasmid-ThermoCas9-sgRNA-homology template	<i>P. putida</i> wild type	(1) XylS/Pm-ThermoCas9 (2) P3 constitutive promoter-sgRNA (3) Homologous recombination flanks (0.5 kb)
Aparicio et al. (2018)	Three-plasmid system:  (1) pSEVA42-SpCas9-tracrRNA (2) pSEVA23-crRNA (3) pSEVA65-Ssr	<i>P. putida</i> wild type	(1) Native constitutive promoter-SpCas9 (2) Native constitutive promoter-tracrRNA (3) Leader-crRNA (4) XylS/Pm-Ssr (5) ssDNA oligos
Cook et al. (2018)	Three-plasmid system:  (1) pRK2-SpCas9 (2) pBBR1-UP-sgRNA (3) pJOE-Suicide plasmid-homology template	<i>P. putida</i> wild type	(1) Constitutive promoter-SpCas9 (2) Constitutive promoter-sgRNA (3) AraC/ParaB- $\alpha\beta\lambda$ operon (4) Homologous recombination flanks (0.5–1 kb)
Sun et al. (2018a)	Two-plasmid system:  (1) pCas-RK2K plasmid-sgRNA targeting the ori of pSEVA64-gRNA (2) pSEVA64-sgRNA-homology template	<i>P. putida</i> wild type with SpCas9 or Cas12a and $\lambda$ Red recombinase	(1) Constitutive promoter-SpCas9/Cas12a (2) Constitutive promoter- $\alpha\beta\lambda$ operon (3) RhaRS/PrhaB-sgRNA-sp targeting the ori of pSEVA64-gRNA (4) Constitutive promoter sgRNA (5) Homologous recombination flanks (0.5 kb)
Zhou et al. (2020)	One-plasmid system:  (1) Plasmid-sgRNA targeting a palindromic sequence in the plasmid-sgRNA with the targeting spacer-homology template	<i>P. putida</i> wild type with SpCas9n and $\lambda$ Red recombinase	(1) Pmin constitutive promoter-SpCas9n (2) PxyIA- $\alpha\beta\lambda$ operon (3) Ptrc-sgRNA (4) Pvan-sgRNA targeting a palindromic sequence in the plasmid (5) Homologous recombination flanks (0.5 kb)

the cells incorporated the right nucleotide swap only when the changed nucleotide was hardly recognized by the endogenous MMR of *P. putida* and it was located 2-nt distance to the PAM. On the contrary, if the changed nucleotide was either easily recognized by the MMR or located 6 or 17 nt far away from the PAM, all the cells lacked the expected mutation (Aparicio et al., 2018). Similar to the previously published systems, Cook et al. (2018) published 1 month later a strategy of three plasmids based on the SpCas9-sgRNA and the dsDNA  $\lambda$  Red recombineering system. First, a suicide plasmid was integrated in the genome of *P. putida*, constitutively expressing the SpCas9 from an additional plasmid. Next the  $\lambda$  Red recombinase was induced with L-arabinose, and the plasmid bearing the sgRNA was electroporated, cleaving the genome in the targeted locus. In comparison with the work of Aparicio et al. (2018) in which ssDNA oligos were used as substrate of the Ssr

**Table 7**  
CRISPR editing tools applied in *P. putida*.

Tool	Purpose	Limitations	Applications	Efficiency	Time spent	References
<b>Thermocas9-sgRNA (One-plasmid system)</b>	Deletion of <i>pyrF</i> gene	(1) The recombination efficiency of the plasmid co-integration in the genome of <i>P. putida</i> (2) Decreased the number of potential target sites due to the relatively larger PAM in compared with the needed PAM of SpCas9 (5'-NGG-3')	-	<i>pyrF</i> (702 bp) 50 %	~ 3–4 days	Mougiakos et al. (2017)
<b>SpCas9-crRNA-tracrRNA and Ssr ssDNA recombinase (Three-plasmid system)</b>	(1) Deletion of <i>pyrF</i> , <i>endA-1</i> and <i>flgM</i> genes (2) Multiplex deletion of <i>endA-1</i> and <i>flgM</i> genes (3) Deletion fragments in the <i>flgM</i> gene with different DNA lengths (4) Point mutations in the <i>pyrF</i> gene	(1) Low efficiency for multiplex gene deletions (2) Low efficiencies when the deleted fragment is larger than 5 kb (3) Nucleotide changes recognized by the MMR or located in any position within the spacer sequence except in the first two bases, will not be implemented. (4) Plasmid curing	-	(1) 50–80 % for single deletions (2) 3 % for multiplex deletions (3) 51 % (Deletion length 1.9kb) 13 % (Deletion length 4.9 kb) 1 % (Deletion length 69.1 kb) (4) 97 % (nt change is not recognized my MMR and it is located 2nt away from the PAM	~ 4–5 days	Aparicio et al. (2018)
<b>SpCas9-sgRNA and dsDNA Redβ recombinase (Three-plasmid system)</b>	Deletion of <i>IvaA</i> , <i>pvdJ</i> , <i>fpvA</i> and <i>gcvP-1</i> genes	Plasmid curing	-	<i>IvaA</i> (1032 bp) 90 % <i>pvdJ</i> (1848 bp) 100 % <i>fpvA</i> (2391 bp) 96.7 % <i>gcvP-1</i> (2844 bp) 87 %	~ 4 days	Cook et al. (2018)
<b>SpCas9-sgRNA and dsDNA Redβ recombinase (Two-plasmid system)</b> <b>Fncas12a-crRNA and dsDNA Redβ recombinase (Two-plasmid system)</b>	(1) Deletion of 8 genes ( <i>nicC</i> , PP_0552, PP_3361, PP_3733, PP_3889, PP_3846, PP_1706 and PP_5301) and 2 DNA fragments (PP_3947-PP_3948 and PP_3939-PP_3940) with SpCas9 (2) Replacement/Insertion of <i>rhlA</i> , <i>dCas9</i> and <i>T7-RNA polymerase</i> genes (3) Single nucleotide substitutions in the <i>nicC</i> gene (4) Deletion of 2 genes (PP_3361, PP_5301) with Cas12a	Multiplex gene deletions was not possible	-	(1) 80–100 % for deletions shorter than 3 kb (2) 85–100 % for deletions larger than 3 kb (3) 70 % Insertion length of 4.5 kb 100 % Insertion length of 4.1 kb 95 % Insertion length of 0.8 kb (4) 100 % for gene substitutions	~ 5 days including plasmid curing	Sun et al. (2018a)
<b>ratAPOBEC1-Cas9n (One-plasmid system)</b>	Cytidine mutations within <i>cadR</i> and <i>ompR</i> genes		-	90–100 %	~ 2 days	Chen et al. (2018a)
<b>ratAPOBEC1-Cas9n (One-plasmid and two-plasmid systems)</b>	(1) Cytidine mutations within <i>hmgA</i> , <i>pobA</i> , <i>quiC</i> and <i>ttaA</i> genes (2) Multiplex base editing:  – Double loci: <i>pobA</i> and <i>quiC</i> – Triple loci: <i>pobA</i> , <i>quiC</i> and <i>TrpE</i>		Enhancing the protocatechuic acid production	(1) 80–100 % (2) Double loci: 80–100 % Triple loci: 25–35 %	~ 2 days	Sun et al. (2020)
<b>SpCas9n-sgRNA and dsDNA Redβ recombinase (One-plasmid system)</b>	(1) Deletion of 5 individual genes: <i>icd</i> , <i>tesA</i> , <i>tesB</i> , <i>ferR</i> and <i>tesBII</i> (2) Deletion of several fragments: <i>vanAB</i> & <i>fcs-ech-vdh</i> (3) Multiplex deletions: <i>testB</i> & <i>testBII</i> (4) Replacements of 2 genes:  – <i>pyrF</i> substituted by <i>Cas9n</i> & <i>gam-bet-exo</i> genes – <i>ferR</i> substituted by <i>fcs-ech-vdh</i>  (5) Insertion of individual genes/ fragments: mutated <i>phaC1</i> , <i>vanAB</i> , <i>fcs-ech-vdh</i> , two copies of <i>fcs-ech-vdh</i> & pPROBE-GT DNA sequence (15 kb)	The constitutive expression of Cas9n	Enhancing the <i>mcl</i> -PHA production using ferulic acid as substrate	100 %	~ 4 days	Zhou et al. (2020)

(continued on next page)

Table 7 (continued)

Tool	Purpose	Limitations	Applications	Efficiency	Time spent	References
	(6) Multiplex insertions: <i>fcs-ech-vdh</i> & <i>vanAB</i>					
	(7) Multiplex deletions and insertions					
	- <i>phaZ</i> was deleted and <i>phaC1</i> inserted					
	- <i>ferR</i> was deleted and <i>fcs-ech-vdh</i> together with <i>vanAB</i> inserted					
	- <i>ferR</i> was deleted and <i>fcs-ech-vdh</i> together with two copies of <i>vanAB</i> inserted					
INTEGRATE	Disruption of <i>nirC</i> , <i>nirD</i> , <i>bdhA</i> and <i>PP_3889</i> genes	Plasmid curing	–	–	~ 2 days	Vo et al. (2020)

recombinase to create the desired mutations, here, after the DSB, a linear DNA fragment was created and used by the  $\lambda$  Red recombinase to boost recombination efficiencies. Four genes between 1 and 8 kb were deleted with efficiencies ranging from 85 to 100 %. Per contra, when the suicide vector and the plasmid carrying the sgRNA were electroporated together, the knock-out efficiencies dramatically dropped to less than 10 % (Cook et al., 2018).

Expectedly, Cas12a was further proven an efficient genome editing tool in *P. putida*. The functionality of the staggered cutting style of FnCas12a (from *Francisella novicida*) was preliminary demonstrated by deleting two genes with 100 % efficiency with assistance of the  $\lambda$  Red recombinase (Sun et al., 2018a). It is, however, important to take into account that the required AT-rich (5'-TTN-3') PAM for FnCas12a is less abundant in the GC-rich genome of *P. putida* than the 5'-NGG-3' of SpCas9. In contrast with the previous studies, the employed two-plasmid strategy additionally incorporated novel features to speed up the plasmid-curing process. To such end, a self-curing plasmid was designed, incorporating the *SacB* gene, but also, conditionally expressing a sgRNA (RhaRS/PrhaB) directed to the origin of replication of the additional plasmid. Therefore, induction with sucrose and L-rhamnose forced the cell to lose both plasmids. In this study, the high efficiency of the system was also demonstrated with SpCas9 generating short and large deletions, single-nucleotide mutations and for the first time, gene insertions up to 4.5 kb (Sun et al., 2018a).

An alternative purpose of CRISPR as counter-selection tool for recombineering-mediated base editing is the use of base editors fused to a Cas9 nickase or dead Cas9 (dCas9). The nickase variant of Cas9 has been developed by mutating only the RuvC (D10A) or HNH (H840A or N863A) nuclease domain (Rees and Liu, 2018). Each individual silent mutation inactivates the endonuclease activity of the corresponding previously mentioned domain while retaining the DNA binding specificity, generating the Cas9n (D10A) or the CasH840A (H840A), both causing single-stranded DNA breaks (SSB) (Ran et al., 2013). When the mutations are present in both domains, the dCas9 is catalytically inactive (see Section 3.5.2 CRISPR for transcriptional regulation section). Two types of base editors have been developed: cytosine base editors (CBEs) and adenine base editors (ABEs), both catalyzing deamination reactions. CBEs convert cytosine into uridine (read as thymidine by the polymerase), whereas ABEs convert adenosine into inosine (read as guanine by the polymerase). Collectively, four different DNA alterations are possible: C to T, A to G, G to A and T to C. In bacteria, in which NHEJ repair mechanisms for DSB are typically absent, base editors coupled to a Cas9 nickase or dCas9 catalyze specific nucleotide mutations within the ssDNA editable window without the need of homologous recombination system nor a repair template, rendering a useful tool by circumventing DSB lethality (Standage-Beier et al., 2015; Zhang et al., 2020b; Zheng et al., 2018). In this regard, Chen et al., 2018a used the cytosine deaminase (ratAPOBEC1) fused to the N terminus of the Cas9n together with the sgRNA, editing cytosine bases in *P. putida*. All the C(s) at positions 3–8 (counting the PAM as positions 21–23) were efficiently

mutated to T(s). Specifically, the tool was proven 90–100 % efficient for the introduction of stop codons in the *cadR* and *ompR* gene coding sequences of *P. putida* KT2440. Additionally, the *sacB* gene was incorporated in the plasmid as a fast curing approach (Chen et al. (2018a)). Recently, Sun et al. (2020) developed an efficient multiplex base editing system in *P. putida* by using the uracil DNA glycosylase inhibitor and by engineering both the ratAPOBEC1 domain and the PAM specificity of the Cas9n. As result, the base editing efficiency on single genes was increased from 40–60 % to 80–100 %, the editable window was significantly narrowed and the PAM specificity was modified from 5'-NGG-3' to 5'-NG-3', increasing the number of target sites. Moreover, the system was used to multiplex editing two genes *pobA* and *quiC* with an efficiency of 90–100 % and three genes *pobA*, *quiC* and *TrpE* with 25–35 % efficiency. Ultimately, the production of protocatechuic acid was improved, demonstrating the utility of the tool with metabolic purposes (Sun et al., 2020).

In the Section 3.3 Recombineering or the previously mentioned work of Aparicio et al. (2018), single-nucleotide substitutions are also achieved via recombineering alone or in combination with CRISPR, instead of using base-editors. In spite of the high efficiency of the base-editors accomplished in a short period of ~2 days, some factors to consider are (i) the inability to make some nucleotide substitutions, limited by the mechanism of action of the available base-editors, (ii) the absence of a PAM in the desired locus and, (iii) the lack of discrimination between the bases that can potentially be used as substrate by the base-editor within the editing window (Rees and Liu, 2018).

The most recent publication uses Cas9n to edit the genome of *P. putida* and overcomes limitations from the above-mentioned publications (Zhou et al., 2020). Zhou et al. (2020) designed a strategy, in which a module comprised of the Cas9n and the  $\lambda$  Red recombineering system under the control of a constitutive minimum promoter (Pmin) and the inducible xylose promoter (Pxy1A), respectively, was initially integrated in genome of *P. putida*, replacing the *pyrF* gene. In that way, only one plasmid was necessary to edit *P. putida*'s genome with unprecedented efficiency levels (100 %). This plasmid had 5 crucial elements: (i) the *pyrF* gene between the upstream and downstream homologous regions of the target site, (ii) the *gfp* gene under control of the P<sub>lac</sub> promoter, (iii) the sgRNA together with a spacer directed to the target site, expressed from the P<sub>trc</sub> promoter, (iv) a palindromic sequence and, (v) the sgRNA under the control of P<sub>van</sub> promoter, targeting the palindromic sequence. Consequently, once the *pyrF* gene was integrated in the genome of *P. putida*, the second sgRNA was induced for self-curing of the plasmid, which was easily screenable due to the loss of GFP signal. The *pyrF* gene was next deleted, therefore used as selection and counter-selection marker. In this way, continual rounds of genome editing were possible as well as impressive efficiencies for single and multiplex gene deletions, insertions and replacements, highlighting the editing of large DNA fragments (> 5 kb). Furthermore, for the first time, Zhou et al. (2020) used their developed Cas9n tool, for a metabolic engineering application, going beyond the proof of concept. Multiple

editing rounds of *P. putida* KT2440 enhanced production of medium-chain length polyhydroxyalcanoates (mcl-PHA) using ferulic acid as carbon source (Zhou et al., 2020).

Recently, two novel CRISPR-associated transposons have been characterized from two different organisms, *Scytonema hofmanni* and *Vibrio cholerae*, expanding the possibilities of genome engineering for prokaryotes and eukaryotes. They consist of Tn7-like transposases subunits, and nuclease-deficient type V-K and type I-F CRISPR-Cas systems, respectively (Klompe et al., 2019; Strecker et al., 2019). The Tn7-like transposons are guided by the crRNA to the target site, where the transposon cargo is integrated. In particular, the insertion and transposable elements of the Tn7-like transposon from *Vibrio cholerae* have been optimized and applied as a genome editing tool, called INTEGRATE, in various bacteria, including *P. putida*. One-plasmid system, in which all the different elements (*tniQ-cas8-cas7-cas6* operon, *tnsA-tnsB-tnsC* operon and the donor DNA) are under the control of the J23119 constitutive promoter, was transformed in *P. putida* and efficiently targeted *nirC*, *nirD*, *bdhA* and *PP\_3889* genes, flanked by a 5'-CC'-3' PAM (Vo et al., 2020). This new CRISPR technology opens new possibilities for genome engineering without the need of homologous recombination, selectable markers or transposon attachment sites, such as the *attTn7*.

In conclusion, the CRISPR technology alone or in combination with ss- or ds-DNA recombineering systems is currently the most efficient and high throughput tool for genome editing of *P. putida*. Probably, almost any type of CRISPR-Cas system can be easily deployed in this bacterium. The current limiting factor is the presence of the PAM near the target site, though, the SpCas9 relies on the simple PAM 5'-NGG-3', highly abundant in the GC rich *P. putida* genome. Besides, Cas9 orthologs with more flexible PAMs have been described (Hu et al., 2018; Nishimasu et al., 2018; Walton et al., 2020). However, the greatest limitation is the multiplex editing efficiencies of this organism. Considering that the maximum multiplexed edited genes achieved in *P. putida* is currently three, we are far from the numbers achieved in *E. coli* (4 deletions and 3 insertions) (Ao et al., 2018; Feng et al., 2018), and *S. cerevisiae* (6 deletions) (Zhang et al., 2019).

Challenges related to high efficiencies of multiplexing CRISPR/Recombineering systems can be due to: (i) the efficiency of the guide RNA, (ii) the recombineering efficiency, (iii) the editing conditions, such as the status of the cells and, (iv) the plasmid design in combination with the regulatory elements controlling the CRISPR and recombineering components. Besides, the potential of CRISPR-Cas technology goes beyond tool development as a proof of concept and applications need to be further implemented in *P. putida*, such as construction of genetic circuits to control cellular behavior or phenotype (sugar utilization, phage resistance, chemotaxis) (Nielsen and Voigt, 2014) as well as metabolic engineering strategies to increase yield and productivity of a target compound.

### 3.5.2. CRISPR for transcriptional regulation

Besides the Cas9 genome editing methods, another CRISPR method based on the dCas9, called CRISPR interference (CRISPRi), has been employed for regulating gene expression in *P. putida* (Table 8) (Qi et al., 2013). The dCas9 can be simply directed to the promoter region of a gene of interest in order to block the RNA polymerase from transcribing it (Fig. 3). In this way, CRISPRi enables targeted gene repression in a short period and with minimal effort, as it requires only an available PAM and the assembly of the corresponding gRNA in the target plasmid. Repression levels can be fine-tuned by either placing the gRNA in different positions of the target gene (Bikard et al., 2013) or by controlling the expression of dCas9 or gRNA with an inducible promoter. Specifically, when dCas9 binds to the promoter region, the downregulation is the most effective and is gradually decreased by changing its position into the coding sequence (Qi et al., 2013; Tan et al., 2018). Additionally, within the coding sequence, targeting the non-template DNA strand, specifically close to the ATG, is responsible for high repression levels, while targeting the template DNA strand is proven to be less effective (Larson et al., 2013). Of particular interest is the effectiveness of CRISPRi when targeting essential genes, which is not possible with traditional deletion strategies. Unlike deletion strategies, CRISPRi enables temporary and partial depletion of the gene expression

**Table 8**  
Regulation tools applied in *P. putida*.

Tool	Purpose	Regulation mode	Limitations	Advantages	Efficiency	Max targets
<b>Transcriptional regulation</b>						
Tan et al. (2018)	(1) Downregulation of <i>pvdH</i> , <i>ftsZ</i> (2) Multiplex downregulation of <i>pvdH</i> , <i>flgB</i>	(1) Ptrc-SpasdCas9 (2) Ptet-sgRNA	(1) Leakiness up to 50 % (2) Specific PAM requirements	Easy cloning	90–300 fold	2
Sun et al. (2018a)	Downregulation of plasmid encoded <i>egfp</i>	(1) Native constitutive promoter-SpdCas9 (2) RhaRS/PrhaB -sgRNA	(1) Low transformation efficiency	Easy cloning	75 %	1
Kim et al. (2019)	Downregulation of plasmid encoded <i>gfp</i> and GlpR regulator	(1) RhaRS/PrhaB-SpdCas9 (2) J23119-sgRNA		(1) Low leakiness (2) Easy cloning	11-fold	1
Batianis et al. (2020)	(1) Downregulation of chromosomal expressed <i>msgfp</i> , <i>pyrF</i> , <i>ftsZ</i> (2) Multiplex downregulation of chromosomal expressed <i>yfp</i> , <i>mCherry</i> , <i>ftsZ</i>	(1) XylS/Pm-SpdCas9 (2) PEM7-sgRNA or native constitutive promoter-crRNA	(1) Decreased growth rates from the GC-rich SpdCas9	(1) Tunable repression (up to 5 levels) (2) Low leakiness (3) Easy cloning	55–88 %	3
Banerjee et al. (2020)	Multiplex downregulation of 14 genes	(1) lacUV5- FndCas12a (2) tRNA ligase promoter/terminator-gRNA	Unequal downregulation levels per target gene	(1) Short repetitive crRNA sequences	50 %	9
<b>Post-transcriptional regulation</b>						
Apura et al. (2020)	(1) Downregulation of chromosomal expressed <i>acnB</i> , <i>sdh</i> , <i>gfp</i> , <i>yfp</i> (2) Upregulation of chromosomal expressed <i>gfp</i>	XylS/Pm-sRNA	Undefined design principles	(1) No heterologous protein expression (2) Modular regulation (down- or upregulation)	20–40 % down-regulation 35–40 % up-regulation	1
<b>Post-translational regulation</b>						
Volke et al. (2020b)	Minimize the basal expression of Xyls/Pm	XylS/Pm-NIa protease	Individual gene engineering	ND	ND	1

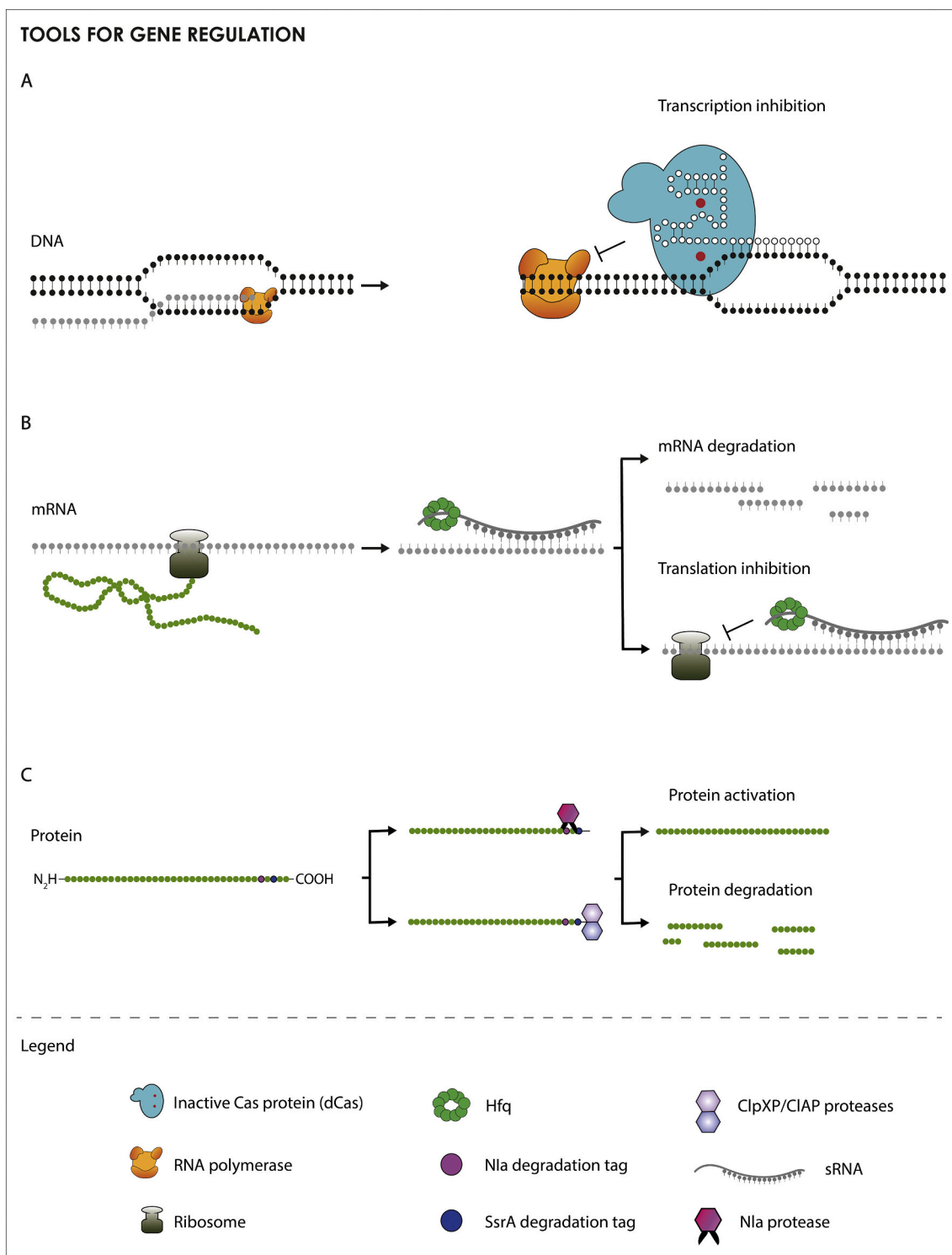


**Fig. 3.** Tools for gene regulation in *P. putida*. A) Dead Cas9 (dCas9) and sgRNA, directed by the spacer, bind to the target, without inducing DSB. The presence of the dCas9 in the promoter region or the beginning of the gene, blocks the DNA polymerase to transcribe the target gene, resulting in transcription inhibition and therefore, gene downregulation. B) sRNAs. The sRNAs are complementary to regions of the mRNA. When dsRNA molecules are created two possible effects can occur: post-transcription inhibition by blocking the ribosome to translate the mRNA into proteins or mRNA degradation induced by the cell machinery. C) Protein sequence with Nla and SsrA degradation tags. In presence of degradation tags, the protein is cleaved. In presence of ClpXP/CIAP proteases, the degradation tag is removed, resulting in protein activation.

allowing downregulation of essential loci without being lethal to the host. Especially important are the inducible CRISPRi systems because they offer the possibility of controlling the repression timing, crucial for modulating the central metabolism to increase fluxes towards a target compound or to uncouple growth from production. Another notable

feature of this method is that multiple genes can be simultaneously repressed by co-expressing several gRNAs at the same time (Hawkins et al., 2015). Given all these features, CRISPRi has been exploited as a powerful tool for metabolic engineering approaches or high-throughput gene characterization studies.

In *P. putida*, the first CRISPRi tool was presented by Tan et al. (2018). They developed a one-plasmid CRISPRi system based on the type II dCas9 homologue of *Streptococcus pasteurianus*. In this study, the *S. pasteurianus* dCas9 gene was integrated into the genomic attTn7 site of *P. putida*, while the sgRNA was placed in a broad-host range pBBR1 plasmid. To enable dynamic regulation, the expression of dCas9 and sgRNA was controlled by the LacI/Ptac expression system and the constitutive Ptet promoter, respectively. At first, they repressed the *ftsZ* gene, essential for cell division, and the *pvdH* gene, which is involved in the production of the fluorescent siderophore pyoverdine. The system functioned effectively, resulting either in filamentous cell morphology instead of the WT rod-shape or in 300-fold reduced pyoverdine fluorescence compared to the non-induced conditions. However, in the case of *pvdH*, ~50 % repression was observed in the absence of inducers indicating leaky expression of the dCas9 from the Ptac promoter. The ability of dCas9 to interfere with multiple genes simultaneously was demonstrated by repressing both, the *flgB* (encodes the flagellar basal body rod protein) and the *pvdH* genes. Cells harboring the double *flgB-pvdH* sgRNAs exhibited reduced swimming radius on soft agar plates and 90-fold reduction in pyoverdine fluorescence levels compared to the non-induced cells. This contrasts with the 300-fold reduction detected in the single repression of *pvdH* indicating the reduced efficiency of multiplexing. Moreover, even though tunable repression was achieved as a function of the inducer concentration (IPTG) in *Pseudomonas aeruginosa*, this was not tested in *P. putida*. At last, it is important to note that the *S. pasteurianus* dCas9 requires highly specific PAM sequences (5'-NNGTGA-3' or 5'-NNGCGA-3') which are considerably less abundant in the genome of *P. putida* compared with the simpler PAM motif 5'-NGG-3' of the commonly used SpCas9.

This system was rapidly followed by another one-plasmid CRISPRi tool developed by Sun et al., 2018a. This time the standard SpdCas9 was utilized under the control of its native Sp promoter, while the sgRNA was placed under the inducible control of the PrhaB promoter. The system was simply tested against a plasmid-encoded eGFP protein resulting in ~75 % repression of fluorescence levels. However, this study lacked any further characterization or applications of the system.

Recently, Kim et al. (2019) applied CRISPRi for metabolic engineering in *P. putida*. Using a one-plasmid system, in which the SpdCas9 was tightly expressed by the inducible PrhaB promoter and the sgRNA by the constitutive BBa\_J23119 promoter, they repressed the GlpR regulator to increase the glycerol-dependent production of mevalonate. This regulator is known to repress the expression of two enzymes (GlpK and GlpD), responsible for the utilization of glycerol in *P. putida* KT2440 (Nikel et al., 2015). It was shown that the repression of the GlpR regulator resulted in a significantly reduced lag-phase and therefore in 1.9-fold higher biomass and 3.3-fold increased mevalonate production. In addition, to quantify the repression levels of their system, a plasmid-encoded GFP was targeted showing an 11-fold reduction in fluorescence levels.

Although these systems showed high repression levels against target genes, they are all afflicted by either leaky expression or the inability to fine-tune repression. Therefore, these bottlenecks may hinder their potential in advanced engineering approaches. To achieve a more robust CRISPRi tool, Batianis et al. (2020), presented two new variants of a one-plasmid CRISPRi system (either sgRNA-based or crRNA-based). Their system relied on the inducible expression of the SpdCas9 via the XylS/Pm expression system which proved to be the most efficient compared to two other promoters (ChnR/PchnB, CprK1/PDB3). At first, the performance of the sgRNA-based plasmid was tested against a chromosomally expressed *msgfp* and the native *ftsZ* gene. By using different concentrations of 3MB (0, 0.01, 0.1, 0.5 and 1 mM), the *msgfp* fluorescence was decreased up to 15 % (leakiness), 55 %, 63 %, 66 % and 88 %, highlighting the tunable activity of the system. In the case of the *ftsZ* gene, the low CRISPRi leakiness did not result in visible filaments indicating the tight control of the dCas9. Next, three chromosomal targets (*yfp*, *mCherry*, *ftsZ*) were simultaneously repressed with both the sgRNA- and

crRNA-based plasmids. It was shown that both plasmids performed similarly against the chosen targets resulting in synthetic filamentation and decreased fluorescence intensities of 55–65 % for mCherry and 55–60 % for yellow fluorescent protein (YFP). Another notable finding of this study was that downregulation of essential genes is more efficient in a *P. putida* strain lacking the main component of the homologous recombination machinery, RecA. By downregulating the essential *pyrF* gene, in both the WT and RecA- strains, growth was arrested for 10h and 20h, respectively. It was hypothesized that this phenomenon is due to the increased genetic stability of the CRISPRi system under stressful conditions (such as depletion of essential genes) in strains with reduced ability of homologous recombination.

Recently, a newly developed CRISPRi system has been used to optimize the production of indigoidine in *P. putida* (Banerjee et al., 2020). This system was specifically designed for efficient simultaneous repression of multiple genes. The greatest challenge of the multiplex CRISPRi is the instability of the crRNA caused by the repeated sequences. Taking this into account, they used the endonuclease deficient Fncas12a (FndCas12a) since its crRNA is 19 bp long compared to the 76 bp of the Cas9. The FndCas12a was expressed from the placUV5 promoter, while each crRNA was under the control of different *P. putida* tRNA ligase promoter/terminator pairs. After some computational predictions for increase the growth coupled production of indigoidine, 14 genes were simultaneously targeted. The efficiency of the multiplex downregulation was evaluated by RNAseq showing that 9 out of the 14 genes had decreased mRNA levels with a 50 % reduction at best. These modest reduction levels of the multiplex CRISPRi are consistent with the efficiencies presented by Tan et al. (2018) and Batianis et al. (2020). Nevertheless, the engineered strain carrying the multiplex CRISPRi plasmid had 2.5- and 28-fold improved titers of indigoidine when grown in glucose and galactose, respectively.

This system is a significant advancement of the CRISPRi technology, regardless the target host, as so far only a few studies have shown the applicability of such long gRNA arrays in metabolic engineering.

### 3.6. sRNAs for post-transcriptional regulation

Small RNAs (sRNAs) are regulatory RNAs of about 40–500 nucleotides that bind to mRNAs and are involved in post-transcriptional regulation in response to stress conditions, in biofilm formation or virulence (Waters and Storz, 2009). They can down-regulate or even up-regulate the expression of the targeted genes, by interfering with their mRNA stability and/or translation. In bacteria, they are classified as cis-encoded sRNAs and the extensively applied trans-encoded sRNAs (Vazquez-Anderson and Contreras, 2013; Villa et al., 2018). Cis-encoded sRNAs, such as the sRNA-responsive toehold switches, are based on base pairing to fully complementary regions in the RNA transcript of the regulated gene. The trans-encoded sRNAs, are typically 50 – 400 nucleotide long and present imperfect complementarity to their target mRNAs. They frequently bind with global RNA chaperones, such as Hfq, for their annealing and stability to the target mRNA. Typically, the trans-encoded sRNAs bind to the RBS to constrain translation initiation or to trigger mRNA degradation. Otherwise, sRNAs may prompt translation or prevent mRNA degradation by base pairing to the 5' or 3' untranslated region resulting in gene upregulation (Storz et al., 2011; Updegrove et al., 2016; Waters and Storz, 2009).

sRNAs-based tools are widely applied in synthetic biology and metabolic engineering as they do not require additional heterologous proteins to function (Gottesman, 2004). In this way, and in contrast with other gene regulators (e.g. dCas9), any metabolic burden to the host cell is limited (Gaida et al., 2013). Moreover, due to its trans-acting modular base-pair complementation, tunable regulation and interference with multiple genes simultaneously is possible (Copeland et al., 2014). Also, similarly with the CRISPRi technologies, sRNAs enable the depletion of essential genes where deletion strategies are lethal.

Although sRNAs-based strategies have been employed extensively in

several non-model bacterial chassis (Chaudhary et al., 2015; Liu et al., 2014; Sun et al., 2018b), only two studies have been currently presented in *P. putida* (Table 8). The first sRNA-based genetic device was presented by (Calles et al., 2019). The authors developed a genetic circuit for minimizing the basal expression of strong inducible promoters in the absence of inducer. A key part of this genetic circuit is a *cis*-encoded sRNA composed by the target-binding sequence ('seed sequence') and the *E. coli* scaffold sequence, MicC. MicC recruits the host's RNA chaperone Hfq, known to facilitate the binding of the 'seed sequence' with target mRNA resulting in mRNA degradation (Na et al., 2013).

Although it was proven that *cis*-repressing sRNAs are functional in *P. putida*, indicating the ability of the MicC scaffold to interact with the native *P. putida* Hfq, no additional technical details (e.g. repression levels, tunability) were provided.

Recently, the first sRNA tool for *a la carte* targeted gene down- or upregulation was developed by Apura et al. (2020). This tool relies on the inducible expression of a small target specific sRNA "seed sequence" (20–30 nt) along with the MicC scaffold followed by a transcription terminator. The expression of both elements was driven by the XylS/Pm expression system. After experimentally proving that the *P. putida* Hfq was able to recognize and bind with the *E. coli* MicC scaffold, the system was utilized to downregulate the expression of four chromosomal expressed genes (*acnB*, *sdhB*, *gfp*, *yfp*). "Seed sequences" complementary to the *acnB* (targeting the RBS and the start codon) and *sdhB* (targeting the coding sequence) mRNAs were designed and introduced upstream of the MicC scaffold. After induction with 3MB, the activity of the aconitase and succinate dehydrogenase decreased by ~40 % and ~20 %, respectively, compared to the control. In addition, it is noteworthy that they managed to up-regulate the expression of target genes by simply changing the seed complementary to a different position of the target mRNA. "Seed sequences" complementary to the 3'-end or an internal region of the *gfp* transcript increased by 40 % and 35 % the GFP fluorescence, respectively. With these results they proved the modular function of this sRNA-based gene regulator to either down- or upregulate target genes in *P. putida*. However, due to the mechanistic and structural complexity of sRNAs, it was not possible to determine design principles for optimal "seed sequences". Thus, the researchers had to test various interaction regions to achieve the desired output.

### 3.7. Post-translational regulation

The simplest approach for controlling the activity of a protein is to regulate its concentration by changing the rate of transcription or translation as described above. However, post-translational regulation can make the cellular processes even more predictable by reducing the impact of gene expression noise (Acar et al., 2010; Ghim and Almaas, 2008). In general, interfering at the post-translational level directly controls the protein concentration but is more energy demanding as the protein is produced only to be degraded (Tan and Prather, 2017). Several methods have been developed to control the abundance of proteins at post-translational level into bacteria. Often, these methods rely on the insertion of a signal peptide in the sequence of the protein of interest and the inducible expression of the corresponding degradation machinery.

The only post-translational synthetic tool for regulation of protein levels in *P. putida* is the FENIX system (Table 8). FENIX was initially developed in *E. coli* (Durante-Rodríguez et al., 2018) and later applied in *P. putida* (Volke et al., 2020b). This system employs a double protease mechanism for the post-translational activation of protein function. The protein of interest is engineered to carry the N1a and SsrA protein degradation tags at the C terminus (Fig. 3). As a result, the endogenous ClpXP and ClpAP proteases recognize the SsrA tag and constitutively degrade the protein, while after induction of the heterologous N1a gene, the SsrA tag is cleaved allowing the accumulation of the target protein (Fig. 3). Within *E. coli*, FENIX was used to increase the production of poly-3-hydroxybutyrate by de-coupling production from growth

(Durante-Rodríguez et al., 2018) whereas in *P. putida* it was employed to minimize the basal expression of target proteins from the strong Pm promoter (see Section 2.2.2 Inducible promoters). To such end, the heterologous module comprised by the *xylS* gene under the control of its native promoter and the *nia* protease encoding gene under the control of the XylS/Pm expression system, were integrated into the *attTn7* site in the genome of *P. putida*. Additionally, the hybrid N1a/SsrA proteolytic tag was added at the C-terminal of the GOI, which in turn is expressed from the Pm promoter in replicative vectors. Consequently, upon the addition of 3-methylbenzoate (3-MB), the GOI with the hybrid tag as well as the N1a protease are induced. Thus, only when the simultaneous expression of both genes surpassed a threshold, the N1a protease relieved the degradation SsrA tag, followed by a stable production of the target gene (Volke et al., 2020b).

## 4. *In silico* metabolic models and databases

Advancements in DNA sequencing, and therefore the identification of enzymes associated with their corresponding reactions, have facilitated the evolution of *in silico* metabolic networks. Metabolism can be defined as the entire reaction set which occurs in cells in order to maintain life (Stephanopoulos et al., 1998). Thus, the correspondence between enzymes and reactions can be used for the reconstruction of a network resulting in a metabolic model. Of the many available class of metabolic models, the constraint-based genome-scale metabolic models (GEMs) and the kinetic metabolic models are the most widely applied in metabolic engineering. A GEM consists of a stoichiometric reconstruction of all reactions retrieved from an organism's genome annotation and literature, along with an accompanying set of constraints on the fluxes of each reaction in the system. This class of models can be employed to better understand, describe and predict biological phenomena as well as for computer-assisted metabolic engineering. Furthermore, they can be used in combination with computational strain optimization methods (CSOMs) to solve a practical problem (or set of problems) relevant to strain design. Powered by phenotype prediction methods such as flux balance analysis (FBA) (Burgard et al., 2003; Orth et al., 2010; Varma and Palsson, 1994), the CSOMs can automatically search for answers in particular metabolic questions such as: (i) which reactions should be removed from the model to couple the production of specific compound to growth or, (ii) which heterologous reactions could be added to achieve a desirable functionality in a given host. The most common tasks for these methods are gene deletion, gene over expression, heterologous insertion, and, more recently, cofactor specificity swapping (Maia et al., 2016). However, GEMs are unable to describe regulation at the enzymatic and post-translational level as they incorporate only stoichiometric constraints (Miskovic et al., 2015). This limitation can be overcome by integrating kinetic information resulting in a new class of metabolic models: the kinetic metabolic models. Kinetic models are based on information of the enzyme mechanisms and can describe changes on metabolites concentration over time. To such end, they comprise values for metabolite concentrations, reaction rate equations and kinetic parameters. This kind of modelling is often applied to simulate small-scale metabolic pathways such as the tricarboxylic acid (TCA) cycle of glycolysis. Dynamic representations of large-scale systems are also possible; however, their construction remains challenging due to the lack of experimental kinetic information to build proper reaction rate equations.

### 4.1. Constraint-based metabolic models

So far, seven *P. putida* KT2440 GEMs have been developed aiming to further understand and ultimately re-wire the strain's metabolism (Table 9). In 2008, Puchalka et al. (2008) reconstructed and manually curated a (at the time) complete GEM on the basis of annotated genome sequence, information from biochemical databases and literature data. The model (iJP815) consisted of 815 gene products, 824 intracellular

Table 9

Comparison of the different GEMs available for *P. putida*.

Model	Genes	Reactions	Metabolites	Carbons supporting growth	Growth rate accuracy	Gene essentiality accuracy
iJN746	746 (14 %)	950	911	61 <sup>b</sup>	73 % <sup>a</sup>	57 % <sup>b</sup>
iJP815	815 (15 %)	877	888	41 <sup>b</sup>	92 % <sup>a</sup>	64 %
PpuMBEL1071	900 (16 %)	1071	1044	ND	51 % <sup>a</sup>	ND
iJP962	962 (17 %)	1070	992	43 <sup>b</sup>	82 % <sup>a</sup>	69 %
iJP962 <sup>extended</sup>	1050 (19 %)	1256	1122	51 <sup>b</sup>	62 % <sup>b</sup>	65 % <sup>b</sup>
PpuQY1140	1140 (21 %)	1171	1104	63 <sup>b</sup>	91 %	63 % <sup>b</sup>
iJN1462	1462 (27 %)	2929	2155	226	91 %	85 %

ND (Not defined).

<sup>a</sup> As summarized by Yuan et al. (2017).<sup>b</sup> As summarized by Nogales et al. (2020).

and 62 extracellular metabolites connected by 877 reactions. It was experimentally validated with data from continuous cell cultures, high-throughput phenotyping (BIOLOG) data, <sup>13</sup>C-measurement of internal flux distributions, and specifically generated knock-out mutants. Among other, the model predicted auxotrophies, which were correctly in 75 % of the cases and was used to explore the metabolic potential of *P. putida*. Moreover, systematic analyses revealed that the metabolic network structure is the main factor determining the accuracy of predictions, whereas biomass composition has negligible influence. Additionally, the model was used in combination with and OptKnock strategy (Burgard et al., 2003) to predict deletion strategies for increasing the availability of acetyl-CoA and therefore the production of PHAs. A double-mutant lacking the 6-phosphogluconolactonase (PGL) and periplasmic glucose dehydrogenase (GCD) was predicted to produce 29 % more acetyl-CoA than the wild type growing on glucose as a carbon source.

The model iJN746, by Nogales et al. (2008) was built in a similar manner. The model contains 746 genes, 950 reactions, and 911 metabolites including biodegradation reactions of aromatic compounds and PHA metabolism. Its predictive ability was assessed by comparison with experimental data, such as growth rates on glucose and gene essentiality (Nogales et al., 2020. Note: as there was no experimental gene essentiality study at that time, the authors used a study carried out in *P. aeruginosa* as a proxy). In addition, using FBA, the production efficiency of PHAs from different carbon sources was evaluated, showing fatty acids as the most prominent substrate. This model has been utilised in several metabolic studies mainly to provide information about metabolism or to describe metabolic flux distributions (Fig. 4).

Another reconstruction, PpuMBEL1071, built by Sohn et al. (2010) quickly followed these models. In contrast with the two previous GEMs, in which the biomass equation was acquired from *E. coli* models, the researchers experimentally determined the biomass composition and the maintenance energy of *P. putida* to create a new strain-specific biomass equation. After validating the model using experimental data, *in silico* metabolic analysis was performed to elucidate the capability of *P. putida* to produce PHA as well as to degrade various aromatic compounds. Finally, the model was utilised to develop a strategy to enhance the survival rate under anaerobic conditions. The predictions resulted in several conclusions such as the expression of the oxygen-independent ATP-forming reaction acetate kinase (AckA).

Noteworthy, 3 years later, a model-driven metabolic engineering application using both iJP815 and PpuMBEL1071 models was presented by Poblete-Castro et al. (2013). In combination with the FluxDesign CSOM, they identified candidate gene deletions which increase the synthesis of PHAs in *P. putida* grown on glucose. In agreement with Puchalka et al. (2008), the deletion of the glucose dehydrogenase (encoded by *gcd*) was also predicted as the target with the highest potential for increasing PHA synthesis. Following this prediction, they managed to increase the PHA content by 60 % in shake flask and 100 % in bioreactors compared to parental strain. The great performance of the engineered strain highlights the potential of model-driven strategies for metabolic engineering.

A fourth GEM, iJP962 (Oberhardt et al., 2011), along with the

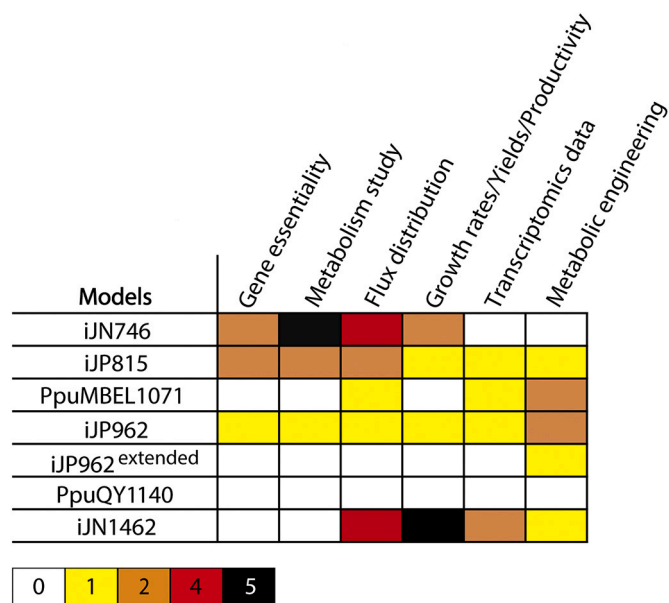


Fig. 4. Heat map of studies that have employed the *P. putida* GEMs. Colours in the heat map indicate the number of studies. References for each model in the figure are as follows: iJN746 (Chavarría et al., 2012; Escapa et al., 2012; Finley et al., 2010; Koehorst et al., 2016; Kruyer and Peralta-Yahya, 2017; Molina-Henares et al., 2010; Sudarsan et al., 2016, 2014), iJP815 (Hintermayer and Weuster-Botz, 2017; Koehorst et al., 2016; Kremling et al., 2012; Molina-Henares et al., 2010; van Duuren et al., 2013), PpuMBEL1071 (Beckers et al., 2016; Poblete-Castro et al., 2013), iJP962 (D'Arrigo et al., 2019; Kampers et al., 2019a; Koehorst et al., 2016; Occhipinti et al., 2018) and iJN1462 (Banerjee et al., 2020; Bator et al., 2020b; Blank et al., 2020; La Rosa et al., 2015; Molina et al., 2019a, 2019b; Niu et al., 2020; Sánchez-Clemente et al., 2018)

*P. aeruginosa* model iMO1056 (Oberhardt et al., 2008), was built via a proposed pipeline called 'model reconciliation' whereby non-biological differences were removed from genome-scale reconstructions while keeping such reconstructions as true as possible to the underlying biological data on which they were based. This GEM, which comprises 197 more reactions than its ancestor, was validated based on experimental data and compared with the iJP815 GEM. Both models presented equal accuracy in predicting growth in various carbon sources, however iJP962 was slightly more accurate in predicting gene essentiality. Later, the model was updated based on the genome reannotation of the strain and further experimental data (Belda et al., 2016) resulting in a new extended version (iJP962<sup>extended</sup>) with 186 additional reactions. Recently, (Kampers et al., 2019a) used iJP962 in combination with comparative genomics to address key O<sub>2</sub>-dependent processes in order to identify the requirements for the strain to grow under anoxic conditions. The predictions suggested the heterologous expression of the acetate kinase from *Escherichia coli* for O<sub>2</sub>-independent ATP production, a

class I dihydroorotate dehydrogenase and a class III anaerobic ribonucleotide triphosphate reductase from *Lactobacillus lactis* for the synthesis of essential metabolites. Driven by these predictions and through adaptive laboratory evolution, the researchers made the strictly aerobic *P. putida* able to grow under micro-oxic conditions.

Even though five *P. putida* KT2440 GEMs were available to this point, as shown in Table 9, the simulations among them were considerably inconsistent. Motivated by this fact, Yuan et al. (2017) built model PpuQY1140 aiming to provide a more reliable reconstruction. At first, all available GEMs were compared to identify the discrepancies leading to contrary calculations. Mistakes were corrected based on literature so that all the calculated synthesis and uptake rates were similar. Subsequently, they built a pathway-consensus model and further updated it with the latest genome annotation data. To assess the accuracy of the PpuQY1140 model, *in silico* growth rates from all models were compared with the experimentally measured values of the wild type strain as well as of several mutants. The results showed the high accuracy of the model, compared to the other reconstructions, in predicting growth rates.

The latest and most complete GEM, iJN1462, was constructed by Nogales et al. (2020). iJN1462 represents a significant expansion compared to the previous *P. putida* GEMs and is just as comparable to other high-quality *E. coli* models. iJN1462 was manually enhanced with in-depth bibliographic information related to *P. putida* metabolism. In particular, the model contains 410 unique citations related to its content while 2048 reactions are supported with at least one citation. Its main advantages are: i) the strain-specific metabolism: new catabolic pathways were included, supporting the diverse growth sources for both carbon and nitrogen, ii) a new detailed *P. putida*-specific biomass objective function based on existing experimental data and, iii) significant expansion of the cell envelope biosynthesis and cofactor, and prosthetic group biosynthesis. The model was validated using experimental data including viability on various nutrient sources, growth rates, <sup>13</sup>C carbon flux analysis, as well as gene essentiality determined by knockout libraries generated independently. It was shown that iJN1462 presented considerably higher correlation between the experimental data and *in silico* predictions, compared to previous *P. putida* GEMs. Recently, the capabilities of iJN1462 model in metabolic engineering were showcased by Banerjee et al. (2020). The model was used in combination with the MCS algorithm (von Kamp and Klant, 2017) to identify a minimal set of reactions which elimination would increase the growth-coupled production of indigoidine. Following the predictions, they managed to significantly increase both titer and yield of indigoidine, demonstrating the usefulness of thoroughly validated constraint-based models in metabolic engineering.

Despite of the various reconstructions available to date, only a few studies have actually employed them to address a specific problem. A summary of the number of investigations and the applications in which each GEM has been used is represented in Fig. 4. Noteworthy, only three of these studies demonstrated experimentally their usefulness in predicting and proposing solutions to a metabolic problem. The establishment of GEMs as a reliable and effective tool for metabolic engineering in *P. putida* requires their further improvement. To increase reliability and decrease the solution space, additional information such as omics data, should be included. Omics data have been used extensively to validate model predictions and to further constrain the calculated metabolic fluxes. Data sets derived from transcriptomics and proteomics studies can be integrated into GEMs using a variety of algorithms (Koehorst et al., 2016; Dahal et al., 2020). In this way, context-specific models are generated by determining the subset of genes that are expressed and translated under a specific metabolic state. Similarly, metabolomics and fluxomics data have been used (in other organisms) to accurately constrain and predict the internal flux distributions as well as substrate uptake rates (Rienksma et al., 2014; Dahal et al., 2020; Öyås et al., 2020).

#### 4.2. Kinetic models

A series of dynamic models have been deployed for *P. putida* with the goal of elucidating specific part of metabolism. Notably among those are the models by Koutinas et al. (2011, 2010) and Tsipa et al. (2018), which linked biomass growth and substrate consumption rates to the gene regulatory programmes that control these processes. Silva-Rocha et al. (2011) and Silva-Rocha and de Lorenzo (2013) developed an approach based on Boolean formalisms and logic-gate like analogies to described catabolic and regulatory event as well as the layout of biodegradation networks in *P. putida*-mt2. These models, which were experimentally validated in independent experiments, contributed to disentangle the complex structure of the circuits underlying the functioning of the TOL plasmid and pathways involved in metabolism of aromatic compounds. Of importance as well are the works of Kremling et al. (2012) and Wolf et al. (2015), who developed detailed kinetic models of the phosphotransferase transport systems (PTS) in *P. putida* and thereby contributed to elucidate the interplay between specific transporters and the central metabolism. Chavarría et al. (2016) modelled the fructose uptake in *P. putida* KT2440 considering transcriptional regulation, enzymatic activity and intracellular and extracellular metabolite concentrations. The fructose transport simulation revealed that fructose uptake requires an additional supply of PEP which is maintained even when fructose is depleted from the medium. In the same year, Sudarsan et al. (2016) developed a kinetic model of the  $\beta$ -ketoadipate (ortho-cleavage) pathway to evaluate benzoate degradation in *P. putida* KT2440. The model includes enzymes and transport mechanistic rate expressions which were experimentally validated by a benzoate-limited continuous culture. Predictions on the *in vivo* operations indicated flux regulation by the benzoate transporter and the enzymes forming and cleaving catechol.

Although these small-scale models are useful to describe particular metabolic and/or regulatory processes for a specific purpose of a small subset of metabolism, they are unable of reliably predicting the dynamic behaviour of larger networks and their use for large-scale metabolic engineering is therefore limited (Diez et al., 2009). Nevertheless, well-curated large-scale kinetic models are potentially very useful to such problems. The first and only large-scale kinetic model for *P. putida* was recently developed by Tokic et al. (2020). For its construction, the iJN1462 GEM was thermodynamically curated by first estimating the standard Gibbs energy of formation of metabolites, second adjusting these values for ionic strength and pH in the studied physiological condition, and finally using these values together with the concentrations of metabolites to calculate the transformed Gibbs free energy of reactions. Standard Gibbs free energies were determined for all reactions and metabolites included in pathways of the central metabolism (TCA cycle, glycolysis, pentose phosphate pathway, gluconeogenesis). After several rounds of curation using literature data and advanced computational approaches, the size of the model was reduced to obtain three different-complexity core models of increasing scale and complexity (D1, D2, D3). In this way, modellers can trade-off between the accuracy of the models and the model complexity. Using the D2 reduced model, they evaluated its computational accuracy against experimental data to: i) simulate the metabolic responses of several single-gene knockouts growing in glucose and, ii) improve the response of *P. putida* to the stress conditions of increased ATP demand.

#### 4.3. Databases

Comprehensive genetic and metabolic information of *P. putida* KT2440 is easily accessible for any researcher through numerous online databases. These databases provide a wide range of knowledge related to the strain's genome, enzymes and metabolic pathways, and various computational or visualisation tools. They enable easy navigation to the genes and metabolism of the strain with parallel reference to the respective literature. In addition to the standard databases such as

KEGG, NCBI, UniProt and BRENDA, *P. putida*'s genome and annotation are also included in the Pseudomonas Genome database ([pseudomonas.com](http://pseudomonas.com)) as well as in BioCyc ([BioCyc.org](http://BioCyc.org)). The re-annotated data from Belda et al. (2016) can also be explored and downloaded using the MicroScope platform (<https://www.genoscope.cns.fr/agg/microscope>).

The Pseudomonas Genome database is continually updated with curated genome re-annotations and metadata of multiple *Pseudomonas* strains while provides tools for large-scale comparative analysis and visualization among them. This database relies on high-quality updates of gene annotations through regular review of the literature via a community-based approach.

BioCyc ([BioCyc.org](http://BioCyc.org)) is a collection of 17,000 organism-specific Pathway/Genome Databases (PGDBs), each containing the full genome and predicted metabolic network of one organism, including metabolites, enzymes, reactions, metabolic pathways, predicted operators, transport systems, and pathway-hole fillers. The BioCyc databases are organized in: (i) Tier 1 PGDBs that have received at least 1 year of manual curation (5 available Tier 1 PGDBs), (ii) Tier 2 PGDBs that have received moderate (less than a year) amounts of review and are usually not updated on an ongoing basis (51 available Tier 2 PGDBs) and, (iii) Tier 3 PGDBs that were created computationally and received no subsequent manual review or updating (16976 available Tier 3 PGDBs). Noteworthy, the *P. putida* KT2440 PGDB was recently upgraded (Feb. 2020) from Tier 3 to Tier 2. The specific upgrades are summarized in <http://pathwaytools.blogspot.com/2020/02/a-new-tier-2-pgdb-for-pseudomonas.html>. This remarkable upgrade adds value to the available genetic and metabolic information of the strain by providing further detailed and reliable data. Moreover, it clearly highlights the increased popularity of *P. putida* KT2440, given that only 51 out of the 17,000 strains are included in Tier 2 status.

## 5. Conclusions and future directions

Significant advances in the SynBio toolbox of *P. putida* have been made recently, especially with the incorporation of novel tools such as CRISPR-based, recombineering and sRNAs. With this comprehensive review, we map and assess the extensive genetic toolbox that this bacterium currently has. However, the scientific community still relies on traditional methods for genome editing of *P. putida* with industrial application purposes. So far, these novel developed tools, although advantageous, have barely reached the application stage (Fig. 5). The arrival of such novel tools in the field of *P. putida* seems to have lagged behind other important SynBio chassis, such as *E. coli*, *Bacillus*, *Streptomyces*, *Clostridium* or cyanobacteria. Consequently, the unexplored potential of these recent tools lies ahead, with very substantial room for improvement.

Although different synthetic libraries of genetic regulatory elements are currently available in *P. putida*, they have not yet been further exploited for modulating gene expression levels, which is necessary for proper functioning of metabolic pathways. Besides, the number of biosensors applied to *P. putida* is very limited in comparison to other bacterial chassis like *E. coli*, *B. subtilis* or cyanobacteria, which have a wide variety of transcriptional factors-based biosensors, riboswitches or riboregulators (Liu et al., 2017; Till et al., 2020). In this regard, the implementation of biosensors will help to monitor concentrations of different metabolites, and thus, optimize metabolic pathways, whereas riboswitches and riboregulators enable to fine-tune gene expression levels with a tight control and dynamic ranges in response to ligand concentrations. Ultimately, programming synthetic genetic circuits as it has been done for *E. coli* (Nielsen et al., 2016), will be a powerful addition as we could control multiple cellular functions of *P. putida* in response to the environment.

Additionally, progress in the *P. putida* recombineering field should be done towards new ways to search for new recombinases. High-throughput methods such as Serial Enrichment for efficient Recombineering, SEER (Wannier et al., 2020) provide a new avenue for discovery

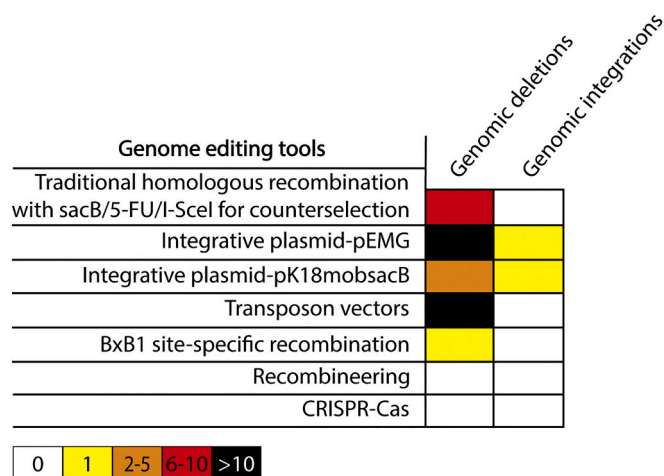


**Fig. 5.** Heat map of studies published in 2020 using genome editing tools for gene deletions and integrations in *P. putida* KT2440. Colours in the heat map indicate the number of studies. The studies do not include the first original paper, in which the tool was developed. Studies using traditional homologous recombination and different strategies for counterselection such as sacB, 5-FU (5-fluorouracil) or I-SceI: Cha et al., 2020; García-Hidalgo et al., 2020; Henríquez et al., 2020; Incha et al., 2020; Ma et al., 2020; Mohamed et al., 2020; Nitschel et al., 2020; Poblete-Castro et al., 2020; Williamson et al., 2020. Studies using the pEMG integrative plasmid: Algar et al., 2020; Bator et al., 2020b, 2020a; van Duuren et al., 2020; Hobmeier et al., 2020; Hueso-Gil et al., 2020; Li et al., 2020; Martínez-García et al., 2020a; Mikkel et al., 2020; Rosendahl et al., 2020; Tiso et al., 2020. Studies using the pK18mobsacB integrative plasmid: Bentley et al., 2020; Liang et al., 2020; Niu et al., 2020; Park et al., 2020; Sumi et al., 2020; Upadhyay et al., 2020. Studies using transposon vectors: (Algar et al., 2020; Batianis et al., 2020; Bator et al., 2020b; Fedeson et al., 2020; Hobmeier et al., 2020; Incha et al., 2020; Köbbing et al., 2020; Mikkel et al., 2020; Sumi et al., 2020; Thompson et al., 2020; Tiso et al., 2020; Volke et al., 2020b; Wehrmann et al., 2020; Zhang et al., 2020a). Study using the BxB1 site-specific recombinase: Elmore et al., 2020.

of recombinases among hundreds of proteins. This technology allows the screening of large libraries, increasing the chances of identifying new promising candidates. Alternatively, better recombinases could be obtained without the need of further mining if the current ones were optimized. For example, recombinase protein engineering is still a poorly explored option, but it begins to take shape in synthetic biologists' minds. So far, sequence optimization has been performed only in native RBSs to strengthen recombinase protein expression (Wannier et al., 2020), but the time will soon come when the own enzyme will be the fine-tuned. Furthermore, studies have shown that functionality can be established and enhanced by co-expression of recombinases with certain single-stranded DNA-binding proteins (SSB) (Wannier et al., 2020). Interactions between SSAPs and exogenous SSBs can stimulate recombinases to work in previously recalcitrant species (Filsinger et al., 2020). This approach could present a valuable opportunity for heterologous systems that have been previously shown to be ineffective in *P. putida*. Ultimately, improved protocols with efficient recombinases will jumpstart the long-awaited use of recombineering as the genome editing tool of choice in *P. putida*. Overcoming current challenges such as multiplexing and automation will enable streamlining of the genome engineering processes, facilitating fast undirected randomized evolution and rational directed mutagenesis. Consequently, this will accelerate substantial biotechnological endeavors such as genome mining (Borrero-de Acuña and Poblete-Castro, 2020) or genome recoding (Isaacs et al., 2011) along a myriad of metabolic and environmental applications.

Similarly, the potential of CRISPR-Cas technology goes beyond tool development as a proof of concept. Applications such as construction of genetic circuits to control cellular behavior or phenotype (sugar

utilization, phage resistance, chemotaxis) (Nielsen and Voigt, 2014) as well as metabolic engineering strategies to increase yield and productivity of a target compound, need to be further implemented in *P. putida*. While there is thus far only a single study on CRISPR for metabolic engineering applications in *P. putida* (Zhou et al., 2020), various studies in other bacteria, including *E. coli*, *Clostridium*, *Streptomyces*, *Synechocystis* and *Synechococcus* species have demonstrated the usefulness of CRISPR for the production of industrial relevant compounds, ranging from alcohols, amino acids, terpenoids, organic acids, fatty acids to antibiotics, anti-tumors or phytochemicals, summarized by Mouggiakos et al. (2018).

Regarding tools for transcription regulation, different CRISPRi-based tools with small variations have been used in *P. putida* as a proof of concept. Recently, the first work was published combining *in silico* predictions with CRISPRi to control metabolic fluxes towards a compound of interest (Banerjee et al., 2020). The application of CRISPRi as a metabolic pathway engineering tool as well as its deployment as a genome-wide perturbation screening method, in combination with bioinformatic tools, will put a step forward towards high-throughput genome-scale analysis of *P. putida*. Works on different bacteria have taken advantage of this powerful tool, by creating gene repression CRISPRi libraries to study the downregulation effect of essential genes on growth rates, gene morphology, chemical phenotypes and modes of action of antibiotics (Peters et al., 2016; Yao et al., 2020) as well as to increase fluxes towards L-lactate in *Synechocystis* sp. PCC 6803 (Yao et al., 2020), 3-hydroxybutyrate (3HB) in *Clostridium ljungdahlii* (Woolston et al., 2018), rapamycin in *Streptomyces rapamycinicus* (Tian et al., 2020) or malate in *E. coli* (Gao et al., 2018). Notably, CRISPRi is additionally utilized as regulatory element in advanced DNA-encoded devices such as genetic circuits (Dinh and Prather, 2019; Moser et al., 2018). Especially in *P. putida*, in which the native gene repressors are not well characterized, CRISPRi would provide an additional option for the design and construction of genetic circuits. Similarly to CRISPRi, sRNAs have been published very recently in *P. putida* as alternative tool for post-transcriptional control. Due to the very recent development of the tool in *P. putida*, the application stage has not arrived yet. In contrast, sRNAs have been used for the engineering of synthetic circuits as well as of metabolic pathways in microorganisms such as *E. coli* (Kang et al., 2014), *B. subtilis* (Yang et al., 2018), *Synechocystis* sp. PCC 6803 (Sun et al., 2018a) or in *C. acetobutylicum* (Cho and Lee, 2017). In the near future, we expect a significant increase in the implementation of the above-mentioned technologies, which will highlight a new era of high-throughput metabolic engineering and functional genetic characterization.

Lastly, the available tools for regulating protein abundance at post-translational level are still limited in *P. putida*. Even though FENIX has proven to be an efficient tool, it needs further application as in *E. coli*, in which it has been utilized to effectively downregulate competing enzymes for increasing the production of glucaric acid (Brockman and Prather, 2015) and medium-chain fatty acids (Torella et al., 2013). Although FENIX enables inducible post-translational protein activation, over the last decades proteases have been proven suitable regulators for post-translational protein inactivation. However, native protease systems are not well-characterized in *P. putida*. Therefore, future work might shed light into it. Alternatively, the protein degradation system from *Mesoplasma florum* (mf-Lon) could be adapted for *P. putida*, in a similar way that was done for *E. coli*, in which mf-Lon allowed regulating protein levels regardless the native proteases (Cameron and Collins, 2014).

Similar to the genetic tools, the metabolic and regulatory models of *P. putida* keep increasing in number. However, their application in metabolic engineering still lags significantly behind those for other microbes, which reflects either their low quality (unto large extend due to the insufficiently accurate annotations available) or the inability of the researchers to exploit them easily due to lack of a user-friendly interface. GEM of *P. putida*'s require the incorporation of additional biochemical and genetic information which will increase

their reliability and accuracy. For example, GECKO (Sánchez et al., 2017) is a recent approach to integrate quantitative measurements of metabolites and protein levels into GEMs. GECKO uses data such enzyme abundance to further constrain each metabolic flux, securing that fluxes do not overdraw the maximum capacity. GECKO-like models have been developed with great success for several microbial chassis such as *Streptomyces coelicolor* (Sulheim et al., 2020), *E. coli* (Ye et al., 2020) and *Bacillus subtilis* (Massaiu et al., 2019). In addition to GEMs, further development of the *P. putida*'s dynamics models of for different parts of metabolism is required as only one large scale kinetic model is currently available. Major challenges for developing accurate genome-scale dynamic models are the lack of experimental datasets (metabolomics, proteomics and comparative fluxomics) for both the wild type strain and a series of mutants, as well as the scarcity of experimentally determined parameters.

In summary, most of the genetic tools that are nowadays used in SynBio for different purposes have reached *P. putida* as well. However, their applications are not yet very widespread. Advances in the deployment of *in vivo* biosensors and novel tools, such as CRISPR or recombineering need to be made to overcome the development barrier, reaching an application stage with high throughput and genome-scale studies. In this regard, it might be possible to generate comprehensive datasets at a short term, paving the way for the successful implementation of the design, build, test and learn (DBTL) cycle for the production of any compound of interest (Carbonell et al., 2018). The DBTL cycle is an engineering framework that enables to systematize strategies for the development of tailor-made microbes and biological systems. Therefore, it is crucial the combination of the "wet" and "dry" synthetic biology tools to accelerate the delivery of tailored strains with an optimal titer, rate and yield, as well as to increase their robustness for use in industrial settings. Furthermore, once a cycle is completed, the acquired knowledge can be used to make better predictions on how the next strain should be engineered. On top of that, the rational engineered strain can be subjected to adaptive laboratory evolution; a powerful tool that enable to evolve strains, overcoming physiological barriers (Carbonell et al., 2018; Hamedirad et al., 2019; Opgenorth et al., 2019). The genome of the evolved strain can be then sequenced to identify the mutations that may improve the performance of the strain under the desired conditions. This newly acquired knowledge is then fed back into the DBTL cycle to refine designs with better accuracy and efficacy, leading ultimately to an optimized strain for subsequent use in a scaled-up process. We see this engineering workflow as determinant to empower *P. putida* as a flexible, robust SynBio platform to accelerate the development of biotechnology products and thereby to contribute significantly to shift from the current dominant linear economy to a more circular one.

## Funding

This work is part of several research programs; Putida for plastics, with project number GSGT.2019.028, SafeChassis: Implementing and Assessing Safeguards for Lifestyle Engineering of a Versatile Industrial Chassis, with project number 15814, both funded by the Dutch Research Council (NWO) and IBISBA with project numbers 730976 and 871118, as well as Empowerputida (nr. 635536) funded by the European Union's Horizon 2020 Research and Innovation Programme.

## Author statement

- All authors have participated in (a) conception and design, or analysis and interpretation of the data; (b) drafting the article or revising it critically for important intellectual content; and (c) approval of the final version.
- This manuscript has not been submitted to, nor is under review at, another journal or other publishing venue.

- The authors have no affiliation with any organization with a direct or indirect financial interest in the subject matter discussed in the manuscript

## References

- Acar, M., Pando, B.F., Arnold, F.H., Elowitz, M.B., Van Oudenaarden, A., 2010. A general mechanism for network-dosage compensation in gene circuits. *Science* 329, 1656–1660. <https://doi.org/10.1126/science.1190544>.
- Adli, M., 2018. The CRISPR tool kit for genome editing and beyond. *Nat. Commun.* 9, 1911. <https://doi.org/10.1038/s41467-018-04252-2>.
- Algar, E., Al-Ramahi, Y., de Lorenzo, V., Martínez-García, E., 2020. Environmental performance of *Pseudomonas putida* with a uracylated genome. *ChemBioChem*. <https://doi.org/10.1002/cbic.202000330>.
- Amarelle, V., Sanches-Medeiros, A., Silva-Rocha, R., Guazzaroni, M.-E., 2019. Expanding the toolbox of broad host-range transcriptional terminators for probiobacteria through metagenomics. *ACS Synth. Biol.* 8, 647–654. <https://doi.org/10.1021/acssynbio.8b00507>.
- Ao, X., Yao, Y., Li, T., Yang, T.-T., Dong, X., Zheng, Z.-T., Chen, G.-Q., Wu, Q., Guo, Y., 2018. A multiplex genome editing method for *Escherichia coli* based on CRISPR-Cas12a. *Front. Microbiol.* 9, 2307. <https://doi.org/10.3389/fmicb.2018.02307>.
- Aparicio, T., de Lorenzo, V., Martínez-García, E., 2015. Broadening the SEVA plasmid repertoire to facilitate genomic editing of Gram-negative bacteria. In: *Hydrocarbon and Lipid Microbiology Protocols: Genetic, Genomic and System Analyses of Pure Cultures*.
- Aparicio, T., Jensen, S.I., Nielsen, A.T., de Lorenzo, V., Martínez-García, E., 2016. The Ssr protein (T1E\_1405) from *Pseudomonas putida* DOT-T1E enables oligonucleotide-based recombineering in platform strain *P. putida* EM42. *Biotechnol. J.* 11, 1309–1319. <https://doi.org/10.1002/biot.201600317>.
- Aparicio, T., de Lorenzo, V., Martínez-García, E., 2018. CRISPR/Cas9-based counterselection boosts recombineering efficiency in *Pseudomonas putida*. *Biotechnol. J.* 13, 1700161. <https://doi.org/10.1002/biot.201700161>.
- Aparicio, T., de Lorenzo, V., Martínez-García, E., 2019. Improved thermotolerance of genome-reduced *Pseudomonas putida* EM42 enables effective functioning of the PL/cI857 system. *Biotechnol. J.* 14, 1800483. <https://doi.org/10.1002/biot.201800483>.
- Aparicio, T., Nyerges, A., Martínez-García, E., de Lorenzo, V., 2020. High-efficiency multi-site genomic editing of *Pseudomonas putida* through thermoinducible ssDNA recombineering. *iScience* 23, 100946. <https://doi.org/10.1016/j.isci.2020.100946>.
- Apura, P., Saramago, M., Peregrina, A., Viegas, S.C., Carvalho, S.M., Saraiva, L.M., Arraiano, C.M., Domingues, S., 2020. Tailor-made sRNAs: a plasmid tool to control the expression of target mRNAs in *Pseudomonas putida*. *Plasmid* 109, 102503. <https://doi.org/10.1016/j.plasmid.2020.102503>.
- Arakawa, H., Lodygin, D., Buerstedde, J.M., 2001. Mutants loxP vectors for selectable marker recycle and conditional knock-outs. *BMC Biotechnol.* <https://doi.org/10.1186/1472-6750-1-7>.
- Bagdasarian, M.M., Amann, E., Lurz, R., Rückert, B., Bagdasarian, M., 1983. Activity of the hybrid trp-lac (tac) promoter of *Escherichia coli* in *Pseudomonas putida*. Construction of broad-host-range, controlled-expression vectors. *Gene* 26, 273–282. [https://doi.org/10.1016/0378-1119\(83\)90197-X](https://doi.org/10.1016/0378-1119(83)90197-X).
- Banerjee, D., Eng, T., Lau, A.K., Sasaki, Y., Wang, B., Chen, Y., Prah, J.-P., Singan, V.R., Herbert, R.A., Liu, Y., Tanjore, D., Petzold, C.J., Keasling, J.D., Mukhopadhyay, A., 2020. Genome-scale metabolic rewiring improves titers rates and yields of the non-native product indigoidine at scale. *Nat. Commun.* 11, 5385. <https://doi.org/10.1038/s41467-020-19171-4>.
- Batiani, C., Kozaeva, E., Damalas, S.G., Martín-Pascual, M., Volke, D.C., Nikel, P.I., Martins dos Santos, V.A.P., 2020. An expanded CRISPRi toolbox for tunable control of gene expression in *Pseudomonas putida*. *Microb. Biotechnol.* 13, 368–385. <https://doi.org/10.1111/1751-7915.13533>.
- Bator, I., Karmainski, T., Tiso, T., Blank, L.M., 2020a. Killing two birds with one stone – strain engineering facilitates the development of a unique rhannolipid production process. *Front. Bioeng. Biotechnol.* 8. <https://doi.org/10.3389/fbioe.2020.00899>.
- Bator, I., Wittgens, A., Rosenau, F., Tiso, T., Blank, L.M., 2020b. Comparison of three xylase pathways in *Pseudomonas putida* KT2440 for the synthesis of valuable products. *Front. Bioeng. Biotechnol.* 7. <https://doi.org/10.3389/fbioe.2019.00480>.
- Beckers, V., Poblete-Castro, I., Tomasch, J., Wittmann, C., 2016. Integrated analysis of gene expression and metabolic fluxes in PHA-producing *Pseudomonas putida* grown on glycerol. *Microb. Cell Factories* 15, 73. <https://doi.org/10.1186/s12934-016-0470-2>.
- Belda, E., van Heck, R.G.A., José Lopez-Sánchez, M., Cruveiller, S., Barbe, V., Fraser, C., Klenk, H.-P., Petersen, J., Morgat, A., Nikel, P.I., Vallenet, D., Rouy, Z., Sekowska, A., Martins Dos Santos, V.A.P., de Lorenzo, V., Danchin, A., Médigue, C., 2016. The revisited genome of *Pseudomonas putida* KT2440 enlightens its value as a robust metabolic chassis. *Environ. Microbiol.* 18, 3403–3424. <https://doi.org/10.1111/1462-2920.13230>.
- Benedetti, I., Nikel, P.I., de Lorenzo, V., 2016. Data on the standardization of a cyclohexanone-responsive expression system for Gram-negative bacteria. *Data in Brief* 6, 738–744. <https://doi.org/10.1016/j.dib.2016.01.022>.
- Bentley, G.J., Narayanan, N., Jha, R.K., Salvachúa, D., Elmore, J.R., Peabody, G.L., Black, B.A., Ramirez, K., De Capite, A., Michener, W.E., Werner, A.Z., Klingeman, D. M., Schindel, H.S., Nelson, R., Foust, L., Guss, A.M., Dale, T., Johnson, C.W., Beckham, G.T., 2020. Engineering glucose metabolism for enhanced muconic acid production in *Pseudomonas putida* KT2440. *Metab. Eng.* 59, 64–75. <https://doi.org/10.1016/j.ymben.2020.01.001>.
- Bikard, D., Jiang, W., Samai, P., Hochschild, A., Zhang, F., Marraffini, L.A., 2013. Programmable repression and activation of bacterial gene expression using an engineered CRISPR-Cas system. *Nucleic Acids Res.* 41, 7429–7437. <https://doi.org/10.1093/nar/gkt520>.
- Blank, L.M., Narancic, T., Mampel, J., Tiso, T., O'Connor, K., 2020. Biotechnological upcycling of plastic waste and other non-conventional feedstocks in a circular economy. In: *Current Opinion in Biotechnology. Energy Biotechnology* ● *Environmental Biotechnology*, Vol. 62, pp. 212–219. <https://doi.org/10.1016/j.copbio.2019.11.011>.
- Blatny, J.M., Brautaset, T., Winther-Larsen, H.C., Haugan, K., Valla, S., 1997. Construction and use of a versatile set of broad-host-range cloning and expression vectors based on the RK2 replicon. *Appl. Environ. Microbiol.* 63, 370–379. <https://doi.org/10.1128/AEM.63.2.370-379.1997>.
- Borrero-de Acuña, J.M., Poblete-Castro, I., 2020. Expanding the reach of recombineering to environmental bacteria. In: *Trends in Biotechnology*. Elsevier Ltd. <https://doi.org/10.1016/j.tibtech.2020.03.014>.
- Bouwman, P., van der Gulden, H., van der Heijden, I., Drost, R., Klijn, C.N., Prasetyanti, P., Pieterse, M., Wientjens, E., Seibler, J., Hogervorst, F.B.L., Jonkers, J., 2013. A high-throughput functional complementation assay for classification of BRCA1 missense variants. *Cancer Discov.* <https://doi.org/10.1158/2159-8290.CD-13-0094>.
- Brockman, I.M., Prather, K.L.J., 2015. Dynamic knockdown of *E. coli* central metabolism for redirecting fluxes of primary metabolites. *Metab. Eng.* 28, 104–113. <https://doi.org/10.1016/j.ymben.2014.12.005>.
- Bruckbauer, S.T., Kvitko, B.H., Karkhoff-Schweizer, R.R., Schweizer, H.P., 2015. Tn5/7-lux: a versatile tool for the identification and capture of promoters in Gram-negative bacteria. *BMC Microbiol.* 15. <https://doi.org/10.1186/s12866-015-0354-3>.
- Burgard, A.P., Pharkya, P., Maranas, C.D., 2003. OptKnock: a bilevel programming framework for identifying gene knockout strategies for microbial strain optimization. *Biotechnol. Bioeng.* 84, 647–657. <https://doi.org/10.1002/bit.10803>.
- Calero, P., Jensen, S.I., Nielsen, A.T., 2016. Broad-host-range ProUSER vectors enable fast characterization of inducible promoters and optimization of p-coumaric acid production in *Pseudomonas putida* KT2440. *ACS Synth. Biol.* 5, 741–753. <https://doi.org/10.1021/acssynbio.6b00081>.
- Calles, B., Goñi-Moreno, Á., Lorenzo, V., 2019. Digitalizing heterologous gene expression in Gram-negative bacteria with a portable ON/OFF module. *Mol. Syst. Biol.* 15. <https://doi.org/10.15252/msb.20188777>.
- Cameron, D.E., Collins, J.J., 2014. Tunable protein degradation in bacteria. *Nat. Biotechnol.* 32, 1276–1281. <https://doi.org/10.1038/nbt.3053>.
- Carbonell, P., Jervis, A.J., Robinson, C.J., Yan, C., Dunstan, M., Swainston, N., Vinaixa, M., Hollywood, K.A., Currin, A., Rattray, N.J.W., Taylor, S., Spiess, R., Sung, R., Williams, A.R., Fellows, D., Stanford, N.J., Mulherin, P., Le Feuvre, R., Barran, P., Goodacre, R., Turner, N.J., Goble, C., Chen, G.G., Kell, D.B., Micklefield, J., Breitling, R., Takano, E., Faulon, J.-L., Scrutton, N.S., 2018. An automated Design-Build-Test-Learn pipeline for enhanced microbial production of fine chemicals. *Commun Biol* 1, 66. <https://doi.org/10.1038/s42003-018-0076-9>.
- Cha, D., Ha, H.S., Lee, S.K., 2020. Metabolic engineering of *Pseudomonas putida* for the production of various types of short-chain-length polyhydroxyalkanoates from levulinic acid. *Bioresour. Technol.* 309, 123332. <https://doi.org/10.1016/j.biortech.2020.123332>.
- Chaslus-Dancla, E., Martel, J.L., Carlier, C., Lafont, J.P., Courvalin, P., 1986. Emergence of aminoglycoside 3-N-acetyltransferase IV in *Escherichia coli* and *Salmonella typhimurium* isolated from animals in France. *Antimicrob. Agents Chemother.* 29, 239–243. <https://doi.org/10.1128/AAC.29.2.239>.
- Chaslus-Dancla, E., Pohl, P., Meurisse, M., Marin, M., Lafont, J.P., 1991. High genetic homology between plasmids of human and animal origins conferring resistance to the aminoglycosides gentamicin and apramycin. *Antimicrob. Agents Chemother.* 35, 590–593. <https://doi.org/10.1128/AAC.35.3.590>.
- Chaudhary, A.K., Na, D., Lee, E.Y., 2015. Rapid and high-throughput construction of microbial cell-factories with regulatory noncoding RNAs. *Biotechnol. Adv.* 33, 914–930. <https://doi.org/10.1016/j.biotechadv.2015.05.009>.
- Chavarría, M., Kleijn, R.J., Sauer, U., Pflüger-Grau, K., de Lorenzo, V., 2012. Regulatory tasks of the phosphoenolpyruvate-phosphotransferase system of *Pseudomonas putida* in central carbon metabolism. *mBio* 3. <https://doi.org/10.1128/mBio.00028-12>.
- Chavarría, M., Goñi-Moreno, Á., de Lorenzo, V., Nikel, P.I., 2016. A metabolic widget adjusts the phosphoenolpyruvate-dependent fructose influx in *Pseudomonas putida*. *mSystems* 1. <https://doi.org/10.1128/mSystems.00154-16>.
- Chen, Y., Rice, P.A., 2003. New insight into site-specific recombination from Flp recombinase-DNA structures. *Annu. Rev. Biophys. Biomol. Struct.* <https://doi.org/10.1146/annurev.biophys.32.110601.141732>.
- Chen, Z., Ling, W., Shang, G., 2016. Recombineering and I-SceI-mediated *Pseudomonas putida* KT2440 scarless gene deletion. *FEMS Microbiol. Lett.* 363. <https://doi.org/10.1093/femsle/fnw231>.
- Chen, W., Zhang, Ya, Zhang, Yifei, Pi, Y., Gu, T., Song, L., Wang, Y., Ji, Q., 2018a. CRISPR/Cas9-based genome editing in *Pseudomonas aeruginosa* and cytidine deaminase-mediated base editing in *Pseudomonas* species. *iScience* 6, 222–231. <https://doi.org/10.1016/j.isci.2018.07.024>.
- Chen, Y., Ho, J.M.L., Shis, D.L., Gupta, C., Long, J., Wagner, D.S., Ott, W., Josić, K., Bennett, M.R., 2018b. Tuning the dynamic range of bacterial promoters regulated by ligand-inducible transcription factors. *Nat. Commun.* 9, 64. <https://doi.org/10.1038/s41467-017-02473-5>.
- Cho, C., Lee, S.Y., 2017. Efficient gene knockdown in *Clostridium acetobutylicum* by synthetic small regulatory RNAs: a *C. acetobutylicum* synthetic sRNA system. *Biotechnol. Bioeng.* 114, 374–383. <https://doi.org/10.1002/bit.26077>.

- Choi, K.R., Lee, S.Y., 2016. CRISPR technologies for bacterial systems: current achievements and future directions. *Biotechnol. Adv.* 34, 1180–1209. <https://doi.org/10.1016/j.biotechadv.2016.08.002>.
- Choi, K.R., Lee, S.Y., 2020. Protocols for RecET-based markerless gene knockout and integration to express heterologous biosynthetic gene clusters in *Pseudomonas putida*. *Microb. Biotechnol.* 13, 199–209. <https://doi.org/10.1111/1751-7915.13374>.
- Choi, K.R., Cho, J.S., Cho, I.J., Park, D., Lee, S.Y., 2018. Markerless gene knockout and integration to express heterologous biosynthetic gene clusters in *Pseudomonas putida*. *Metab. Eng.* 47, 463–474. <https://doi.org/10.1016/j.ymben.2018.05.003>.
- Cook, T.B., Rand, J.M., Nurani, W., Courtney, D.K., Liu, S.A., Pfeleger, B.F., 2018. Genetic tools for reliable gene expression and recombining in *Pseudomonas putida*. *J. Ind. Microbiol. Biotechnol.* 45, 517–527. <https://doi.org/10.1007/s10295-017-2001-5>.
- Copeland, M.F., Politz, M.C., Pfeleger, B.F., 2014. Application of TALEs, CRISPR/Cas and sRNAs as trans-acting regulators in prokaryotes. In: *Current Opinion in Biotechnology*. Elsevier Ltd. <https://doi.org/10.1016/j.copbio.2014.02.010>
- Court, D.R., Sawitzke, J.A., Thomason, L.C., 2002. Genetic engineering using homologous recombination. *Annu. Rev. Genet.* 36, 361–388. <https://doi.org/10.1146/annurev.genet.36.061102.093104>.
- D'Arrigo, I., Cardoso, J.G.R., Rennig, M., Sonnenschein, N., Herrgård, M.J., Long, K.S., 2019. Analysis of *Pseudomonas putida* growth on non-trivial carbon sources using transcriptomics and genome-scale modelling. *Environ. Microbiol. Rep.* 11, 87–97. <https://doi.org/10.1111/1751-7915.12704>.
- Dahal, S., Yurkovich, J.T., Xu, H., Palsson, B.O., Yang, L., 2020. Synthesizing systems biology knowledge from omics using genome-scale models. *Proteomics* 20, 1900282. <https://doi.org/10.1002/pmic.201900282>.
- Damalas, S.G., Batiannis, C., Martín-Pascual, M., de Lorenzo, V., 2020. SEVA 3.1: enabling interoperability of DNA assembly among the SEVA, BioBricks and Type IIS restriction enzyme standards. *Microb. Biotechnol.* 14.
- Dammeyer, T., Steinwand, M., Krüger, S.-C., Dübel, S., Hust, M., Timmis, K.N., 2011. Efficient production of soluble recombinant single chain Fv fragments by a *Pseudomonas putida* strain KT2440 cell factory. *Microb. Cell Factories* 10, 11. <https://doi.org/10.1186/1475-2859-10-11>.
- Datsenko, K.A., Wanner, B.L., 2000. One-step inactivation of chromosomal genes in *Escherichia coli* K-12 using PCR products. *Proc. Natl. Acad. Sci. U. S. A.* 97, 6640–6645. <https://doi.org/10.1073/pnas.120163297>.
- Davies, J., O'Connor, S., 1978. Enzymatic modification of aminoglycoside antibiotics: 3-N-acetyltransferase with broad specificity that determines resistance to the novel aminoglycoside apramycin. *Antimicrob. Agents Chemother.* 14, 69–72. <https://doi.org/10.1128/AAC.14.1.69>.
- Day, D.L., Yasinow, D., McDonough, J., Shuster, C.W., 1984. Use of ureidopenicillins for selection of plasmid vector transformants in *Pseudomonas aeruginosa* and *Pseudomonas putida*. *J. Bacteriol.* 157, 937–939.
- de Lorenzo, V., 1992. Genetic engineering strategies for environmental applications. *Curr. Opin. Biotechnol.* 3, 227–231. [https://doi.org/10.1016/0958-1669\(92\)90097-3](https://doi.org/10.1016/0958-1669(92)90097-3).
- de Lorenzo, V., Eltis, L., Kessler, B., Timmis, K.N., 1993. Analysis of *Pseudomonas* gene products using lacIq/P<sub>trp</sub>-lac plasmids and transposons that confer conditional phenotypes. *Gene* 123, 17–24. [https://doi.org/10.1016/0378-1119\(93\)90533-9](https://doi.org/10.1016/0378-1119(93)90533-9).
- de Lorenzo, V., Herrero, M., Sánchez, J.M., Timmis, K.N., 1998. Mini-transposons in microbial ecology and environmental biotechnology. *FEMS Microbiol. Ecol.* 27, 211–224. <https://doi.org/10.1111/j.1574-6941.1998.tb00538.x>.
- de Lorenzo, V., Krasnogor, N., Schmidt, M., 2021. For the sake of the bioeconomy: define what a Synthetic Biology Chassis is! *New Biotechnol.* 60, 44–51. <https://doi.org/10.1016/j.nbt.2020.08.004>.
- Diez, M.S., Lam, C.M.C., Leprince, A., dos Santos, V.A.P.M., 2009. (Re-)construction, characterization and modeling of systems for synthetic biology. *Biotechnol. J.* 4, 1382–1391. <https://doi.org/10.1002/biot.200900173>.
- Dinh, C.V., Prather, K.L.J., 2019. Development of an autonomous and bifunctional quorum-sensing circuit for metabolic flux control in engineered *Escherichia coli*. *Proc. Natl. Acad. Sci. U. S. A.* 116, 25562–25568. <https://doi.org/10.1073/pnas.1911144116>.
- Domröse, A., Wehmann, R., Thies, S., Jaeger, K.-E., Drepper, T., Loeschcke, A., 2017. Rapid generation of recombinant *Pseudomonas putida* secondary metabolite producers using yT<sub>REX</sub>. *Synth. Syst. Biotechnol.* 2, 310–319. <https://doi.org/10.1016/j.synbio.2017.11.001>.
- Domröse, A., Hage-Hülsmann, J., Thies, S., Wehmann, R., Kruse, L., Otto, M., Wierckx, N., Jaeger, K.E., Drepper, T., Loeschcke, A., 2019. *Pseudomonas putida* rDNA is a favored site for the expression of biosynthetic genes. *Sci. Rep.* 9. <https://doi.org/10.1038/s41598-019-43405-1>.
- Dos Santos, V.A.P.M., Heim, S., Moore, E.R.B., Strätz, M., Timmis, K.N., 2004. Insights into the genomic basis of niche specificity of *Pseudomonas putida* KT2440. *Environ. Microbiol.* 6, 1264–1286. <https://doi.org/10.1111/j.1462-2920.2004.00734.x>.
- Durante-Rodríguez, G., De Lorenzo, V., Nikel, P.I., 2018. A post-translational metabolic switch enables complete decoupling of bacterial growth from biopolymer production in engineered *Escherichia coli*. *ACS Synth. Biol.* 7, 2686–2697. <https://doi.org/10.1021/acssynbio.8b00345>.
- Dvořák, P., de Lorenzo, V., 2018. Refactoring the upper sugar metabolism of *Pseudomonas putida* for co-utilization of cellobiose, xylose, and glucose. *Metab. Eng.* 48, 94–108. <https://doi.org/10.1016/j.ymben.2018.05.019>.
- e Silva, S. de A., Echeverrigaray, S., 2012. Bacterial promoter features description and their application on *E. coli* in silico prediction and recognition approaches. In: Prez-Sánchez, H. (Ed.), *Bioinformatics*. InTech. <https://doi.org/10.5772/48149>.
- Ebinuma, H., Nakahama, K., Nanto, K., 2015. Enrichments of gene replacement events by *Agrobacterium*-mediated recombine-mediated cassette exchange. *Mol. Breed.* <https://doi.org/10.1007/s11032-015-0215-7>.
- Ellis, H.M., Yu, D., DiTizio, T., Court, D.L., 2001. High efficiency mutagenesis, repair, and engineering of chromosomal DNA using single-stranded oligonucleotides. *Proc. Natl. Acad. Sci. U. S. A.* 98, 6742–6746. <https://doi.org/10.1073/pnas.121164898>.
- Elmore, J.R., Furches, A., Wolff, G.N., Gorday, K., Guss, A.M., 2017. Development of a high efficiency integration system and promoter library for rapid modification of *Pseudomonas putida* KT2440. *Metab. Eng. Commun.* 5, 1–8. <https://doi.org/10.1016/j.meten.2017.04.001>.
- Elmore, J.R., Dexter, G.N., Salvachúa, D., O'Brien, M., Klingeman, D.M., Gorday, K., Michener, J.K., Peterson, D.J., Beckham, G.T., Guss, A.M., 2020. Engineered *Pseudomonas putida* simultaneously catabolizes five major components of corn stover lignocellulose: glucose, xylose, arabinose, p-coumaric acid, and acetic acid. *Metab. Eng.* 62, 62–71. <https://doi.org/10.1016/j.ymben.2020.08.001>.
- Escapa, I.F., García, J.L., Bühler, B., Blank, L.M., Prieto, M.A., 2012. The polyhydroxyalkanoate metabolism controls carbon and energy spillage in *Pseudomonas putida*. *Environ. Microbiol.* 14, 1049–1063. <https://doi.org/10.1111/j.1462-2920.2011.02684.x>.
- Fedeson, D.T., Saake, P., Calero, P., Nikel, P.I., Ducat, D.C., 2020. Biotransformation of 2,4-dinitrotoluene in a phototrophic co-culture of engineered *Synechococcus elongatus* and *Pseudomonas putida*. *Microb. Biotechnol.* 13, 997–1011. <https://doi.org/10.1111/1751-7915.13544>.
- Feng, X., Zhao, D., Zhang, X., Ding, X., Bi, C., 2018. CRISPR/Cas9 assisted multiplex genome editing technique in *Escherichia coli*. *Biotechnol. J.* 13, 1700604. <https://doi.org/10.1002/biot.201700604>.
- Fernández, M., Conde, S., de la Torre, J., Molina-Santiago, C., Ramos, J.-L., Duque, E., 2012. Mechanisms of resistance to chloramphenicol in *Pseudomonas putida* KT2440. *Antimicrob. Agents Chemother.* 56, 1001–1009. <https://doi.org/10.1128/AAC.05398-11>.
- Filsinger, G., Wannier, T., Pedersen, F.B., Zhang, J., Lutz, I., Stork, D., Debnath, A., Gozzi, K., Kuchwara, H., Volf, V., Wang, S., Rios, X., Gregg, C., Lajoie, M., Shipman, S., Aach, J., Laub, M., Church, G., 2020. Characterizing the portability of RecT-mediated oligonucleotide recombination. *bioRxiv*. <https://doi.org/10.1101/2020.04.14.041095>, 2020.04.14.041095.
- Finley, S.D., Broadbelt, L.J., Hatzimanikatis, V., 2010. In silico feasibility of novel biodegradation pathways for 1,2,4-trichlorobenzene. *BMC Syst. Biol.* 4, 7. <https://doi.org/10.1186/1752-0509-4-7>.
- Freed, E., Fenster, J., Smolinski, S.L., Walker, J., Henard, C.A., Gill, R., Eckert, C.A., 2018. Building a genome engineering toolbox in nonmodel prokaryotic microbes. *Biotechnol. Bioeng.* 115, 2120–2138. <https://doi.org/10.1002/bit.26727>.
- Gaida, S.M., Al-Hinai, M.A., Indurthi, D.C., Nicolaou, S.A., Papoutsakis, E.P., 2013. Synthetic tolerance: three noncoding small RNAs, DsrA, ArcZ and RprA, acting supra-additively against acid stress. *Nucleic Acids Res.* 41, 8726–8737. <https://doi.org/10.1093/nar/gkt651>.
- Gaj, T., Sirk, S.J., Barbas, C.F., 2014. Expanding the scope of site-specific recombinases for genetic and metabolic engineering. *Biotechnol. Bioeng.* <https://doi.org/10.1002/bit.25096>.
- Galata, V., Fehlmann, T., Backes, C., Keller, A., 2019. PLSDB: a resource of complete bacterial plasmids. *Nucleic Acids Res.* 47, D195–D202. <https://doi.org/10.1093/nar/gky1050>.
- Gallagher, R.R., Li, Z., Lewis, A.O., Isaacs, F.J., 2014. Rapid editing and evolution of bacterial genomes using libraries of synthetic DNA. *Nat. Protoc.* 9, 2301–2316. <https://doi.org/10.1038/nprot.2014.082>.
- Gao, C., Wang, S., Hu, G., Guo, L., Chen, X., Xu, P., Liu, L., 2018. Engineering *Escherichia coli* for malate production by integrating modular pathway characterization with CRISPRi-guided multiplexed metabolic tuning. *Biotechnol. Bioeng.* 115, 661–672. <https://doi.org/10.1002/bit.26486>.
- García-Hidalgo, J., Brink, D.P., Ravi, K., Paul, C.J., Lidén, G., Gorwa-Grauslund, M.F., 2020. Vanillin production in *Pseudomonas*: whole-genome sequencing of *Pseudomonas* sp. Strain 9.1 and reannotation of *Pseudomonas putida* CalA as a vanillin reductase. *Appl. Environ. Microbiol.* 86. <https://doi.org/10.1128/AEM.02442-19>.
- Gawin, A., Valla, S., Brautaset, T., 2017. The XylS/Pm regulator/promoter system and its use in fundamental studies of bacterial gene expression, recombinant protein production and metabolic engineering. *Microb. Biotechnol.* 10, 702–718. <https://doi.org/10.1111/1751-7915.12701>.
- Gemperlein, K., Zipf, G., Bernauer, H.S., Müller, R., Wenzel, S.C., 2016. Metabolic engineering of *Pseudomonas putida* for production of docosaheptaenoic acid based on a myxobacterial PUFA synthase. *Metab. Eng.* 33, 98–108. <https://doi.org/10.1016/j.ymben.2015.11.001>.
- Ghim, C.M., Almaas, E., 2008. Genetic noise control via protein oligomerization. *BMC Syst. Biol.* 2, 1–13. <https://doi.org/10.1186/1752-0509-2-94>.
- Gisler, S., Gonçalves, J.P., Akhtar, W., de Jong, J., Pindyurin, A.V., Wessels, L.F.A., van Lohuizen, M., 2019. Multiplexed Cas9 targeting reveals genomic location effects and gRNA-based staggered breaks influencing mutation efficiency. *Nat. Commun.* 10, 1598. <https://doi.org/10.1038/s41467-019-09551-w>.
- Gottesman, S., 2004. The small RNA regulators of *Escherichia coli*: roles and mechanisms. *Annu. Rev. Microbiol.* 58, 303–328. <https://doi.org/10.1146/annurev.micro.58.030603.123841>.
- Graf, N., Altenbuchner, J., 2013. Functional characterization and application of a tightly regulated MekR/P mekA expression system in *Escherichia coli* and *Pseudomonas putida*. *Appl. Microbiol. Biotechnol.* 97, 8239–8251. <https://doi.org/10.1007/s00253-013-5030-7>.
- Grindley, N.D.F., Whiteson, K.L., Rice, P.A., 2006. Mechanisms of site-specific recombination. *Annu. Rev. Biochem.* <https://doi.org/10.1146/annurev.biochem.73.011303.073908>.
- Grossman, T.H., Kawasaki, E.S., Punreddy, S.R., Osburne, M.S., 1998. Spontaneous CAMP-dependent derepression of gene expression in stationary phase plays a role in

- recombinant expression instability. *Gene* 209, 95–103. [https://doi.org/10.1016/S0378-1119\(98\)00020-1](https://doi.org/10.1016/S0378-1119(98)00020-1).
- Guan, X., Ramanathan, S., Garriss, J.P., Shetty, R.S., Ensor, M., Bachas, L.G., Daunert, S., 2000. Chlorocatechol detection based on a clc operon/reporter gene system. *Anal. Chem.* 72, 2423–2427. <https://doi.org/10.1021/ac9913917>.
- Hamedirad, M., Chao, R., Weisberg, S., Lian, J., Sinha, S., Zhao, H., 2019. Towards a fully automated algorithm driven platform for biosystems design. *Nat. Commun.* 10, 5150. <https://doi.org/10.1038/s41467-019-13189-z>.
- Hammer, K., Mijakovic, I., Jensen, P.R., 2006. Synthetic promoter libraries – tuning of gene expression. *Trends Biotechnol.* 24, 53–55. <https://doi.org/10.1016/j.tibtech.2005.12.003>.
- Hawkins, J.S., Wong, S., Peters, J.M., Almeida, R., Qi, L.S., 2015. Targeted transcriptional repression in bacteria using CRISPR interference (CRISPRi). *Methods Mol. Biol.* 1311, 349–362. [https://doi.org/10.1007/978-1-4939-2687-9\\_23](https://doi.org/10.1007/978-1-4939-2687-9_23).
- Henriquez, T., Stein, N.V., Jung, H., 2020. Resistance to bipyridyls mediated by the TgABC efflux system in *Pseudomonas putida* KT2440. *Front. Microbiol.* 11 <https://doi.org/10.3389/fmicb.2020.01974>.
- Hintermayer, S.B., Weuster-Botz, D., 2017. Experimental validation of in silico estimated biomass yields of *Pseudomonas putida* KT2440. *Biotechnol. J.* 12, 1600720. <https://doi.org/10.1002/biot.201600720>.
- Hobmeier, K., Löwe, H., Liefeldt, S., Kremling, A., Pflüger-Grau, K., 2020. A nitrate-blind *P. putida* strain boosts PHA production in a synthetic mixed culture. *Front. Bioeng. Biotechnol.* 8. <https://doi.org/10.3389/fbioe.2020.00486>.
- Hoffmann, J., Altenbuchner, J., 2015. Functional characterization of the mannitol promoter of *Pseudomonas fluorescens* DSM 50106 and its application for a mannitol-inducible expression system for *Pseudomonas putida* KT2440. *PLoS One* 10, e0133248. <https://doi.org/10.1371/journal.pone.0133248>.
- Hogenkamp, F., Hilgers, F., Knapp, A., Klaus, O., Bier, C., Binder, D., Jaeger, K.-E., Drepper, T., Pietruszka, J., 2021. Effect of photocaged isopropyl  $\beta$ -d-1-thiogalactopyranoside solubility on the light responsiveness of LacI-controlled expression systems in different bacteria. *ChemBioChem* 22, 539–547. <https://doi.org/10.1002/cbic.202000377>.
- Hu, J.H., Miller, S.M., Geurts, M.H., Tang, W., Chen, L., Sun, N., Zeina, C.M., Gao, X., Rees, H.A., Lin, Z., Liu, D.R., 2018. Evolved Cas9 variants with broad PAM compatibility and high DNA specificity. *Nature* 556, 57–63. <https://doi.org/10.1038/nature26155>.
- Hueso-Gil, A., Nyerges, A., Pál, C., Calles, B., de Lorenzo, V., 2019. Multiple-site diversification of regulatory sequences enables interspecies operability of genetic devices. *ACS Synth. Biol.* <https://doi.org/10.1021/acssynbio.9b00375>.
- Hueso-Gil, A., Calles, B., de Lorenzo, V., 2020. The Wsp intermembrane complex mediates metabolic control of the swim-attach decision of *Pseudomonas putida*. *Environ. Microbiol.* 22, 3535–3547. <https://doi.org/10.1111/1462-2920.15126>.
- Hüsken, L.E., Beeftink, R., de Bont, J.A.M., Wery, J., 2001. High-rate 3-methylcatechol production in *Pseudomonas putida* strains by means of a novel expression system. *Appl. Microbiol. Biotechnol.* 55, 571–577. <https://doi.org/10.1007/s002530000566>.
- Incha, M.R., Thompson, M.G., Blake-Hedges, J.M., Liu, Y., Pearson, A.N., Schmidt, M., Gin, J.W., Petzold, C.J., Deutschbauer, A.M., Keasling, J.D., 2020. Leveraging host metabolism for bisdemethoxycurcumin production in *Pseudomonas putida*. *Metab. Eng. Commun.* 10, e00119 <https://doi.org/10.1016/j.mec.2019.e00119>.
- Isaacs, F.J., Carr, P.A., Wang, H.H., Lajoie, M.J., Sterling, B., Kraal, L., Tolonen, A.C., Gianoulis, T.A., Goodman, D.B., Reppas, N.B., Emig, C.J., Bang, D., Hwang, S.J., Jewett, M.C., Jacobson, J.M., Church, G.M., 2011. Precise manipulation of chromosomes in vivo enables genome-wide codon replacement. *Science* 333, 348–353. <https://doi.org/10.1126/science.1205822>.
- Jaganathan, D., Ramasamy, K., Sellamuthu, G., Jayabalan, S., Venkataraman, G., 2018. CRISPR for crop improvement: an update review. *Front. Plant Sci.* 9 <https://doi.org/10.3389/fpls.2018.00985>.
- Jahn, M., Vorpahl, C., Hübschmann, T., Harms, H., Müller, S., 2016. Copy number variability of expression plasmids determined by cell sorting and Droplet Digital PCR. *Microb. Cell Factories* 15, 211. <https://doi.org/10.1186/s12934-016-0610-8>.
- Jiang, F., Doudna, J.A., 2017. CRISPR–Cas9 structures and mechanisms. *Annu. Rev. Biophys.* 46, 505–529. <https://doi.org/10.1146/annurev-biophys-062215-010822>.
- Kampers, Linde F.C., Van Heck, R.G.A., Donati, S., Saccenti, E., Volkers, R.J.M., Schaap, P.J., Suarez-Diez, M., Nikel, P.I., Martins Dos Santos, V.A.P., 2019a. In silico-guided engineering of *Pseudomonas putida* towards growth under micro-oxic conditions. *Microb. Cell Factories* 18, 179. <https://doi.org/10.1186/s12934-019-1227-5>.
- Kampers, Linde F.C., Volkers, R.J.M., Martins Dos Santos, V.A.P., 2019b. *Pseudomonas putida* KT2440 is HV1 certified, not GRAS. *Microb. Biotechnol.* 12, 845–848. <https://doi.org/10.1111/1751-7915.13443>.
- Kang, Z., Zhang, C., Zhang, Junli, Jin, P., Zhang, Juan, Du, G., Chen, J., 2014. Small RNA regulators in bacteria: powerful tools for metabolic engineering and synthetic biology. *Appl. Microbiol. Biotechnol.* 98, 3413–3424. <https://doi.org/10.1007/s00253-014-5569-y>.
- Karunakaran, P., Blatny, J.M., Ertesvåg, H., Valla, S., 1998. Species-dependent phenotypes of replication-temperature-sensitive trfA mutants of plasmid RK2: a codon-neutral base substitution stimulates temperature sensitivity by leading to reduced levels of trfA expression. *J. Bacteriol.* 180, 3793–3798.
- Kemp, L.R., Dunstan, M.S., Fisher, K., Warwicker, J., Leys, D., 2013. The transcriptional regulator CprK detects chlorination by combining direct and indirect readout mechanisms. *Philos. Trans. R. Soc. B* 368, 20120323. <https://doi.org/10.1098/rstb.2012.0323>.
- Khetrapal, V., Mehreshahi, K., Rafee, S., Chen, S., Lim, C.L., Chen, S.L., 2015. A set of powerful negative selection systems for unmodified Enterobacteriaceae. *Nucleic Acids Res.* 43, e83. <https://doi.org/10.1093/nar/gkv248>.
- Kim, S.K., Yoon, P.K., Kim, S.-J., Woo, S.-G., Rha, E., Lee, H., Yeom, S.-J., Kim, H., Lee, D.-H., Lee, S.-G., 2019. CRISPR interference-mediated gene regulation in *Pseudomonas putida* KT2440. *Microb. Biotechnol.* <https://doi.org/10.1111/1751-7915.13382>.
- Klompe, S.E., Vo, P.L.H., Halpin-Healy, T.S., Sternberg, S.H., 2019. Transposon-encoded CRISPR–Cas systems direct RNA-guided DNA integration. *Nature* 571, 219–225. <https://doi.org/10.1038/s41586-019-1323-z>.
- Köbbing, S., Blank, L.M., Wierckx, N., 2020. Characterization of context-dependent effects on synthetic promoters. *Front. Bioeng. Biotechnol.* 8, 551. <https://doi.org/10.3389/fbioe.2020.00551>.
- Koehorst, J.J., van Dam, J.C.J., van Heck, R.G.A., Saccenti, E., dos Santos, V.A.P.M., Suarez-Diez, M., Schaap, P.J., 2016. Comparison of 432 *Pseudomonas* strains through integration of genomic, functional, metabolic and expression data. *Sci. Rep.* 6, 38699. <https://doi.org/10.1038/srep38699>.
- Koutinas, M., Lam, M.-C., Kiparissides, A., Silva-Rocha, R., Godinho, M., Livingstone, A.G., Pistikopoulos, E.N., Lorenzo, V.D., Santos, V.A.P.M.D., Mantalaris, A., 2010. The regulatory logic of m-xylene biodegradation by *Pseudomonas putida* mt-2 exposed by dynamic modelling of the principal node Ps/Pr of the TOL plasmid. *Environ. Microbiol.* 12, 1705–1718. <https://doi.org/10.1111/j.1462-2920.2010.02245.x>.
- Koutinas, M., Kiparissides, A., de Lorenzo, V., Santos, V.A.P.M.D., Pistikopoulos, E.N., Mantalaris, A., 2011. Predicting microbial growth kinetics with the use of genetic circuit models. In: 21st European Symposium on Computer Aided Process Engineering. Presented at the 21st European Symposium on Computer Aided Process Engineering. Elsevier, pp. 1321–1325. <https://doi.org/10.1016/B978-0-444-54298-4.50043-X>.
- Kovach, M.E., Elzer, P.H., Steven Hill, D., Robertson, G.T., Farris, M.A., Roop, R.M., Peterson, K.M., 1995. Four new derivatives of the broad-host-range cloning vector pBBR1MCS, carrying different antibiotic-resistance cassettes. *Gene* 166, 175–176. [https://doi.org/10.1016/0378-1119\(95\)00584-1](https://doi.org/10.1016/0378-1119(95)00584-1).
- Krebs, A.R., Dessus-Babus, S., Burger, L., Schübeler, D., 2014. High-throughput engineering of a mammalian genome reveals building principles of methylation states at CG rich regions. *eLife*. <https://doi.org/10.7554/eLife.04094>.
- Kremling, A., Pflüger-Grau, K., Chavarría, M., Puchalka, J., dos Santos, V., Lorenzo, V., 2012. Modeling and analysis of flux distributions in the two branches of the phosphotransferase system in *Pseudomonas putida*. *BMC Syst. Biol.* 6, 149. <https://doi.org/10.1186/1752-0509-6-149>.
- Kruyer, N.S., Peralta-Yahya, P., 2017. Metabolic engineering strategies to bio-adipic acid production. *Curr. Opin. Biotechnol.* 45, 136–143. <https://doi.org/10.1016/j.copbio.2017.03.006>.
- La Rosa, R., Nogales, J., Rojo, F., 2015. The Crc/CrcZ-CrcY global regulatory system helps the integration of gluconeogenic and glycolytic metabolism in *Pseudomonas putida*. *Environ. Microbiol.* 17, 3362–3378. <https://doi.org/10.1111/1462-2920.12812>.
- Lambert, J.M., Bongers, R.S., Kleerebezem, M., 2007. Cre-lox-based system for multiple gene deletions and selectable-marker removal in *Lactobacillus plantarum*. *Appl. Environ. Microbiol.* <https://doi.org/10.1128/AEM.01473-06>.
- Lambertsen, L., Sternberg, C., Molin, S., 2004. Mini-Tn7 transposons for site-specific tagging of bacteria with fluorescent proteins. *Environ. Microbiol.* 6, 726–732. <https://doi.org/10.1111/j.1462-2920.2004.00605.x>.
- Larson, M.H., Gilbert, L.A., Wang, X., Lim, W.A., Weissman, J.S., Qi, L.S., 2013. CRISPR interference (CRISPRi) for sequence-specific control of gene expression. *Nat. Protoc.* 8, 2180–2196. <https://doi.org/10.1038/nprot.2013.132>.
- Lauritsen, I., Porse, A., Sommer, M.O.A., Nørholm, M.H.H., 2017. A versatile one-step CRISPR-Cas9 based approach to plasmid-curing. *Microb. Cell Factories* 16, 135. <https://doi.org/10.1186/s12934-017-0748-z>.
- Leprince, A., de Lorenzo, V., Völler, P., van Passel, M.W.J., Martins dos Santos, V.A.P., 2012a. Random and cyclical deletion of large DNA segments in the genome of *Pseudomonas putida*. *Environ. Microbiol.* 14, 1444–1453. <https://doi.org/10.1111/j.1462-2920.2012.02730.x>.
- Leprince, A., Janus, D., de Lorenzo, V., Santos, V.M.D., 2012b. Streamlining of a *Pseudomonas putida* genome using a combinatorial deletion method based on minitransposon insertion and the Flp-FRT recombination system. *Methods Mol. Biol.* 813, 249–266. [https://doi.org/10.1007/978-1-61779-412-4\\_15](https://doi.org/10.1007/978-1-61779-412-4_15).
- Leprince, A., van Passel, M.W.J., dos Santos, V.A.P.M., 2012c. Streamlining genomes: toward the generation of simplified and stabilized microbial systems. *Curr. Opin. Biotechnol.* 23, 651–658. <https://doi.org/10.1016/j.copbio.2012.05.001>.
- Li, L., Liu, X., Wei, K., Lu, Y., Jiang, W., 2019. Synthetic biology approaches for chromosomal integration of genes and pathways in industrial microbial systems. *Biotechnol. Adv.* 37, 730–745. <https://doi.org/10.1016/j.biotechadv.2019.04.002>.
- Li, W.-J., Narancic, T., Kenny, S.T., Niehoff, P.-J., O'Connor, K., Blank, L.M., Wierckx, N., 2020. Unraveling 1,4-butanediol metabolism in *Pseudomonas putida* KT2440. *Front. Microbiol.* 11 <https://doi.org/10.3389/fmicb.2020.00382>.
- Liang, P., Zhang, Y., Xu, B., Zhao, Y., Liu, X., Gao, W., Ma, T., Yang, C., Wang, S., Liu, R., 2020. Deletion of genomic islands in the *Pseudomonas putida* KT2440 genome can create an optimal chassis for synthetic biology applications. *Microb. Cell Factories* 19, 70. <https://doi.org/10.1186/s12934-020-01329-w>.
- Lin, L., Cheng, Y., Pu, Y., Sun, S., Li, X., Jin, M., Pierson, E.A., Gross, D.C., Dale, B.E., Dai, S.Y., Ragauskas, A.J., Yuan, J.S., 2016. Systems biology-guided biodesign of consolidated lignin conversion. *Green Chem.* 18, 5536–5547. <https://doi.org/10.1039/C6GC00131D>.
- Liu, Y.-X., Wang, M., Wang, X.-J., 2014. Endogenous Small RNA Clusters in Plants. *Genomics Proteomics Bioinforma. Spec. Issue Ribogenomics* 12, 64–71. <https://doi.org/10.1016/j.gpb.2014.04.003>.
- Liu, Yang, Liu, Ye, Wang, M., 2017. Design, optimization and application of small molecule biosensor in metabolic engineering. *Front. Microbiol.* 8 <https://doi.org/10.3389/fmicb.2017.02012>.

- Loeschcke, A., Markert, A., Wilhelm, S., Wirtz, A., Rosenau, F., Jaeger, K.-E., Drepper, T., 2013. TREC: a universal tool for the transfer and expression of biosynthetic pathways in bacteria. *ACS Synth. Biol.* 2, 22–33. <https://doi.org/10.1021/sb3000657>.
- Luo, X., Yang, Y., Ling, W., Zhuang, H., Li, Q., Shang, G., 2016. *Pseudomonas putida* KT2440 markerless gene deletion using a combination of  $\lambda$  Red recombineering and Cre/loxP site-specific recombination. *FEMS Microbiol. Lett.* <https://doi.org/10.1093/femsle/fnw014>.
- Ma, C., Mu, Q., Wang, L., Shi, Y., Zhu, L., Zhang, S., Xue, Y., Tao, Y., Ma, Y., Yu, B., 2020. Bio-production of high-purity propionate by engineering l-threonine degradation pathway in *Pseudomonas putida*. *Appl. Microbiol. Biotechnol.* 104, 5303–5313. <https://doi.org/10.1007/s00253-020-10619-7>.
- Maia, P., Rocha, M., Rocha, I., 2016. In silico constraint-based strain optimization methods: the quest for optimal cell factories. *Microbiol. Mol. Biol. Rev.* 80, 45–67. <https://doi.org/10.1128/MMBR.00014-15>.
- Marinelli, L.J., Hatfull, G.F., Piri, M., 2012. Recombineering. *Bacteriophage* 2, 5–14. <https://doi.org/10.4161/bact.18778>.
- Martínez-García, E., de Lorenzo, V., 2011. Engineering multiple genomic deletions in Gram-negative bacteria: analysis of the multi-resistant antibiotic profile of *Pseudomonas putida* KT2440: Tools for editing Gram-negative genomes. *Environ. Microbiol.* 13, 2702–2716. <https://doi.org/10.1111/j.1462-2920.2011.02538.x>.
- Martínez-García, E., de Lorenzo, V., 2019. *Pseudomonas putida* in the quest of programmable chemistry. In: *Current Opinion in Biotechnology*. Elsevier Ltd. <https://doi.org/10.1016/j.copbio.2019.03.012>.
- Martínez-García, E., Calles, B., Arévalo-Rodríguez, M., de Lorenzo, V., 2011. pBAM1: an all-synthetic genetic tool for analysis and construction of complex bacterial phenotypes. *BMC Microbiol.* 11, 38. <https://doi.org/10.1186/1471-2180-11-38>.
- Martínez-García, E., Nikel, P.I., Aparicio, T., de Lorenzo, V., 2014. *Pseudomonas* 2.0: genetic upgrading of *P. putida* KT2440 as an enhanced host for heterologous gene expression. *Microb. Cell Factories* 13. <https://doi.org/10.1186/s12934-014-0159-3>, 159.
- Martínez-García, E., Aparicio, T., Goñi-Moreno, A., Fraile, S., de Lorenzo, V., 2015. SEVA 2.0: an update of the Standard European Vector Architecture for de-/re-construction of bacterial functionalities. *Nucleic Acids Res.* 43, D1183–D1189. <https://doi.org/10.1093/nar/gku1114>.
- Martínez-García, E., Fraile, S., Espeso, D.R., Vecchiotti, D., Berton, G., de Lorenzo, V., 2020a. Naked bacterium: emerging properties of a surfome-streamlined *Pseudomonas putida* strain. *ACS Synth. Biol.* <https://doi.org/10.1021/acssynbio.0c00272>.
- Martínez-García, E., Goñi-Moreno, A., Bartley, B., McLaughlin, J., Sánchez-Sampedro, L., Pascual del Pozo, H., Prieto Hernández, C., Marletta, A.S., De Lucrezia, D., Sánchez-Fernández, G., Fraile, S., de Lorenzo, V., 2020b. SEVA 3.0: an update of the Standard European Vector Architecture for enabling portability of genetic constructs among diverse bacterial hosts. *Nucleic Acids Res.* 48, D1164–D1170. <https://doi.org/10.1093/nar/gkz1024>.
- Massali, I., Pasotti, L., Sonnenschein, N., Rama, E., Cavaletti, M., Magni, P., Calvio, C., Herrgård, M.J., 2019. Integration of enzymatic data in *Bacillus subtilis* genome-scale metabolic model improves phenotype predictions and enables in silico design of poly- $\gamma$ -glutamic acid production strains. *Microb. Cell Factories* 18, 3. <https://doi.org/10.1186/s12934-018-1052-2>.
- Meyers, A., Furtmann, C., Gesing, K., Tozakidis, I.E.P., Jose, J., 2019. Cell density-dependent auto-inducible promoters for expression of recombinant proteins in *Pseudomonas putida*. *Microb. Biotechnol.* 12, 1003–1013. <https://doi.org/10.1111/1751-7915.13455>.
- Mikkel, K., Tagel, M., Ukkivi, K., Ilves, H., Kivisaar, M., 2020. Integration Host Factor IHF facilitates homologous recombination and mutagenic processes in *Pseudomonas putida*. *DNA Repair* 85, 102745. <https://doi.org/10.1016/j.dnarep.2019.102745>.
- Miskovic, L., Tokic, M., Fengos, G., Hatzimanikatis, V., 2015. Rites of passage: requirements and standards for building kinetic models of metabolic phenotypes. In: *Current Opinion in Biotechnology*. Elsevier Ltd. <https://doi.org/10.1016/j.copbio.2015.08.019>.
- Mohamed, E.T., Werner, A.Z., Salvachúa, D., Singer, C.A., Szostkiewicz, K., Rafael Jiménez-Díaz, M., Eng, T., Radi, M.S., Simmons, B.A., Mukhopadhyay, A., Herrgård, M.J., Singer, S.W., Beckham, G.T., Feist, A.M., 2020. Adaptive laboratory evolution of *Pseudomonas putida* KT2440 improves p-coumaric and ferulic acid catabolism and tolerance. *Metab. Eng. Commun.* 11, e00143. <https://doi.org/10.1016/j.mec.2020.e00143>.
- Molina, L., Rosa, R.L., Nogales, J., Rojo, F., 2019a. Influence of the Crc global regulator on substrate uptake rates and the distribution of metabolic fluxes in *Pseudomonas putida* KT2440 growing in a complete medium. *Environ. Microbiol.* 21, 4446–4459. <https://doi.org/10.1111/1462-2920.14812>.
- Molina, L., Rosa, R.L., Nogales, J., Rojo, F., 2019b. *Pseudomonas putida* KT2440 metabolism undergoes sequential modifications during exponential growth in a complete medium as compounds are gradually consumed. *Environ. Microbiol.* 21, 2375–2390. <https://doi.org/10.1111/1462-2920.14622>.
- Molina-Henares, M.A., Torre, J.D.L., García-Salamanca, A., Molina-Henares, A.J., Herrera, M.C., Ramos, J.L., Duque, E., 2010. Identification of conditionally essential genes for growth of *Pseudomonas putida* KT2440 on minimal medium through the screening of a genome-wide mutant library. *Environ. Microbiol.* 12, 1468–1485. <https://doi.org/10.1111/j.1462-2920.2010.02166.x>.
- Molla, K.A., Yang, Y., 2020. Predicting CRISPR/Cas9-induced mutations for precise genome editing. *Trends Biotechnol.* 38, 136–141. <https://doi.org/10.1016/j.tibtech.2019.08.002>.
- Moon, S.B., Kim, D.Y., Ko, J.-H., Kim, Y.-S., 2019. Recent advances in the CRISPR genome editing tool set. *Exp. Mol. Med.* 51, 1–11. <https://doi.org/10.1038/s12276-019-0339-7>.
- Moser, F., Espah Borujeni, A., Ghodasara, A.N., Cameron, E., Park, Y., Voigt, C.A., 2018. Dynamic control of endogenous metabolism with combinatorial logic circuits. *Mol. Syst. Biol.* 14, e8605. <https://doi.org/10.15252/msb.20188605>.
- Mougiakos, I., Mohanraju, P., Bosma, E.F., Vrouwe, V., Finger Bou, M., Naduthodi, M.L.S., Gussak, A., Brinkman, R.B.L., van Kranenburg, R., van der Oost, J., 2017. Characterizing a thermostable Cas9 for bacterial genome editing and silencing. *Nat. Commun.* 8, 1647. <https://doi.org/10.1038/s41467-017-01591-4>.
- Mougiakos, I., Bosma, E.F., Ganguly, J., van der Oost, J., van Kranenburg, R., 2018. Hijacking CRISPR-Cas for high-throughput bacterial metabolic engineering: advances and prospects. In: *Current Opinion in Biotechnology, Energy biotechnology • Environmental biotechnology*, Vol. 50, pp. 146–157. <https://doi.org/10.1016/j.copbio.2018.01.002>.
- Mutalik, V.K., Guimaraes, J.C., Cambray, G., Lam, C., Christoffersen, M.J., Mai, Q.-A., Tran, A.B., Paull, M., Keasling, J.D., Arkin, A.P., Endy, D., 2013. Precise and reliable gene expression via standard transcription and translation initiation elements. *Nat. Methods* 10, 354–360. <https://doi.org/10.1038/nmeth.2404>.
- Na, D., Yoo, S.M., Chung, H., Park, H., Park, J.H., Lee, S.Y., 2013. Metabolic engineering of *Escherichia coli* using synthetic small regulatory RNAs. *Nat. Biotechnol.* 31, 170–174. <https://doi.org/10.1038/nbt.2461>.
- Nelson, K.E., Weinel, C., Paulsen, I.T., Dodson, R.J., Hilbert, H., Martins dos Santos, V. a P., Fouts, D.E., Gill, S.R., Pop, M., Holmes, M., Brinkac, L., Beanan, M., DeBoy, R.T., Daugherty, S., Kolonay, J., Madupu, R., Nelson, W., White, O., Peterson, J., Khouri, H., Hance, I., Chris Lee, P., Holtzapple, E., Scanlan, D., Tran, K., Moazzez, A., Utterback, T., Rizzo, M., Lee, K., Kosack, D., Moestl, D., Wedler, H., Lauber, J., Stjepandic, D., Hoheisel, J., Straetz, M., Heim, S., Kiewitz, C., Eisen, J.A., Timmis, K. N., Diesterhöft, A., Tümmler, B., Fraser, C.M., 2002. Complete genome sequence and comparative analysis of the metabolically versatile *Pseudomonas putida* KT2440. *Environ. Microbiol.* 4, 799–808. <https://doi.org/10.1046/j.1462-2920.2002.00366.x>.
- Nielsen, A.A., Voigt, C.A., 2014. Multi-input CRISPR/C as genetic circuits that interface host regulatory networks. *Mol. Syst. Biol.* 10, 15252/MSB.20145735, 763.
- Nielsen, A.A.K., Der, B.S., Shin, J., Vaidyanathan, P., Paralanov, V., Strychalski, E.A., Ross, D., Densmore, D., Voigt, C.A., 2016. Genetic circuit design automation. *Science* 352. <https://doi.org/10.1126/science.aac7341>, aac7341.
- Nikel, P.I., de Lorenzo, V., 2013. Implantation of unmarked regulatory and metabolic modules in Gram-negative bacteria with specialised mini-transposon delivery vectors. *J. Biotechnol.* 163, 143–154. <https://doi.org/10.1016/j.jbiotec.2012.05.002>.
- Nikel, P.I., Romero-Campero, F.J., Zeidman, J.A., Goñi-Moreno, A., de Lorenzo, V., 2015. The glycerol-dependent metabolic persistence of *Pseudomonas putida* KT2440 reflects the regulatory logic of the GlpR repressor. *mBio* 6. <https://doi.org/10.1128/mBio.00340-15>.
- Nikel, P.I., Chavarría, M., Danchin, A., de Lorenzo, V., 2016. From dirt to industrial applications: *Pseudomonas putida* as a synthetic biology chassis for hosting harsh biochemical reactions. In: *Current Opinion in Chemical Biology, Synthetic Biology • Synthetic Biomolecule*, Vol. 34, pp. 20–29. <https://doi.org/10.1016/j.cbpa.2016.05.011>.
- Nishimatsu, H., Shi, X., Ishiguro, S., Gao, L., Hirano, S., Okazaki, S., Noda, T., Abudayyeh, O.O., Gootenberg, J.S., Mori, H., Oura, S., Holmes, B., Tanaka, M., Seki, M., Hirano, H., Aburatani, H., Ishitani, R., Ikawa, M., Yachie, N., Zhang, F., Nureki, O., 2018. Engineered CRISPR-Cas9 nuclease with expanded targeting space. *Science* 361, 1259–1262. <https://doi.org/10.1126/science.aas9129>.
- Nitschel, R., Ankenbauer, A., Welsch, I., Wirth, N.T., Massner, C., Ahmad, N., McColm, S., Borges, F., Fotheringham, I., Takors, R., Blombach, B., 2020. Engineering *Pseudomonas putida* KT2440 for the production of isobutanol. *Eng. Life Sci.* 20, 148–159. <https://doi.org/10.1002/elsc.201900151>.
- Niu, W., Willett, H., Mueller, J., He, X., Kramer, L., Ma, B., Guo, J., 2020. Direct biosynthesis of adipic acid from lignin-derived aromatics using engineered *Pseudomonas putida* KT2440. *Metab. Eng.* 59, 151–161. <https://doi.org/10.1016/j.ymben.2020.02.006>.
- Nogales, J., Palsson, B., Thiele, I., 2008. A genome-scale metabolic reconstruction of *Pseudomonas putida* KT2440: iJN746 as a cell factory. *BMC Syst. Biol.* 2, 1–20. <https://doi.org/10.1186/1752-0509-2-79>.
- Nogales, J., Mueller, J., Gudmundsson, S., Canalejo, F.J., Duque, E., Monk, J., Feist, A. M., Ramos, J.L., Niu, W., Palsson, B.O., 2020. High-quality genome-scale metabolic modelling of *Pseudomonas putida* highlights its broad metabolic capabilities. *Environ. Microbiol.* 22, 255–269. <https://doi.org/10.1111/1462-2920.14843>.
- Noirot, P., Kolodner, R.D., 1998. DNA strand invasion promoted by *Escherichia coli* RecT protein. *J. Biol. Chem.* 273, 12274–12280. <https://doi.org/10.1074/jbc.273.20.12274>.
- Nyerges, Á., Csörgö, B., Nagy, I., Bálint, B., Bihari, P., Lázár, V., Apjok, G., Umenhoffer, K., Bogos, B., Pósfai, G., Pál, C., 2016. A highly precise and portable genome engineering method allows comparison of mutational effects across bacterial species. *Proc. Natl. Acad. Sci. U. S. A.* 113, 2502–2507. <https://doi.org/10.1073/pnas.1520040113>.
- Oberhardt, M.A., Puchaika, J., Fryer, K.E., Martins dos Santos, V.A.P., Papin, J.A., 2008. Genome-scale metabolic network analysis of the opportunistic pathogen *Pseudomonas aeruginosa* PAO1. *J. Bacteriol.* 190, 2790–2803. <https://doi.org/10.1128/JB.01583-07>.
- Oberhardt, M.A., Puchaika, J., Martins dos Santos, V.A.P., Papin, J.A., 2011. Reconciliation of genome-scale metabolic reconstructions for comparative systems analysis. *PLoS Comput. Biol.* 7, e1001116. <https://doi.org/10.1371/journal.pcbi.1001116>.

- Occhipinti, A., Eyassu, F., Rahman, T.J., Rahman, P.K.S.M., Angione, C., 2018. In silico engineering of *Pseudomonas* metabolism reveals new biomarkers for increased biosurfactant production. *PeerJ* 6, e6046. <https://doi.org/10.7717/peerj.6046>.
- Oppenorth, P., Costello, Z., Okada, T., Goyal, G., Chen, Y., Gin, J., Benites, V., de Raad, M., Northen, T.R., Deng, K., Deutsch, S., Baidoo, E.E.K., Petzold, C.J., Hillson, N.J., García Martín, H., Beller, H.R., 2019. Lessons from two design-build-test-learn cycles of dodecanol production in *Escherichia coli* aided by machine learning. *ACS Synth. Biol.* 8, 1337–1351. <https://doi.org/10.1021/acssynbio.9b00020>.
- Orth, J.D., Thiele, I., Palsson, B.O., 2010. What is flux balance analysis?. In: *Nature Biotechnology*. Nature Publishing Group. <https://doi.org/10.1038/nbt.1614>.
- Øyås, O., Borrell, S., Trauner, A., Zimmermann, M., Feldmann, J., Liphardt, T., Gagneux, S., Stelling, J., Sauer, U., Zampieri, M., 2020. Model-based integration of genomics and metabolomics reveals SNP functionality in *Mycobacterium tuberculosis*. *Proc. Natl. Acad. Sci. U. S. A.* 117 (15), 8494–8502. <https://doi.org/10.1073/pnas.1915551117>. Epub 2020 Mar 30.
- Park, M.-R., Chen, Y., Thompson, M., Benites, V.T., Fong, B., Petzold, C.J., Baidoo, E.E.K., Gladden, J.M., Adams, P.D., Keasling, J.D., Simmons, B.A., Singer, S.W., 2020. Response of *Pseudomonas putida* to complex, aromatic-rich fractions from biomass. *ChemSusChem* 13, 4455–4467. <https://doi.org/10.1002/cssc.202000268>.
- Peabody, G.L., Elmore, J.R., Martínez-Baird, J., Guss, A.M., 2019. Engineered *Pseudomonas putida* KT2440 co-utilizes galactose and glucose. In: *Biotechnology for Biofuels*. <https://doi.org/10.1186/s13068-019-1627-0>.
- Pellicci, V., Reytrat, J.-M., Gicquel, B., 1996. Generation of unmarked directed mutations in mycobacteria, using sucrose counter-selectable suicide vectors. *Mol. Microbiol.* 20, 919–925. <https://doi.org/10.1111/j.1365-2958.1996.tb02533.x>.
- Peters, J.M., Colavin, A., Shi, H., Czarny, T.L., Larson, M.H., Wong, S., Hawkins, J.S., Lu, C.H.S., Koo, B.-M., Marta, E., Shiver, A.L., Whitehead, E.H., Weissman, J.S., Brown, E.D., Qi, L.S., Huang, K.C., Gross, C.A., 2016. A comprehensive, CRISPR-based functional analysis of essential genes in bacteria. *Cell* 165, 1493–1506. <https://doi.org/10.1016/j.cell.2016.05.003>.
- Pickar-Oliver, A., Gersbach, C.A., 2019. The next generation of CRISPR-Cas technologies and applications. *Nat. Rev. Mol. Cell Biol.* 20, 490–507. <https://doi.org/10.1038/s41580-019-0131-5>.
- Poblete-Castro, I., Becker, J., Dohnt, K., dos Santos, V.M., Wittmann, C., 2012. Industrial biotechnology of *Pseudomonas putida* and related species. *Appl. Microbiol. Biotechnol.* 93, 2279–2290. <https://doi.org/10.1007/s00253-012-3928-0>.
- Poblete-Castro, I., Binger, D., Rodríguez, A., Becker, J., Martins dos Santos, V.A.P., Wittmann, C., 2013. In-silico-driven metabolic engineering of *Pseudomonas putida* for enhanced production of poly-hydroxyalkanoates. *Metab. Eng.* 15, 113–123. <https://doi.org/10.1016/j.ymben.2012.10.004>.
- Poblete-Castro, I., Aravena-Carrasco, C., Orellana-Saez, M., Pacheco, N., Cabrera, A., Borrero-de Acuña, J.M., 2020. Engineering the osmotic state of *Pseudomonas putida* KT2440 for efficient cell disruption and downstream processing of poly(3-hydroxyalkanoates). *Front Bioeng Biotechnol.* 8. <https://doi.org/10.3389/fbioe.2020.00161>.
- Puchalka, J., Oberhardt, M.A., Godinho, M., Bielecka, A., Regenshardt, D., Timmis, K.N., Papin, J.A., Martins Dos Santos, V.A.P., 2008. Genome-scale reconstruction and analysis of the *Pseudomonas putida* KT2440 metabolic network facilitates applications in biotechnology. *PLoS Comput. Biol.* 4. <https://doi.org/10.1371/journal.pcbi.1000210>.
- Qi, L.S., Larson, M.H., Gilbert, L.A., Doudna, J.A., Weissman, J.S., Arkin, A.P., Lim, W.A., 2013. Repurposing CRISPR as an RNA-guided platform for sequence-specific control of gene expression. *Cell* 152, 1173–1183. <https://doi.org/10.1016/j.cell.2013.02.022>.
- Ran, F.A., Hsu, P.D., Lin, C.-Y., Gootenberg, J.S., Konermann, S., Trevino, A.E., Scott, D. A., Inoue, A., Matoba, S., Zhang, Y., Zhang, F., 2013. Double nicking by RNA-guided CRISPR Cas9 for enhanced genome editing specificity. *Cell* 154, 1380–1389. <https://doi.org/10.1016/j.cell.2013.08.021>.
- Ray-Soni, A., Bellecourt, M.J., Landick, R., 2016. Mechanisms of bacterial transcription termination: all good things must end. *Annu. Rev. Biochem.* 85, 319–347. <https://doi.org/10.1146/annurev-biochem-060815-014844>.
- Rees, H.A., Liu, D.R., 2018. Base editing: precision chemistry on the genome and transcriptome of living cells. *Nat. Rev. Genet.* 19, 770–788. <https://doi.org/10.1038/s41576-018-0059-1>.
- Reisbig, M.D., 2003. Factors influencing gene expression and resistance for Gram-negative organisms expressing plasmid-encoded ampC genes of Enterobacter origin. *J. Antimicrob. Chemother.* 51, 1141–1151. <https://doi.org/10.1093/jac/dkg204>.
- Ricaurte, D.E., Martínez-García, E., Nyerges, Á., Pál, C., de Lorenzo, V., Aparicio, T., 2018. A standardized workflow for surveying recombinases expands bacterial genome-editing capabilities. *Microb. Biotechnol.* 11, 176–188. <https://doi.org/10.1111/1751-7915.12846>.
- Rienksma, R.A., Suarez-Diez, M., Spina, L., Schaap, P.J., Martins dos Santos, V.A., 2014. Systems-level modeling of mycobacterial metabolism for the identification of new (multi-)drug targets. *Semin. Immunol.* 26 (6), 610–622. <https://doi.org/10.1016/j.smim.2014.09.013>.
- Roberto, K., Manabu, I., Donald, R.H., 1978. Trans-complementation-dependent replication of a low molecular weight origin fragment from plasmid R6K. *Cell* 15, 1199–1208. [https://doi.org/10.1016/0092-8674\(78\)90046-6](https://doi.org/10.1016/0092-8674(78)90046-6).
- Rosendahl, S., Tamman, H., Brauer, A., Remm, M., Hörak, R., 2020. Chromosomal toxin-antitoxin systems in *Pseudomonas putida* are rather selfish than beneficial. *Sci. Rep.* 10, 9230. <https://doi.org/10.1038/s41598-020-65504-0>.
- Rybalchenko, N., Golub, E.I., Bi, B., Radding, C.M., 2004. Strand invasion promoted by recombination protein  $\beta$  of coliphage  $\lambda$ . *Proc. Natl. Acad. Sci. U. S. A.* 101, 17056–17060. <https://doi.org/10.1073/pnas.0408046101>.
- Salis, H.M., 2011. Chapter two - the ribosome binding site calculator. In: Voigt, C. (Ed.), *Methods in Enzymology, Synthetic Biology Part B*. Academic Press, pp. 19–42. <https://doi.org/10.1016/B978-0-12-385120-8.00002-4>.
- Salis, H.M., Mirsky, E.A., Voigt, C.A., 2009. Automated design of synthetic ribosome binding sites to control protein expression. *Nat. Biotechnol.* 27, 946–950. <https://doi.org/10.1038/nbt.1568>.
- Sánchez, B.J., Zhang, C., Nilsson, A., Lahtvee, P.-J., Kerkhoven, E.J., Nielsen, J., 2017. Improving the phenotype predictions of a yeast genome-scale metabolic model by incorporating enzymatic constraints. *Mol. Syst. Biol.* 13, 935. <https://doi.org/10.15252/msb.20167411>.
- Sánchez-Clemente, R., Igeño, M.I., Población, A.G., Guijo, M.I., Merchán, F., Blasco, R., 2018. Study of pH changes in media during bacterial growth of several environmental strains. *Proceedings* 2, 1297. <https://doi.org/10.3390/proceedings2201297>.
- Schäfer, A., Tauch, A., Jäger, W., Kalinowski, J., Thierbach, G., Pühler, A., 1994. Small mobilizable multi-purpose cloning vectors derived from the *Escherichia coli* plasmids pK18 and pK19: selection of defined deletions in the chromosome of *Corynebacterium glutamicum*. *Gene* 145, 69–73. [https://doi.org/10.1016/0378-1119\(94\)90324-7](https://doi.org/10.1016/0378-1119(94)90324-7).
- Schuster, M., Kahmann, R., 2019. CRISPR-Cas9 genome editing approaches in filamentous fungi and oomycetes. *Fungal Genet. Biol.* 130, 43–53. <https://doi.org/10.1016/j.fgb.2019.04.016>.
- Selle, K., Barrangou, R., 2015. Harnessing CRISPR–Cas systems for bacterial genome editing. *Trends Microbiol.* 23, 225–232. <https://doi.org/10.1016/j.tim.2015.01.008>.
- Shintani, M., Sanchez, Z.K., Kimbara, K., 2015. Genomics of microbial plasmids: classification and identification based on replication and transfer systems and host taxonomy. *Front. Microbiol.* 6. <https://doi.org/10.3389/fmicb.2015.00242>.
- Silva-Rocha, R., de Lorenzo, V., 2013. The TOL network of *Pseudomonas putida* mt-2 processes multiple environmental inputs into a narrow response space. *Environ. Microbiol.* 15, 271–286. <https://doi.org/10.1111/1462-2920.12014>.
- Silva-Rocha, R., Tamames, J., dos Santos, V.M., de Lorenzo, V., 2011. The logicome of environmental bacteria: merging catabolic and regulatory events with Boolean formalisms. *Environ. Microbiol.* 13, 2389–2402. <https://doi.org/10.1111/j.1462-2920.2011.02455.x>.
- Silva-Rocha, R., Martínez-García, E., Calles, B., Chavarría, M., Arce-Rodríguez, A., de las Heras, A., Páez-Espino, A.D., Durante-Rodríguez, G., Kim, J., Nikel, P.I., Platero, R., de Lorenzo, V., 2013. The Standard European Vector Architecture (SEVA): a coherent platform for the analysis and deployment of complex prokaryotic phenotypes. *Nucleic Acids Res.* 41, D666–D675. <https://doi.org/10.1093/nar/gks1119>.
- Sohn, S.B., Kim, T.Y., Park, J.M., Lee, S.Y., 2010. In silico genome-scale metabolic analysis of *Pseudomonas putida* KT2440 for polyhydroxyalkanoate synthesis, degradation of aromatics and anaerobic survival. *Biotechnol. J.* 5, 739–750. <https://doi.org/10.1002/biot.201000124>.
- Standage-Beier, K., Zhang, Q., Wang, X., 2015. Targeted large-scale deletion of bacterial genomes using CRISPR-nickases. *ACS Synth. Biol.* 4, 1217–1225. <https://doi.org/10.1021/acssynbio.5b00132>.
- Stephanopoulos, G., Aristidou, A.A., Nielsen, J.H., 1998. In: Stephanopoulos, Gregory N., Aristidou, Aristos A., Nielsen, Jens (Eds.), *Metabolic Engineering Principles and Methodologies*.
- Storz, G., Vogel, J., Wassarman, K.M., 2011. Regulation by Small RNAs in Bacteria: Expanding Frontiers. *Molecular Cell. Cell Press*. <https://doi.org/10.1016/j.molcel.2011.08.022>.
- Strecker, J., Ladha, A., Gardner, Z., Schmid-Burgk, J.L., Makarova, K.S., Koonin, E.V., Zhang, F., 2019. RNA-guided DNA insertion with CRISPR-associated transposases. *Science* 365, 48–53. <https://doi.org/10.1126/science.aax9181>.
- Sudarsan, S., Dethlefsen, S., Blank, L.M., Siemann-Herzberg, M., Schmid, A., 2014. The functional structure of central carbon metabolism in *Pseudomonas putida* KT2440. *Appl. Environ. Microbiol.* 80, 5292–5303. <https://doi.org/10.1128/AEM.01643-14>.
- Sudarsan, S., Blank, L.M., Dietrich, A., Vielhauer, O., Takors, R., Schmid, A., Reuss, M., 2016. Dynamics of benzoate metabolism in *Pseudomonas putida* KT2440. *Metab. Eng. Commun.* 3, 97–110. <https://doi.org/10.1016/j.meten.2016.03.005>.
- Sulheim, S., Kumelj, T., van Dissel, D., Salehzadeh-Yazdi, A., Du, C., van Wezel, G.P., Nieselt, K., Almaas, E., Wentzel, A., Kerkhoven, E.J., 2020. Enzyme-constrained models and omics analysis of streptomyces coelicolor reveal metabolic changes that enhance heterologous production. *iScience* 23, 101525. <https://doi.org/10.1016/j.isci.2020.101525>.
- Sumi, S., Mutaguchi, N., Ebuchi, T., Tsuchida, H., Yamamoto, T., Suzuki, M., Natsuka, C., Shiratori-Takano, H., Shintani, M., Nojiri, H., Ueda, K., Takano, H., 2020. Light response of *Pseudomonas putida* KT2440 mediated by class II LitR, a photosensor homolog. *J. Bacteriol.* 202. <https://doi.org/10.1128/JB.00146-20>.
- Sun, J., Wang, Q., Jiang, Y., Wen, Z., Yang, L., Wu, J., Yang, S., 2018a. Genome editing and transcriptional repression in *Pseudomonas putida* KT2440 via the type II CRISPR system. *Microb. Cell Factories* 17, 41. <https://doi.org/10.1186/s12934-018-0887-x>.
- Sun, T., Pei, G., Song, X., Chen, L., Zhang, W., 2018b. Discovery and application of stress-responsive sRNAs in cyanobacteria. In: Zhang, W., Song, X. (Eds.), *Synthetic Biology of Cyanobacteria, Advances in Experimental Medicine and Biology*. Singapore, pp. 55–74. [https://doi.org/10.1007/978-981-13-0854-3\\_3](https://doi.org/10.1007/978-981-13-0854-3_3).
- Sun, J., Lu, L.-B., Liang, T.-X., Yang, L.-R., Wu, J.-P., 2020. CRISPR-assisted multiplex base editing system in *Pseudomonas putida* KT2440. *Front. Bioeng. Biotechnol.* 8, 905. <https://doi.org/10.3389/fbioe.2020.00905>.
- Tan, S.Z., Prather, K.L., 2017. Dynamic pathway regulation: recent advances and methods of construction. In: *Current Opinion in Chemical Biology*. Elsevier Ltd. <https://doi.org/10.1016/j.cbpa.2017.10.004>.
- Tan, S.Z., Reisch, C.R., Prather, K.L.J., 2018. A Robust CRISPR Interference Gene Repression System in *Pseudomonas*. <https://doi.org/10.1128/JB>.

- Thompson, M.G., Incha, M.R., Pearson, A.N., Schmidt, M., Sharpless, W.A., Eiben, C.B., Cruz-Morales, P., Blake-Hedges, J.M., Liu, Y., Adams, C.A., Haushalter, R.W., Krishna, R.N., Lichtner, P., Blank, L.M., Mukhopadhyay, A., Deuschbauer, A.M., Shih, P.M., Keasling, J.D., 2020. Fatty acid and alcohol metabolism in *Pseudomonas putida*: functional analysis using random barcode transposon sequencing. *Appl. Environ. Microbiol.* 86 <https://doi.org/10.1128/AEM.01665-20>.
- Tian, J., Yang, G., Gu, Y., Sun, X., Lu, Y., Jiang, W., 2020. Developing an endogenous quorum-sensing based CRISPRi circuit for autonomous and tunable dynamic regulation of multiple targets in industrial *Streptomyces* (preprint). *Bioengineering*. <https://doi.org/10.1101/2020.01.17.910026>.
- Till, P., Toepel, J., Bühler, B., Mach, R.L., Mach-Aigner, A.R., 2020. Regulatory systems for gene expression control in cyanobacteria. *Appl. Microbiol. Biotechnol.* 104, 1977–1991. <https://doi.org/10.1007/s00253-019-10344-w>.
- Tiso, T., Ihling, N., Kubicki, S., Biselli, A., Schonhoff, A., Bator, I., Thies, S., Karmainski, T., Kruth, S., Willenbrink, A.-L., Loeschke, A., Zapp, P., Jupke, A., Jaeger, K.-E., Büchs, J., Blank, L.M., 2020. Integration of genetic and process engineering for optimized rhamnolipid production using *Pseudomonas putida*. *Front Bioeng. Biotechnol.* 8. <https://doi.org/10.3389/fbioe.2020.00976>.
- Tokic, M., Hatzimanikatis, V., Miskovic, L., 2020. Large-scale kinetic metabolic models of *Pseudomonas putida* KT2440 for consistent design of metabolic engineering strategies. *Biotechnol. Biofuels* 13, 1–19. <https://doi.org/10.1186/s13068-020-1665-7>.
- Torella, J.P., Ford, T.J., Kim, S.N., Chen, A.M., Way, J.C., Silver, P.A., 2013. Tailored fatty acid synthesis via dynamic control of fatty acid elongation. *Proc. Natl. Acad. Sci. U. S. A.* 110, 11290–11295. <https://doi.org/10.1073/pnas.1307129110>.
- Tsipas, A., Koutinas, M., Usaku, C., Mantalaris, A., 2018. Optimal bioprocess design through a gene regulatory network – growth kinetic hybrid model: towards replacing monod kinetics. *Metab. Eng.* 48, 129–137. <https://doi.org/10.1016/j.ymben.2018.04.023>.
- Turan, S., Zehe, C., Kuehle, J., Qiao, J., Bode, J., 2013. Recombinase-mediated cassette exchange (RMCE) – a rapidly-expanding toolbox for targeted genomic modifications. *Gene*. <https://doi.org/10.1016/j.gene.2012.11.016>.
- Upadhyay, P., Singh, N.K., Tupe, R., Odenath, A., Lali, A., 2020. Biotransformation of corn bran derived ferulic acid to vanillic acid using engineered *Pseudomonas putida* KT2440. *Prep. Biochem. Biotechnol.* 50, 341–348. <https://doi.org/10.1080/10826068.2019.1697935>.
- Updegrave, T.B., Zhang, A., Storz, G., 2016. Hfq: The flexible RNA matchmaker. In: *Current Opinion in Microbiology*. Elsevier Ltd. <https://doi.org/10.1016/j.mib.2016.02.003>.
- Urtecho, G., Tripp, A.D., Insigne, K.D., Kim, H., Kosuri, S., 2019. Systematic dissection of sequence elements controlling  $\sigma 70$  promoters using a genomically encoded multiplexed reporter assay in *Escherichia coli*. *Biochemistry*. <https://doi.org/10.1021/acs.biochem.7b01069>.
- van Duuren, J.B., Puchalka, J., Mars, A.E., Bücker, R., Eggink, G., Wittmann, C., dos Santos, V.A.M., 2013. Reconciling in vivo and in silico key biological parameters of *Pseudomonas putida*KT2440 during growth on glucose under carbon-limited condition. *BMC Biotechnol.* 13, 93. <https://doi.org/10.1186/1472-6750-13-93>.
- van Duuren, J.B.J.H., de Wild, P.J., Starck, S., Bradtmöller, C., Selzer, M., Mehlmann, K., Schneider, R., Kohlstedt, M., Poblete-Castro, I., Stolzenberger, J., Barton, N., Fritz, M., Scholl, S., Venus, J., Wittmann, C., 2020. Limited life cycle and cost assessment for the bioconversion of lignin-derived aromatics into adipic acid. *Biotechnol. Bioeng.* 117, 1381–1393. <https://doi.org/10.1002/bit.27299>.
- Varma, A., Palsson, B.O., 1994. Stoichiometric flux balance models quantitatively predict growth and metabolic by-product secretion in wild-type *Escherichia coli* W3110. *Appl. Environ. Microbiol.* 60, 3724–3731. <https://doi.org/10.1128/aem.60.10.3724-3731.1994>.
- Vazquez-Anderson, J., Contreras, L.M., 2013. Regulatory RNAs. *RNA Biol.* 10, 1778–1797. <https://doi.org/10.4161/rna.27102>.
- Villa, J.K., Su, Y., Contreras, L.M., Hammond, M.C., 2018. Synthetic biology of small RNAs and riboswitches. In: *Regulating with RNA in Bacteria and Archaea*. ASM Press, Washington, DC, USA, pp. 527–545. <https://doi.org/10.1128/9781683670247.ch31>.
- Vo, P.L.H., Ronda, C., Klompe, S.E., Chen, E.E., Acree, C., Wang, H.H., Sternberg, S.H., 2020. CRISPR RNA-guided integrases for high-efficiency, multiplexed bacterial genome engineering. *Nat. Biotechnol.* <https://doi.org/10.1038/s41587-020-00745-y>.
- Volke, D.C., Friis, L., Wirth, N.T., Turlin, J., Nikel, P.I., 2020a. Synthetic control of plasmid replication enables target- and self-curing of vectors and expedites genome engineering of *Pseudomonas putida*. *Metab. Eng. Commun.* 10, e00126 <https://doi.org/10.1016/j.mec.2020.e00126>.
- Volke, D.C., Turlin, J., Mol, V., Nikel, P.I., 2020b. Physical decoupling of XylS/Pm regulatory elements and conditional proteolysis enable precise control of gene expression in *Pseudomonas putida*. *Microb. Biotechnol.* 13, 222–232. <https://doi.org/10.1111/1751-7915.13383>.
- von Kamp, A., Klamt, S., 2017. Growth-coupled overproduction is feasible for almost all metabolites in five major production organisms. *Nat. Commun.* 8, 15956. <https://doi.org/10.1038/ncomms15956>.
- Walton, R.T., Christie, K.A., Whittaker, M.N., Kleinstiver, B.P., 2020. Unconstrained genome targeting with near-PAMless engineered CRISPR-Cas9 variants. *Science* 368, 290–296. <https://doi.org/10.1126/science.aba8853>.
- Wang, H.H., Isaacs, F.J., Carr, P.A., Sun, Z.Z., Xu, G., Forest, C.R., Church, G.M., 2009. Programming cells by multiplex genome engineering and accelerated evolution. *Nature* 460, 894–898. <https://doi.org/10.1038/nature08187>.
- Wang, Y., Yau, Y.Y., Perkins-Balding, D., Thomson, J.G., 2011. Recombinase technology: applications and possibilities. *Plant Cell Rep.* <https://doi.org/10.1007/s00299-010-0938-1>.
- Wang, H., La Russa, M., Qi, L.S., 2016. CRISPR/Cas9 in genome editing and beyond. *Annu. Rev. Biochem.* 85, 227–264. <https://doi.org/10.1146/annurev-biochem-060815-014607>.
- Wang, X., Lin, L., Dong, J., Ling, J., Wang, W., Wang, H., Zhang, Z., Yu, X., 2018. Simultaneous improvements of *Pseudomonas* cell growth and polyhydroxyalkanoate production from a lignin derivative for lignin-consolidated bioprocessing. *Appl. Environ. Microbiol.* 84 <https://doi.org/10.1128/AEM.01469-18> e01469-18/aem/84/18/e01469-18.atom.
- Wang, G., Zhao, Z., Ke, J., Engel, Y., Shi, Y.M., Robinson, D., Bingol, K., Zhang, Z., Bowen, B., Louie, K., Wang, B., Evans, R., Miyamoto, Y., Cheng, K., Kosina, S., De Raad, M., Silva, L., Luhrs, A., Lubbe, A., Hoyt, D.W., Francavilla, C., Otani, H., Deutsch, S., Washton, N.M., Rubin, E.M., Mouncey, N.J., Visel, A., Northen, T., Cheng, J.F., Bode, H.B., Yoshikuni, Y., 2019. CRAGE enables rapid activation of biosynthetic gene clusters in undomesticated bacteria. *Nat. Microbiol.* <https://doi.org/10.1038/s41564-019-0573-8>.
- Wannier, T.M., Nyerges, A., Kuchwara, H.M., Czikkely, M., Balogh, D., Filsinger, G.T., Borders, N.C., Gregg, C.J., Lajoie, M.J., Rios, X., Pál, C., Church, G.M., 2020. Improved bacterial recombineering by parallelized protein discovery. *bioRxiv*. <https://doi.org/10.1101/2020.01.14.906594>, 2020.01.14.906594.
- Waters, L.S., Storz, G., 2009. Regulatory RNAs in bacteria. *Cell. Cell Press*. <https://doi.org/10.1016/j.cell.2009.01.043>.
- Wehrmann, M., Toussaint, M., Pfannstiel, J., Billard, P., Klebensberger, J., 2020. The cellular response to lanthanum is substrate specific and reveals a novel route for glycerol metabolism in *Pseudomonas putida* KT2440. *MBio* 11, 14.
- Weimer, A., Kohlstedt, M., Volke, D.C., Nikel, P.I., Wittmann, C., 2020. Industrial biotechnology of *Pseudomonas putida*: advances and prospects. *Appl. Microbiol. Biotechnol.* 104, 7745–7766. <https://doi.org/10.1007/s00253-020-10811-9>.
- Williamson, J.J., Bahrin, N., Hardiman, E.M., Bugg, T.D.H., 2020. Production of substituted styrene bioproducts from lignin and lignocellulose using engineered *Pseudomonas putida* KT2440. *Biotechnol. J.* 15, 1900571. <https://doi.org/10.1002/biot.201900571>.
- Wirth, N.T., Kozaeva, E., Nikel, P.I., 2019. Accelerated genome engineering of *Pseudomonas putida* by I-SceI-mediated recombination and CRISPR-Cas9 counterselection. *Microb. Biotechnol.* 13, 233–249. <https://doi.org/10.1111/1751-7915.13396>.
- Wolf, S., Pflüger-Grau, K., Kremling, A., 2015. Modeling the interplay of *Pseudomonas putida* EIIA with the potassium transporter KdpFABC. *J. Mol. Microbiol. Biotechnol.* 25, 178–194. <https://doi.org/10.1159/000381214>.
- Woolston, B.M., Emerson, D.F., Currie, D.H., Stephanopoulos, G., 2018. Redirecting carbon flux in *Clostridium ljungdahlii* using CRISPR interference (CRISPRi). *Metab. Eng.* 48, 243–253. <https://doi.org/10.1016/j.ymben.2018.06.006>.
- Yang, S., Wang, Y., Wei, C., Liu, Q., Jin, X., Du, G., Chen, J., Kang, Z., 2018. A new sRNA-mediated posttranscriptional regulation system for *Bacillus subtilis*. *Biotechnol. Bioeng.* 115, 2986–2995. <https://doi.org/10.1002/bit.26833>.
- Yao, L., Shabestary, K., Björk, S.M., Asplund-Samuelsson, J., Jonsson, H.N., Jahn, M., Hudson, E.P., 2020. Pooled CRISPRi screening of the cyanobacterium *Synechocystis* sp. PCC 6803 for enhanced industrial phenotypes. *Nat. Commun.* 11, 1666. <https://doi.org/10.1038/s41467-020-15491-7>.
- Ye, C., Luo, Q., Guo, L., Gao, C., Xu, N., Zhang, L., Liu, L., Chen, X., 2020. Improving lysine production through construction of an *Escherichia coli* enzyme-constrained model. *Biotechnol. Bioeng.* 117, 3533–3544. <https://doi.org/10.1002/bit.27485>.
- Yuan, Q., Huang, T., Li, P., Hao, T., Li, F., Ma, H., Wang, Z., Zhao, X., Chen, T., Goryanin, I., 2017. Pathway-Consensus approach to metabolic network reconstruction for *Pseudomonas putida* KT2440 by systematic comparison of published models. *PLoS One* 12. <https://doi.org/10.1371/journal.pone.0169437>.
- Zhang, Yueping, Wang, J., Wang, Z., Zhang, Yiming, Shi, S., Nielsen, J., Liu, Z., 2019. A gRNA-trNA array for CRISPR-Cas9 based rapid multiplexed genome editing in *Saccharomyces cerevisiae*. *Nat. Commun.* 10, 1053. <https://doi.org/10.1038/s41467-019-09005-3>.
- Zhang, J.J., Tang, X., Huan, T., Ross, A.C., Moore, B.S., 2020a. Pass-back chain extension expands multimodular assembly line biosynthesis. *Nat. Chem. Biol.* 16, 42–49. <https://doi.org/10.1038/s41589-019-0385-4>.
- Zhang, Y., Zhang, H., Wang, Z., Wu, Z., Wang, Y., Tang, N., Xu, X., Zhao, S., Chen, W., Ji, Q., 2020b. Programmable adenine deamination in bacteria using a Cas9–adenine-deaminase fusion. *Chem. Sci.* 11, 1657–1664. <https://doi.org/10.1039/C9SC03784E>.
- Zheng, K., Wang, Y., Li, N., Jiang, F.-F., Wu, C.-X., Liu, F., Chen, H.-C., Liu, Z.-F., 2018. Highly efficient base editing in bacteria using a Cas9-cytidine deaminase fusion. *Commun. Biol.* 1, 32. <https://doi.org/10.1038/s42003-018-0035-5>.
- Zhou, Y., Lin, L., Wang, H., Zhang, Z., Zhou, J., Jiao, N., 2020. Development of a CRISPR/Cas9n-based tool for metabolic engineering of *Pseudomonas putida* for ferulic acid-to-polyhydroxyalkanoate bioconversion. *Commun. Biol.* 3, 98. <https://doi.org/10.1038/s42003-020-0824-5>.
- Zobel, S., Benedetti, I., Eisenbach, L., de Lorenzo, V., Wierckx, N., Blank, L.M., 2015. Tn7-based device for calibrated heterologous gene expression in *Pseudomonas putida*. *ACS Synth. Biol.* 4, 1341–1351. <https://doi.org/10.1021/acssynbio.5b00058>.